NASA Contractor Report 3422

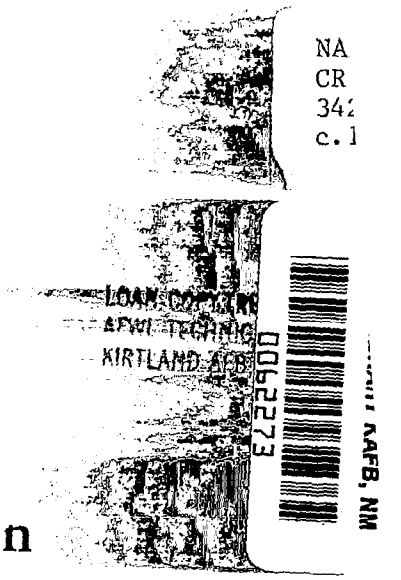

Investigation of Air Solubility in Jet A Fuel at High Pressures

S. D. Rupprecht and G. M. Faeth

GRANT NSG-3306
MAY 1981

NASA

NASA Contractor Report 3422

Investigation of Air Solubility in Jet A Fuel at High Pressures

S. D. Rupprecht and G. M. Faeth
The Pennsylvania State University
University Park, Pennsylvania

Prepared for
Lewis Research Center
under Grant NSG-3306

NASA
National Aeronautics
and Space Administration

Scientific and Technical
Information Branch

1981

TABLE OF CONTENTS

INVESTIGATION OF AIR SOLUBILITY IN JET A FUEL AT HIGH PRESSURES

SUMMARY

This report discusses activities under NASA Grant No. NSG 3306 for the period September 1, 1979 to August 31, 1980. The objective of the investigation was to determine the thermodynamic properties of Jet A fuel saturated with dissolved air at high pressures. This information is needed for the development of the supercritical injector concept.

Supercritical injection involves dissolving air into a fuel prior to injection. As the resulting mixture passes out of the injector, the air comes out of solution, similar to the flashing of a superheated liquid. Flashing is known to improve atomization and the presence of air in the primary zone of a spray flame is known to reduce pollutant emissions. Therefore, supercritical injection has been proposed as a means of improving the performance of spray burners.

The specific objectives of the present investigation are: (1) to measure the solubility and density characteristics of fuel-gas mixtures, and (2) to correlate these results using basic thermodynamic theory. The system Jet A-air was of primary concern; however, the systems Jet A-nitrogen, n-dodecane-nitrogen and n-dodecane-air were also considered, in order to help establish theoretical methods. The range of the experiments involved pressures of 1.03-10.34 MPa and temperatures in the range 298-373K. The theory involved application of the multicomponent form of the Soave equation of state. A computer program was developed to facilitate the computations.

The results of the investigation can be summarized as follows:

1. The present solubility and density measurements could be correlated by selecting reasonable values for the binary interaction parameters in the Soave equation of state. This was accomplished by treating Jet A as a pseudo-compound.

2. For the present test range, the solubility of air in Jet A was roughly proportional to pressure. The solubility also increased with temperature, but the temperature dependence was relatively weak. Maximum observed solubilities were at 373K and 10.34 MPa, where the mass fraction of dissolved air in the liquid was 0.0227-0.0267, depending on the particular sample of Jet A tested.

3. The effect of dissolved air on liquid density was small. Temperature variations resulted in density variations typical of hydrocarbon blends.

4. Solubility predictions are reported over a wider range than the experiments. These results show that the mole fraction of dissolved air approaches a maximum of 0.6 near the thermodynamic critical point of the mixture.

5. Computations were completed for the isentropic expansion of initially saturated dissolved gas mixtures. The presence of dissolved gas appreciably increases the volumetric expansion ratio of the flow, which should result in improved atomization, particularly at low back pressures.

6. The Soave equation of state provided the best correlation of data for conditions not too near the thermodynamic critical point. In contrast, the Redlich-Kwong equation of state provided a fair correlation over the entire range of the data, and was clearly superior in the near critical region.

With thermodynamic properties and solubility levels established, current efforts are examining the supercritical injection concept. This involves evaluation of both injector atomization properties and combustion performance.

NOMENCLATURE

Symbol	Description
a	parameter, Eq. (10)
a_i	parameter, Eq. (13)
a_{ij}	parameter, Eq. (12)
A	parameter, Eq. (18)
b	parameter, Eq. (11)
b_i	parameter, Eq. (14)
B	parameter, Eq. (19)
C_i	ideal gas property constants
C_{pi}	isobaric specific heat of species i
E_i	voltage
f_i	fugacity of species i
F	parameter, Eq. (39)
F'	parameter, Eq. (40)
h	enthalpy
H_i	heights in solubility measuring device
k_{ij}	binary interaction coefficient
K_i	vapor-liquid equilibrium constant
ℓ_i	length from pivot to center of gravity of float i
L	number of unknowns in the system
L_i	lengths along ribbon resistor
n	total number of species
N	total number of intensive properties
M_i	molecular weight of species i
p	pressure

Symbol	Description
R	Universal gas constant
s	entropy
S_i	parameter, Eq. (16)
T	temperature
v	specific volume
V	mole fraction of vapor
V_i	volume of floats in density apparatus
VR	volumetric expansion ratio
x	mass fraction of vapor
x_i	mole fraction of species i in liquid phase
y_i	mole fraction of species i in gas phase
YV	parameter in computer program
Z	compressibility factor
Z_i	parameter in computer program
α	parameter, Eq. (10)
α_i	parameter, Eq. (15)
α_{ij}	parameter, Eq. (12)
β_{ij}	parameter, Eq. (27)
θ	angle between float B and the horizontal
ρ	density
ϕ	angle between floats
ϕ_i	fugacity coefficient of species i
ω_i	accentric factor of species i

Subscripts	Description
A	designates float in density apparatus
B	designates float in density apparatus
c	critical property
E	state after expansion
f	liquid phase
g	vapor phase
i	generic species
I	state prior to expansion
m	mixture property
r	reduced state
ref	reference state

Superscripts	
$( )^{o}$	ideal gas state

1. Introduction

There are numerous systems which involve the combustion of liquid fuels in air, e.g., aircraft propulsion systems, industrial gas turbines, direct injection stratified charge engines, diesel engines, and furnaces to name only a few. The supercritical injection concept has been proposed as a means for improving combustor operation in such systems [1].

Basically, supercritical injection involves operation at conditions where a portion of the liquid flashes to a vapor upon injection. There are two major approaches to the supercritical injection concept: (1) to dissolve a gas (generally air) into the fuel, and (2) preheating the fuel. In either case, the preparation of the fuel occurs upstream of the injector. The flashing process occurs as the pressure of the liquid is reduced, either near the downstream end of the injector passage, or a short distance from the injector within the combustion chamber.

The present investigation considered supercritical injection by means of dissolved gases. Figure 1 is a sketch of this concept for a gas turbine combustor. In this case, air is drawn from the inlet of the combustor, compressed, mixed with the fuel, and allowed to dissolve prior to injection. The resulting single-phase liquid mixture then passes through a conventional pressure atomizing injector. The rapid reduction of fluid pressure at the injector exit results in the spontaneous expansion or flashing of a portion of the dissolved gases to a vapor state.

Several effects, beneficial to the combustion process, are anticipated when supercritical injection is used. The spontaneous appearance of vapor at the injector exit will result in a rapid and significant increase in the specific volume of the flow. This process is analagous to the aerosol flashing process found in commercial spray cans for paints, deodorants, etc. Aerosol flashing studies have shown that flashing causes significant reduction of drop sizes in the spray, when compared with conventional liquid injection [2-4]. Thus, it is believed that supercritical injection can enhance the spray atomization process associated with combustion systems.

Supercritical injection results in intimate mixing between fuel and air, due to the initial uniform state of the dissolved gas mixture prior to injection. It is widely recognized that premixing fuel and air causes reduced production of soot, UHC, CO and NOX. Due to the unusually well-mixed state, supercritical injection has the potential for reducing pollutants to a greater degree than air atomization, if sufficient quantities of air can be dissolved in the fuel.

The present investigation represents the first stage in the evaluation of the supercritical injection concept. The main objective is to determine the extent to which air can be dissolved in fuels typically used

---

*Numbers in brackets denote references.

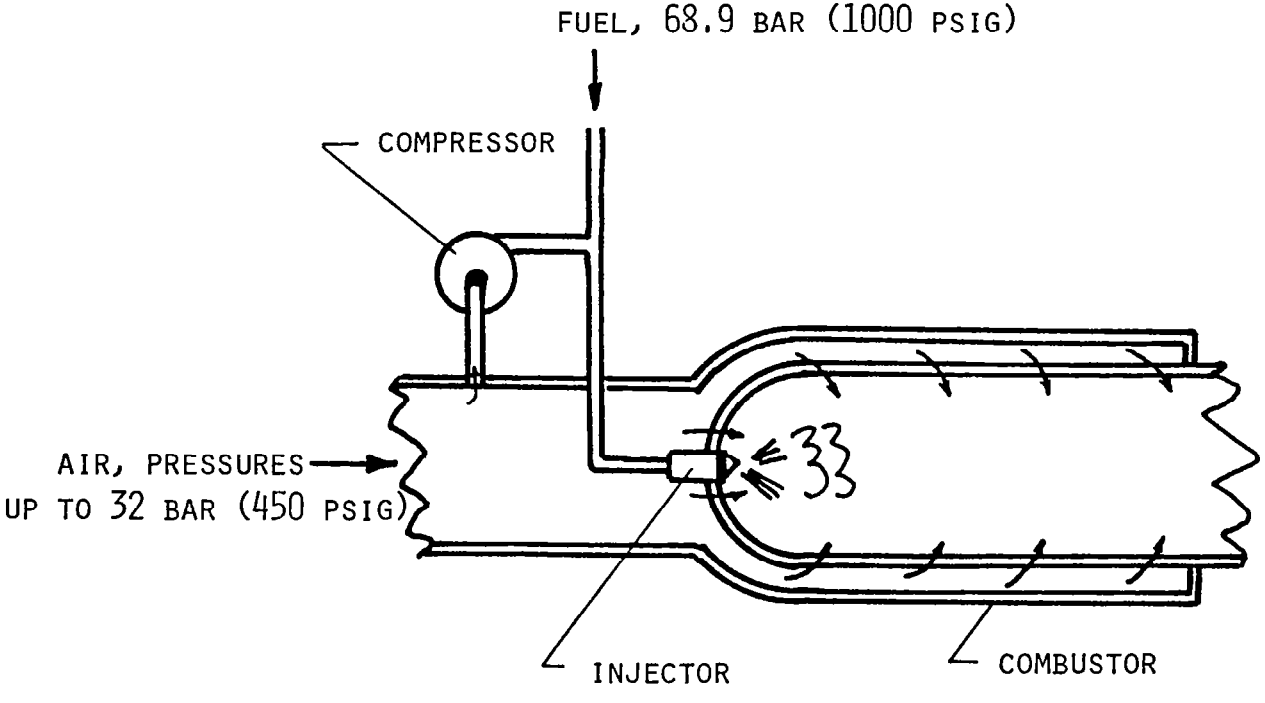

Fig. 1 Supercritical injection concept.

in aircraft propulsion systems. A second major objective is to examine the thermodynamic properties of the resulting fuel-dissolved air mixture. The specific objectives of the research can be summarized as follows:

1. Measure the solubility of gases in liquid fuels for temperature and pressure ranges typical of injector inlet conditions. The fuels considered included dodecane and two samples of Jet A, while the gases were nitrogen and air. Dodecane and nitrogen were included in the investigation in order to provide some results with well-defined systems for checking theoretical results. The temperature and pressure range of the measurements were 297-373K and 1-11 MPa, respectively.

2. Measure the density of saturated fuel-dissolved gas mixtures over a similar range of conditions.

3. Correlate the measurements using multicomponent high pressure thermodynamic theory so that results can be extended to conditions that were not actually tested.

4. Estimate the properties of saturated mixtures during expansion processes, in order to provide information required to predict supercritical injection atomization properties [2-4].

All the results of the investigation are described in this report. The report begins with a discussion of the thermodynamic model. This is followed by a description of the apparatus used to complete the present solubility measurements. The theory is then evaluated using results from both the present and earlier investigations. Following a description of the apparatus used to make density measurements, the density predictions are compared with theory. The report concludes with a discussion of predicted property variations as initially saturated dissolved gas mixtures are isentropically expanded through an injector.

The authors also wish to acknowledge the assistance of H. L. Wysong and D. Grapes during the experimental portion of the investigation. Professor C. H. Wolgemuth, of this department, graciously allowed us to use the density measuring device and provided valuable guidance in its use.

2. Thermodynamic Model

2.1 General Description

The most appealing method for determining the extent to which air may be dissolved in a liquid fuel (solubility of the fuel), for a wide range of conditions, is to employ an equation of state in conjunction with multicomponent phase equilibria theory. By virtue of well established thermodynamic theory, the equation of state may then be employed to also provide thermodynamic property data for the liquid fuel-dissolved gas mixture.

Faeth and coworkers [5-8] employed high pressure thermodynamic theory to predict the dissolved gas concentration at the liquid surface of a fuel droplet immersed in combustion product gases. This involved use of the Redlich-Kwong equation of state which has been

adapted to multicomponent systems through the use of mixing rules developed by Prausnitz and Chueh [9]. In particular, Lazar and Faeth [6] found good agreement between theory and experiment for several pure hydrocarbon-nitrogen systems subjected to high pressure environments (5.07-30.40 MPa). This is of particular interest since high pressures are generally required in order to dissolve appreciable amounts of air into jet fuels.

Recent developments [10-12] have suggested that the Soave modification [13] of the Redlich-Kwong equation of state gives improved results. The major modification of the Soave equation of state is that a Redlich-Kwong constant has been modified to become temperature dependent in order to improve the basic fit of the vapor pressure curve of each species of a multicomponent system. Due to its improved properties, the Soave equation of state has recently been adopted by the American Petroleum Institutes Technical Data Book--Petroleum Refining [14] for vapor-liquid equilibrium calculations. It is, therefore, believed that the Soave equation of state has more promise for accurately modeling high pressure phase equilibria than the Redlich-Kwong version used during earlier work in this laboratory [5-8].

There is one drawback associated with this analytical approach, which would be encountered with either the Soave or Redlich-Kwong equation of state. Inherent in the mixing rules applied to either equation of state is a binary interaction coefficient k_{ij}, which is characteristic of the i-j interaction for each binary pair present in a multicomponent system. This coefficient must be obtained from some experimental information concerning the binary interaction. Most practical jet fuels, however, are complicated blends of hydrocarbons which vary in composition from sample to sample. As a result the literature contains no information on the binary interactions between practical jet fuels and the constituents associated with air (oxygen, nitrogen, carbon dioxide and argon). Therefore, it was necessary to perform solubility experiments with a practical jet fuel in order to determine the binary interaction coefficients. Once the solubility data is collected and correlated with the Soave equation of state, it then becomes feasible to extrapolate the results over a wide range of conditions in order to theoretically investigate the solubility characteristics of a practical jet fuel.

2.2 Phase Equilibrium Considerations

The purpose of phase equilibria thermodynamics is to predict conditions (temperature, pressure, density, composition) which prevail when two or more phases are in equilibrium. A liquid and vapor are considered to be in equilibrium when the following conditions are satisfied:

$$T_g = T_f \tag{1}$$

$$p_g = p_f \tag{2}$$

$$f_{ig} = f_{if} \qquad i = i, 2, 3, \ldots n \tag{3}$$

These equations represent the necessary conditions for equilibrium with respect to the three processes of heat transfer, boundary displacement, and mass transfer. Equilibrium of these processes are represented by temperature pressure and fugacity equality for both phases, in Eqs. (1)-(3). Fugacity is a generalized "partial pressure" of the i-th component, valid for computations at high pressures.† Introducing a fugacity coefficient, this "partial pressure" of the component through the following relationship.

$$f_i = \phi_i x_i p \tag{4}$$

Thermodynamically the fugacity coefficient is defined as

$$RT \ln \phi_i = \int_o^p [v_i - \frac{RT}{p}] \, dp \tag{5}$$

When an appropriate equation of state is employed in Eq. (5) an expression for the fugacity coefficient may be obtained.

The independent intensive properties associated with phase equilibrium between the liquid and vapor phases are p, T, v_f, v_g, x_i and y_i. For a multicomponent system of n individual species the total number of intensive properties is*

$$N = 2n + 2 \tag{6}$$

The number of intensive properties which must be specified to fix the equilibrium state is given by the Gibbs phase rule:

$$\begin{matrix}\text{Number of independent} \\ \text{intensive properties to} \\ \text{fix equilibrium state}\end{matrix} = \begin{matrix}\text{number of} \\ \text{components}\end{matrix} - \begin{matrix}\text{number of} \\ \text{phases}\end{matrix} + 2 \tag{7}$$

For the present investigation the number of phases is two. Therefore, the number of independent intensive properties which need to be specified is equivalent to the number of components present in the system, n. The number of unknowns, L, therefore, becomes

$$L = n + 2 \tag{8}$$

---

†The fugacity represents the intensive potential governing mass transfer between the phases.

*Note that conservation of mass specifies that only n-1 component mole fractions be considered for each phase. The nth mole fraction is specified by the fact that the summation of the mole fractions of each component is unity.

Consequently n + 2 independent equations must be specified in order to solve for the unknown variables. Equations (3) will constitute a system of n equations, where f_{if} and f_{ig} are found for each component of the system. An equation of state, applied once to the liquid phase and once to the vapor phase, will constitute two more equations. Total number of independent equations will, therefore, be n + 2. Simultaneously solving these n + 2 independent equations will completely define all of the independent intensive properties associated with the equilibrium state.

Simultaneously solving n + 2 independent equations, however, represents a large computational effort. For this reason, this investigation employed iterative computer techniques to simultaneously solve the system of independent equations. This involved adapting the Soave equation of state to Starling's [15] multi-purpose vapor-liquid equilibrium computer code.

The main element of Starling's [15] code used in the present calculations was the algorithm for computing bubble points. In this case, the composition of the liquid phase x_i and the temperature of the system is known. It is desired to compute the equilibrium composition of the gas phase, y_i, and the pressure. The method of solution is indicated schematically in Figure 2. The computer program, utilizing the Soave equation of state, is presented in Appendix A.

2.3 Soave Equation of State

The Soave equation of state is similar to the Redlich-Kwong equation of state, however, an additional temperature dependent factor is introduced. The Soave equation of state has the following form [13]

$$p = \frac{RT}{v-b} - \frac{\alpha a}{v(v+b)} \tag{9}$$

Applying Van der Waals one-fluid mixing rules [16], the equation of state may be adapted to multicomponent systems. Applying these mixing rules the parameters of Eq. (9) may be defined as follows:

$$\alpha a = \sum_{i=1}^{n} \sum_{j=1}^{n} x_i x_j \alpha_{ij} a_{ij} \tag{10}$$

$$b = \sum_{i=1}^{n} x_i b_i \tag{11}$$

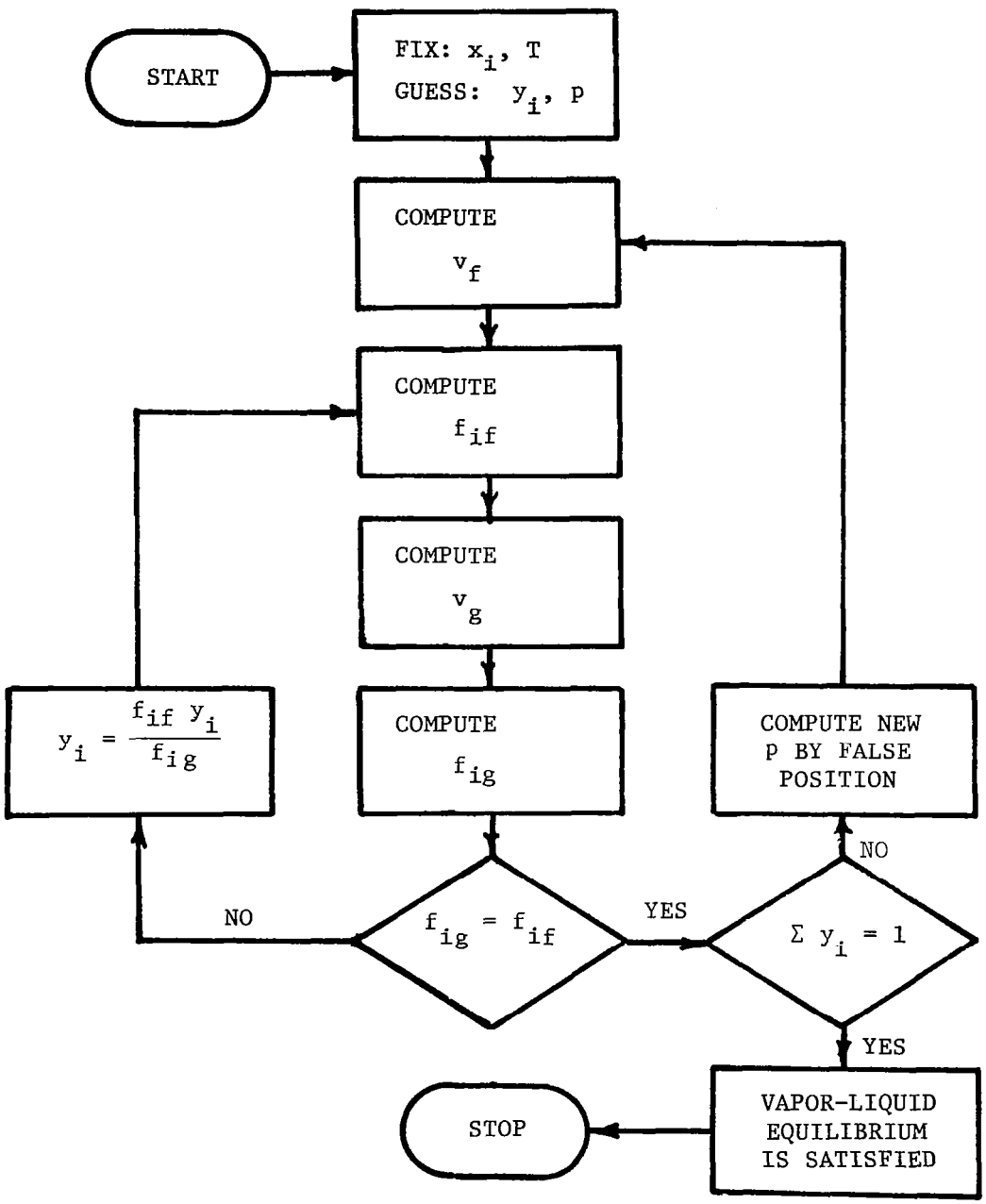

Figure 2. Schematic of bubble-point pressure routine.

where

$$\alpha_{ij}a_{ij} = (1 - k_{ij})(\alpha_i\alpha_j a_i a_j)^{1/2} \tag{12}$$

$$a_i = 0.42747R^2T_{ci}^{\ 2}/p_{ci} \tag{13}$$

$$b_i = 0.08664RT_{ci}/p_{ci} \tag{14}$$

$$\alpha_i = [1 + S_i(1 - T_{ri}^{\ 1/2})]^2 \tag{15}$$

$$S_i = 0.48508 + 1.55171\omega_i - 0.15613\omega_i^{\ 2} \tag{16}$$

where ω_i is the accentric factor of the ith component. It should be noted that Eq. (16) represents a modification of the Soave equation of state due to Grabowski and Daubert [10-11]. Soave's original proposal contained slightly different coefficients than those found in Eq. (16). This correction merely represents a refit of an expanded set of vapor pressure data. The basic form of the regression, however, has remained unaltered.

The constants k_{ij} found in Eq. (12) are the binary interaction coefficients described by Chueh and Prausnitz [17]. These coefficients correct for the effects of deviations from the geometric mean mixing rule for αa and must be determined from data on binary mixtures. To a good approximation the k_{ij} are independent of temperature, pressure, and composition [10]. It is recommneded that the k_{ij} be set equal to zero for interactions between hydrocarbons and interations containing hydrogen [14]. Binary interaction coefficients for interactions between common hydrocarbons and gaseous CO_2, N_2, CO, and O_2 are tabulated in Ref. 14. Analytical correlations are provided for other common hydrocarbon-gas interactions.

Introducing the Soave equation of state into Eq. (5) and integrating yields the following expression for the fugacity coefficient.

$$\ln\phi_i = \frac{b_i}{b}(Z-1) - \ln(Z-B) - \frac{A}{B}\left[\frac{2\Sigma x_i\alpha_{ij}a_{ij}}{\alpha a} - \frac{b_i}{b}\right]\ln\left(1+\frac{B}{Z}\right) \tag{17}$$

where

$$A = \alpha ap/R^2T^2 \tag{18}$$

$$B = bp/RT \tag{19}$$

Due to the appearance of the compressibility factor, Z, in Eq. (17), it is convenient to rewrite the Soave equation of state in terms of the compressibility factor. This may be done by noting:

$$v = Z\frac{RT}{p} \tag{20}$$

Introducing Eqs. (10), (19) and (20) into Eq. (9) yields the following cubic expression:

$$Z^3 - Z^2 + Z(A-B-B^2) - AB = 0 \tag{21}$$

Equation (21) employed twice, once for each phase, and combined with Eq. (17) for each of the n species, will form a set of n + 2 independent equations. The vapor liquid equilibrium state may now be completely specified, assuming that two independent intensive variables have been previously specified. It should be noted that Eq. (21) will yield three roots for each phase. For the vapor phase the greatest root is taken to be the compressibility factor. For the liquid phase the smallest root is taken to be the compressibility factor.

2.4 Enthalpy and Entropy Considerations

Once the system temperature, pressure, density and phase compositions are known, the enthalpy and entropy of departure of each phase may be determined by employing an equation of state in conjunction with the following thermodynamic relations.

$$h - h^o = \int_v^\infty \left[p - T\left(\frac{dp}{dT}\right)_{v,n_T}\right] dv + pv - RT \tag{22}$$

$$s - s^o = \int_v^\infty \left[\frac{R}{v} - \left(\frac{dp}{dT}\right)_{v,n_T}\right] dv + R \sum_i x_i \ln\frac{vp_{ref}}{x_i RT} \tag{23}$$

where h^o and s^o are ideal gas states to be defined later. Substitution of the Soave equation of state into Eqs. (22) and (23) yields

$$h - h^o = \frac{1}{b}\left\{\alpha a - T\left(\frac{d(\alpha a)}{dT}\right)_{v,n_T}\right\} \ln\left(\frac{v}{v+b}\right) + RT(Z-1) \quad (24)$$

$$s - s^o = -R\ln\left(\frac{v}{v-b}\right) - \frac{1}{b}\left(\frac{d(\alpha a)}{dT}\right)_{v,n_T} \ln\left(\frac{v}{v+b}\right) +$$

$$R\sum_i x_i \ln\frac{vp_{ref}}{x_i RT} \quad (25)$$

where

$$\frac{d(\alpha a)}{dT}\Big|_{v,n_T} = \sum_i \sum_j \frac{\beta_{ij}}{2}\left[S_j\left(\frac{\alpha_i}{TT_{cj}}\right)^{1/2} + S_i\left(\frac{\alpha_j}{TT_{ci}}\right)^{1/2}\right] \quad (26)$$

$$\beta_{ij} = x_i x_j (1-k_{ij})(a_i a_j)^{1/2} \quad (27)$$

The ideal gas states for the mixture enthalpy and entropy may be expressed as

$$h^o = \sum_i x_i h_i^o \quad (28)$$

$$s^o = \sum_i x_i s_i^o \quad (29)$$

where the individual component enthalpy and entropy ideal gas states are defined as

$$h^o{}_i(T) = h_i^o\ (T_{ref}) + \int_{T_{ref}}^{T} C^o_{pi}\, dT \quad (30)$$

$$s_i^o(T,p_{ref}) = s_i^o(T_{ref}, p_{ref}) + \int_{T_{ref}}^{T} \frac{C_{pi}^o\, dT}{T} \qquad (31)$$

The reference states defined in Equations (30) and (31) are taken at T_{ref} = 0 K and p_{ref} = 1 atm.

Equations (30) and (31) employed in conjunction with Eqs. (24) through (29) make it possible to determine the absolute enthalpy and entropy of the individual phases existing in equilibrium at a given pressure and temperature.

2.5 Property Considerations

2.5.1 Air Model

Two models were employed to represent the composition of air. The first model considered dry air, having the following composition, on a percent by mole basis: N_2 = 78.0881, O_2 = 20.9495, Ar = 0.9324, and CO_2 = 0.0300. The second model employed simplified air: N_2 = 79 and O_2 = 21 percent, on a molal basis.

2.5.2 Jet A Pseudo-Compound Model

The Soave equation of state requires that the critical pressure, temperature and accentric factor be supplied for each species of a multicomponent system. This information is readily available for most pure substances [14]. Jet A fuels, however, are undefined petroleum fractions. An undefined petroleum fraction must meet standard specifications, but a range of compositions or blends can satisfy these requirements. As a result, the critical pressure, temperature and accentric factor will vary from sample to sample. In order to provide the Soave equation of state with the appropriate component property data, each Jet A fuel sample was modeled as a pseudo-compound (defined by a pseudo-critical temperature, pressure and accentric factor). In addition a pseudo-compound molecular weight was also determined to allow molar to gravimetric unit conversions.

The procedure for creating pseudo-compound models for undefined petroleum fractions is disucssed in detail in the API-Technical Data Book [14]. This procedure only requires that the specific gravity and the characteristic distillation curve of each Jet A fuel sample be provided. The specific gravity and characteristic distillation curves of the two Jet A fuel samples considered in this investigation are shown in Table 1. The subsequent pseudo-properties derived from the API pseudo-compound procedure are shown in Table 2, along with the properties of other pure components considered during this investigation.

Table 1

DISTILLATION CHARACTERISTICS AND SPECIFIC GRAVITY OF JET A 79/80 FUELS

Distilled (%)	Temperature (K)	
	Jet A (79)	Jet A (80)
IBP	434.82	444.26
10	460.93	465.37
30	472.04	477.04
50	488.15	487.59
70	509.82	500.93
90	552.04	522.04
FBP	600.93	547.59
Specific Gravity (60/60°F)	0.8381	0.8095

Table 2

CRITICAL PROPERTY CONSTANTS[a]

Substance	Molecular Weight	T_c (K)	p_c (MPa)	ω
n-Pentane	72.151	469.6	3.37	0.251
n-Hexane	86.178	507.4	2.97	0.296
n-Decane	142.286	617.6	2.11	0.490
n-Dodecane	170.33	628.26	1.82	0.5623
n-Tridecane	184.35	675.76	1.72	0.6231
Jet A[b]	170.1	655.93	1.83	0.4780
Jet A (79)[c]	187.1	677.59	2.34	0.4950
Jet A (80)[c]	200.0	669.26	2.14	0.4950
Nitrogen	28.02	126.26	3.40	0.0450
Oxygen	32.0	154.76	5.08	0.0190
Carbon Dioxide	44.01	304.21	7.38	0.2310
Argon	39.4	150.71	4.86	-0.002

[a]Taken from Ref. 14, unless noted otherwise.

[b]Taken from Ref. 18.

[c]Computed during this investigation.

2.5.3 Ideal Gas Thermal Property Constants

In order to determine the absolute enthalpy and entropy of multicomponent systems, the enthalpy and entropy at ideal gas states must be determined for each component. These individual component ideal gas states are defined in Eqs. (30) and (31). In order to determine these properties the ideal gas isobaric specific heat of the individual component is required. A functional relationship between the isobaric specific heat and absolute temperature is required to properly evaluate the integrals in Eqs. (30) and (31). The API-Technical Data Book [14] suggests the following functional relationship.

$$C^o_{pi} = C_1 + 2\,C_2T + 3\,C_3T^2 + 4\,C_4T^3 + 5\,C_5T^4 \qquad (32)$$

Integrating Eqs. (30) and (31), and consolidating reference states into one constant, yields the following expressions

$$h^o_i = C_o + C_1T + C_2T^2 + C_3T^3 + C_4T^4 + C_5T^5 \qquad (33)$$

$$s^o_i = C_1 \ln T + 2\,C_2T + \frac{3}{2}\,C_3T^2 + \frac{4}{3}\,C_4T^3 + \frac{5}{4}\,C_5T^4 + C_6 \qquad (34)$$

The constants C_i are tabulated in reference [14] for most common substances. Jet A fuels being undefined petroleum fractions are not listed. In addition there is no method available for modeling the ideal gas properties of a Jet A fuel. As a result, the only recourse was to curve fit available ideal gas isobatic specific heat, enthalpy and entropy property data of a typical Jet A fuel. This was done using data supplied by Faith, et al. [18]. Though this data does not specifically represent the two Jet A fuel samples evaluated in this investigation, it will provide reasonable estimates of their actual ideal gas enthalpies and entropies. The curve-fitted Jet A constants, along with other pure component constants used in this investigation, are summarized in Table 3.

3. Gas Solubility Apparatus

3.1 Test Apparatus

High pressure multicomponent phase equilibria experimental studies [19-21] frequently employ gas chromatograph and absorption techniques to determine the gas phase compositions of simple binary and ternary systems. These techniques are less appropriate for the present investigation for two reasons: 1) this investigation is specifically concerned with determining liquid phase compositions as opposed to gas

Table 3

THERMAL PROPERTY CONSTANTS OF IDEAL GASES

Species	$C_0^{\bullet a}$ (kJ/kg)	C_1 (kJ/kg-K)	$C_2 \times 10^3$ (kJ/kg-K^2)	$C_3 \times 10^7$ (kJ/kg-K^3)	$C_4 \times 10^{10}$ (kJ/kg-K^4)	$C_5 \times 10^{14}$ (kJ/kg-K^4)	C_6 (kJ/kg-K)
n-Dodecane	60.966342	-0.077547	3.420590	-13.085368	2.475715	-1.303777	2.272586
Jet A[c]	76.221709	0.127624	3.149567	-11.201976	1.766033	-0.168140	-1.204104
Nitrogen	-2.172470	1.068470	-0.134094	2.155655	-0.786305	0.698494	0.177362
Oxygen	-2.283534	0.952422	-0.281135	6.552125	-4.523085	10.877250	0.520469
Carbon Dioxide	11.113553	0.479100	0.762146	-3.593857	0.847424	-0.577511	1.437543

[a]Datum state, $h^o = 0$ at 0 K.

[b]Datum state, $s^o = 0$ at 0 K and 1 atm.

[c]For formulation studied in Ref. 14.

phase compositions, 2) the varying and complex nature of the undefined petroleum fraction Jet A, makes gas chromatograph and absorption techniques extremely complex. As a result, a new liquid phase gas solubility measuring apparatus was developed for the investigation. This new apparatus was specifically designed to determine the extent to which gases may be dissolved in liquid fuels.

A sketch of the gas solubility apparatus appears in Figure 3. The arrangement consists of a sample preparation chamber and a gas-liquid volume measuring system. The sample preparation chamber has a volume of 1000 ml. The chamber can be pressurized with air or nitrogen. The chamber pressure level is determined with Heisse, absolute pressure gauges (0.1% accuracy, 0-2.1 and 0.10.3 MPa ranges, using two gauges.) The chamber is wrapped with electrical heating coils and insulated to allow a range of sample temperatures. Chamber temperatures are measured with several chromel-alumel thermocouples spot-welded to the outer surface. The liquid sample within the chamber has a volume of approximately 500 ml. The sample is equilibrated by shaking the chamber. Samples are withdrawn from the chamber through a 3.2 mm OD x 0.89 mm wall thickness tube. The sampling tube ends at roughly the center of the liquid sample.

The gas-liquid volume measuring system consists of a vertical glass tube 9.5 mm OD x 1 mm wall thickness, 760 mm long. The tube diameter is reduced at top and bottom to facilitate the connection to flexible Tygon tubing. The lower end of the glass tube is connected to a mercury filled bottle which can be moved vertically to adjust the mercury level in the glass tube. The upper end of the tube can be connected to the valve at the exit of the sampling tube.

3.2 Operation of the Apparatus

The operation of the apparatus proceeds as follows. The liquid sample was set at the desired pressure and temperature level and agitated with the gas-liquid measuring system not connected to the sample tube. Trials indicated that an agitation period of 250-300 s was adequate to achieve equilibration.

Once equilibration was achieved, the sample valve was opened, and the sample line was purged, and the valve was closed once again. The gas-liquid volume measuring system was purged of any earlier sample by raising the mercury column to the top of the Tygon tubing (at the top of the glass tube). The tubing was then connected to the sampling valve. The seal of this connection was checked by dropping the mercury column, which places the upper end of the tube under vacuum. A poor seal was readily detected by subsequent motion of the mercury column. If the seal was adequate, the mercury level was returned to its original position and the sample valve was opened. A sample was withdrawn until the mercury level neared the bottom of the tube and then the valve was closed once again.

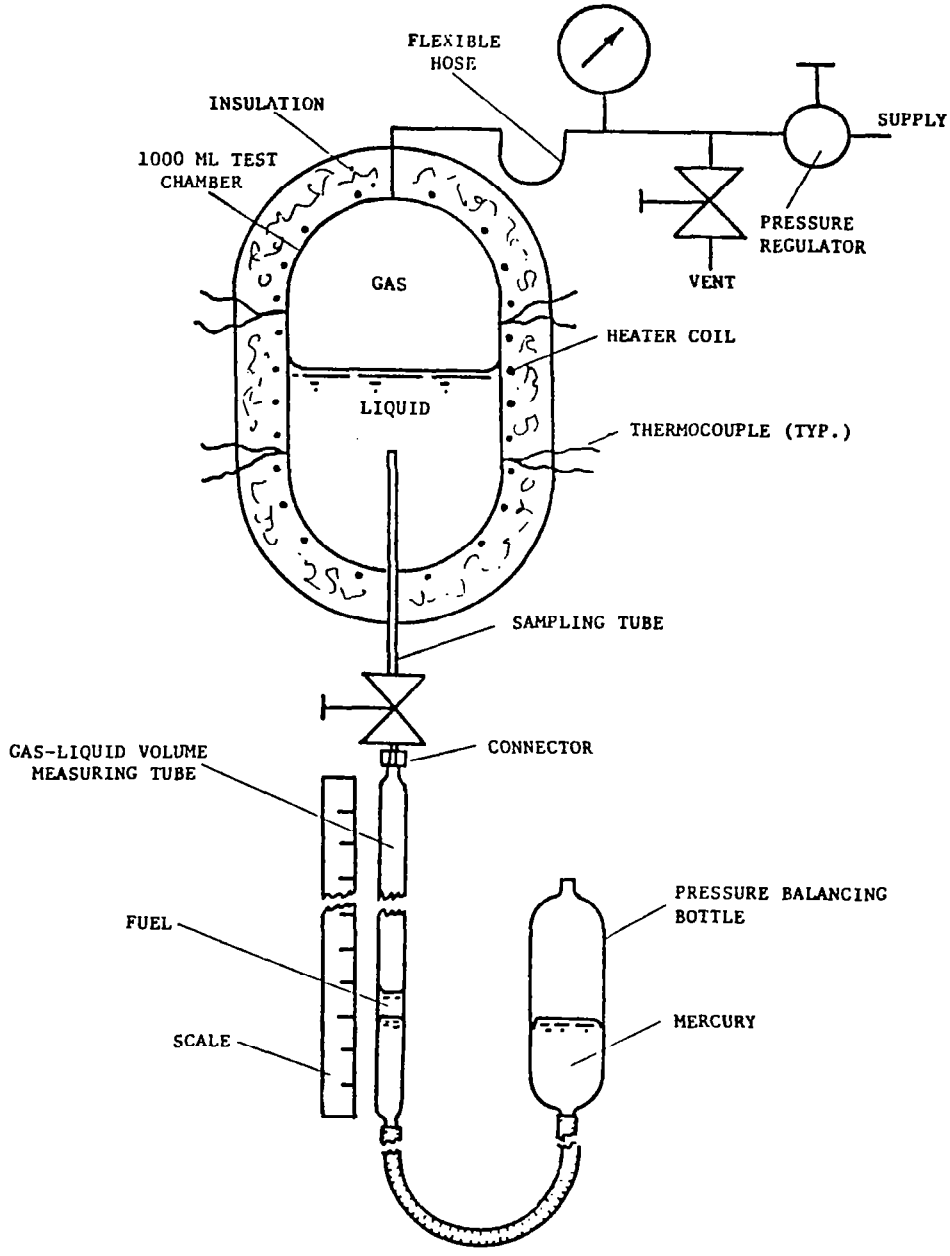

Figure 3. Gas solubility apparatus.

The depressurized sample rapidly separates into gas and liquid phases. The sample was allowed to separate and cool to room temperature conditions. The sample was brought to room pressure by equilizing the mercury levels in the bottle and the sample tube. The volume of liquid and gas was then read from the scale on the sample tube. The gas volume was corrected for the small volume in the Tygon tubing and the sampling valve. The ullage volume was determined by measuring the variation of pressure with scale volume when no sample was present.

The dissolved gas concentration of the test liquids, at atmospheric pressure, is negligible. The vapor pressure of the liquids is also small at room temperature. Therefore, measurement of the gas and liquid volumes in the depressurized sample provides sufficient information to compute the concentration of dissolved gas in the original sample. For this computation the gas phase is assumed to be ideal, which is justified at atmospheric pressure.

From these assumptions, the ratio of the heights of the gas and liquid portions of the sample are as follows

$$H_g/H_f = x_g \rho_f RT/(p x_f M_f) \tag{35}$$

where p and T are the pressure and temperature in the sample tube and x_g and x_f denote the original mole fractions of gas and liquid in the saturated liquid mixture. Noting that $x_f = 1 - x_g$, Eq. (35) can be rewritten as

$$x_g = \left[1 + \frac{\rho_f RTH_f}{pM_f H_g}\right]^{-1} \tag{36}$$

The properties required in Eq. (36) are summarized in Tables 1 and 2. The temperature, pressure and the heights of both phases in the sample tube are measured, yielding x_g immediately from Eq. (36).

4. Solubility Results and Discussion

4.1 Present Experiments

Prior to making solubility predictions, it is necessary to prescribe the binary interaction coefficients, k_{ij}, of all pairs of species to be considered. Values are available in the literature for dodecane [14]. Similar results are not available for the Jet A fuels, therefore, these values were chosen to provide a good match of the present measurements and the predictions. It was found that adequate results were obtained using the literature values for n-tridecane. This is reasonable, since the molecular weight and pseudocritical

properties of Jet A fuels and n-tridecane are similar. All the binary interaction coefficients employed in the computations are summarized in Table 4. The solubility data obtained during the present investigation are summarized in Appendix B.

Predicted and measured solubilities of nitrogen and air in dodecane are illustrated in Figures 4 and 5, respectively. These are plots of the mole fractions of nitrogen and air dissolved in the liquid phase as a function of total pressure, with system temperature as a parameter. The predictions shown are for dry air, results with the approximate air composition are similar. The comparison between predictions and measurements is reasonably good. The average discrepancy between predicted and measured pressures was 5%, for a given liquid phase composition and pressure.

The results, illustrated in Figures 4 and 5, show a nearly linear increase in solubility with increasing pressure. Increasing the temperature also increases the solubility, however, this effect is not large for the present range of test conditions. Comparing the solubility of nitrogen and air in n-dodecane, indicates that air is roughly 15% more soluble than nitrogen. The amount of air dissolved in dodecane was not large for these test conditions, reaching a maximum mole fraction of 0.158 (mass fraction of 0.031) at 373.15K and 10.34 MPa.

Solubility results for Jet A (79) - nitrogen and air systems are illustrated in Figures 6 and 7, respectively. Similar results for Jet A (80) appear in Figures 8 and 9. As before, the predictions are for dry air although the simplified air results are essentially the same. The comparison between predictions and measurements for the Jet A fuels is not as satisfactory as the results for n-dodecane. The greatest discrepancy between predictions and measurements occurs at high pressures, where the error reaches roughly 20 percent. An improved correlation of the data could be obtained by further adjustment of the binary interaction coefficients. This tends to shift the predicted curves up or down, without changing the slope, and would result in reduced maximum errors over the present test range. The use of a series of narrow-cut pseudo-compounds could also be employed to represent the mixture more accurately. This would modify the slope of the solubility prediction. Since Jet A formulations vary, however, it was felt that this level of fitting was unnecessarily accurate for present applications.

The general behavior of the solubility properties of the Jet A fuels, illustrated in Figures 6-9, is similar to dodecane. Solubility increases in roughly a linear fashion with increasing pressure, and is a relatively weak function of temperature over the present test range. The solubility properties of the two Jet A samples are also similar. Maximum solubilities were observed at the maximum temperature and pressure of the tests, 373.15K and 10.34 MPa. At this condition, the mole fractions of air in Jet A (79) and (80) were 0.131 and 0.154, respectively (mass fractions of 0.0227 and 0.0267, respectively).

Table 4

BINARY INTERACTION COEFFICIENTS

	Nitrogen	Oxygen	Carbon Dioxide	Argon
n-Pentane	--	--	0.1278	--
n-Hexane	0.1444	--	--	--
n-Decane	0.1293	--	--	--
n-Dodecane	0.1595	0.1595	0.1389	0.0
n-Tridecane	0.1614	0.1614	0.1387	0.0
Jet A	0.1595	0.1595	0.1389	0.0
Jet A (79)	0.1614	0.1614	0.1387	0.0
Jet A (80)	0.1614	0.1614	0.1387	0.0
Nitrogen	0.0	0.0	-0.0220	0.0
Oxygen	0.0	0.0	0.0	0.0
Carbon Dioxide	-0.0220	0.0	0.0	0.0
Argon	0.0	0.0	0.0	0.0

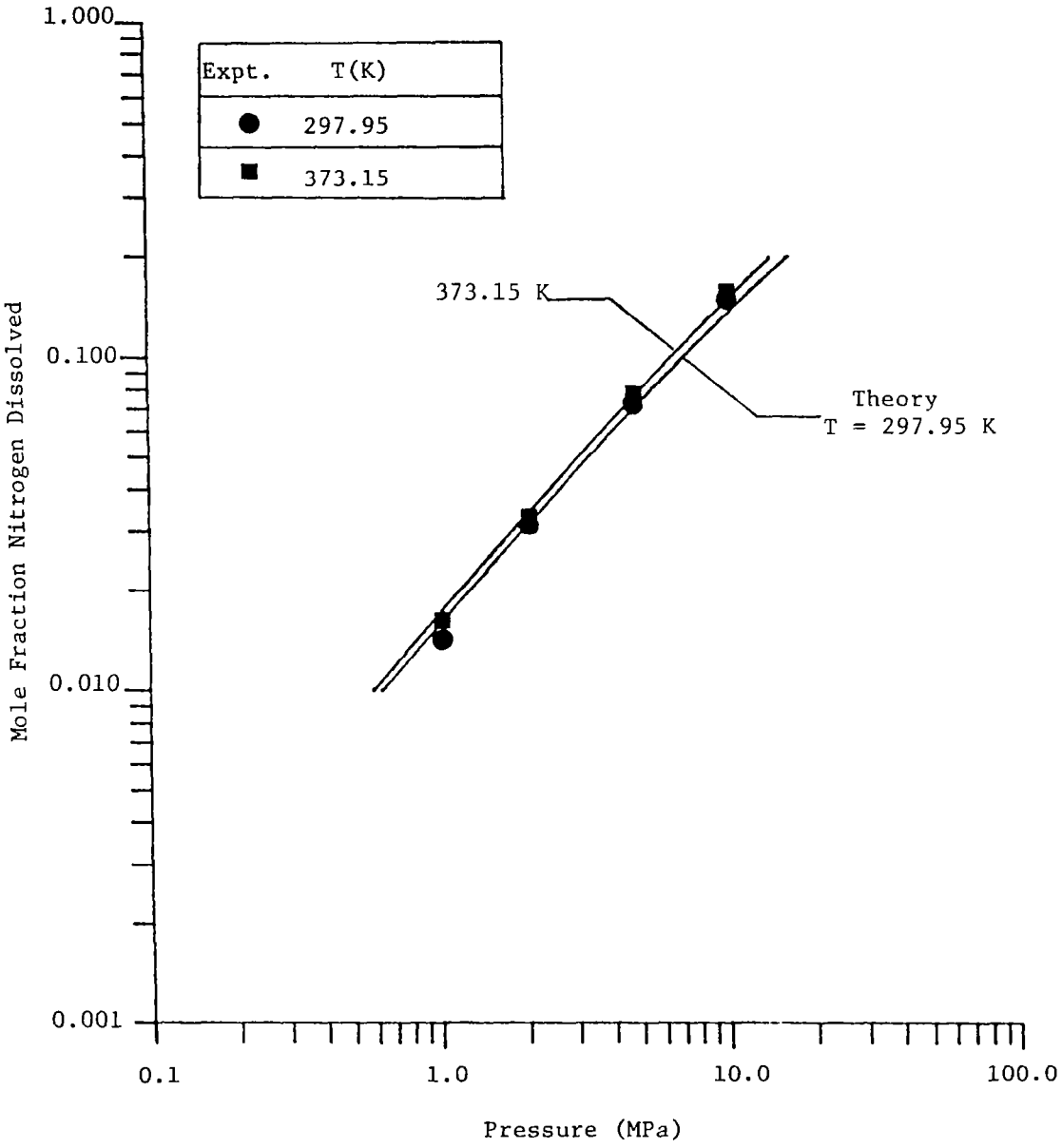

Figure 4. Solubility characteristics of n-dodecane - nitrogen system.

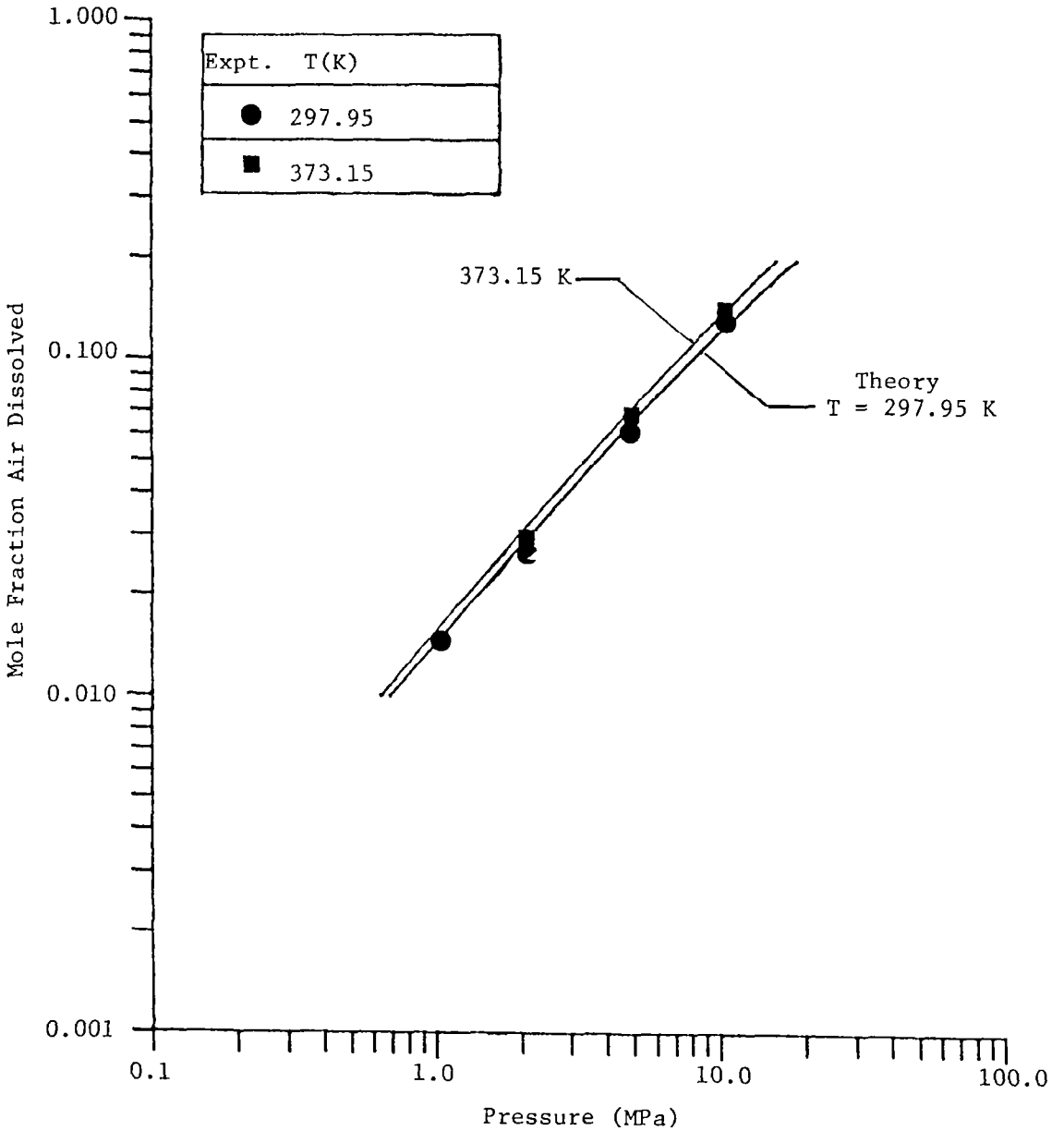

Figure 5. Solubility characteristics of n-dodecane - air system.

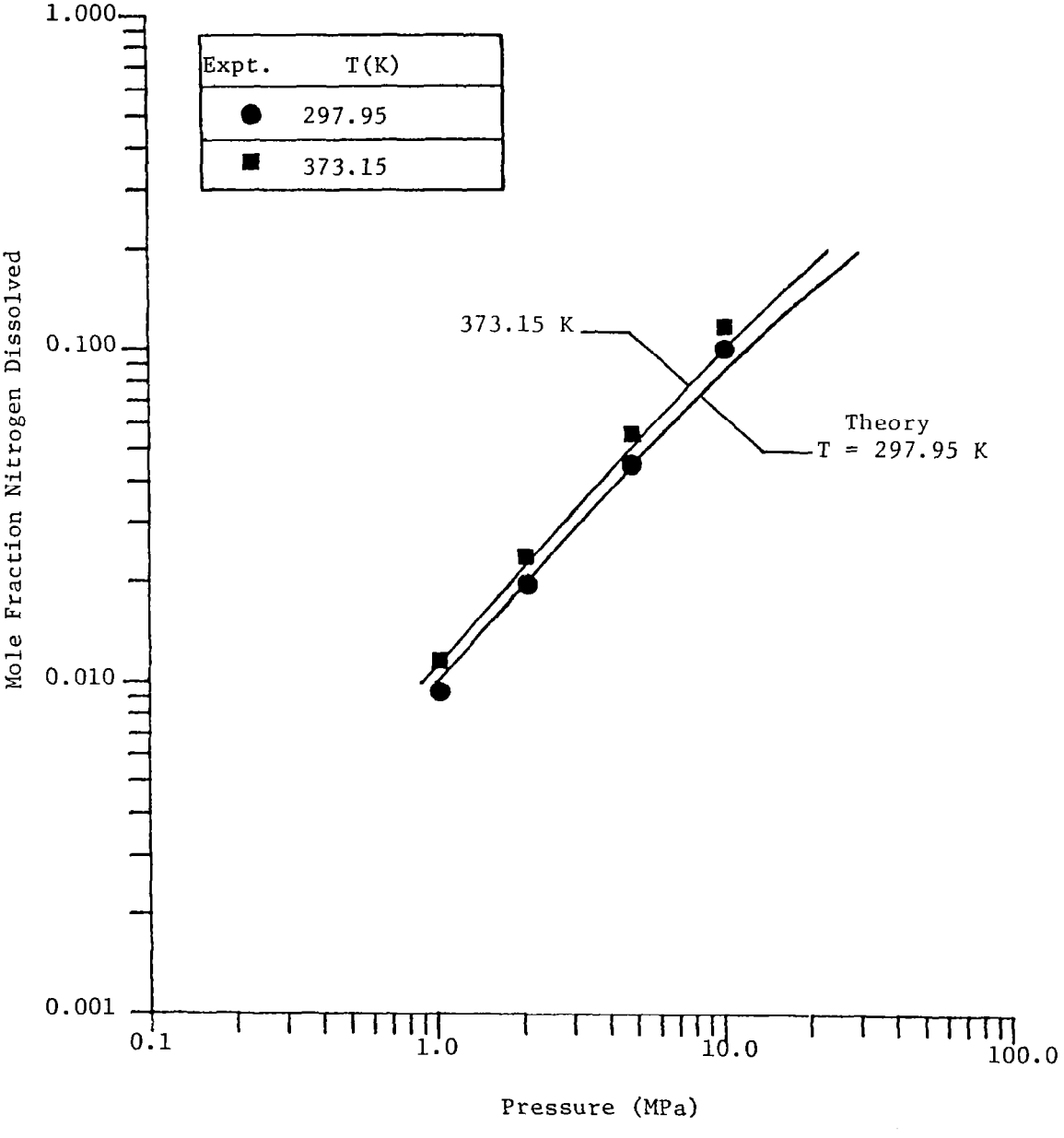

Figure 6. Solubility characteristics of Jet A (79) - nitrogen system.

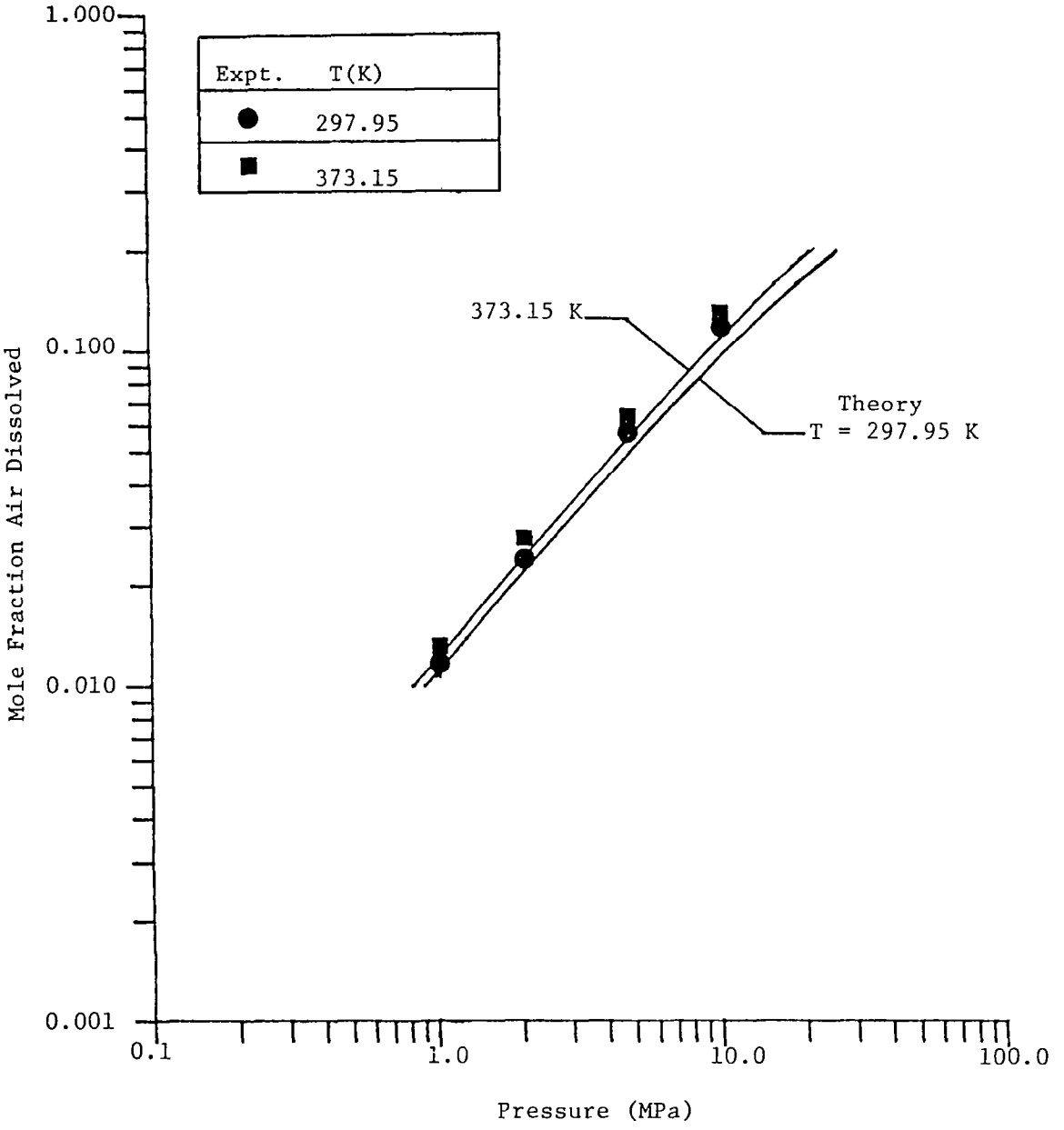

Figure 7. Solubility characteristics of Jet A (79) - air system.

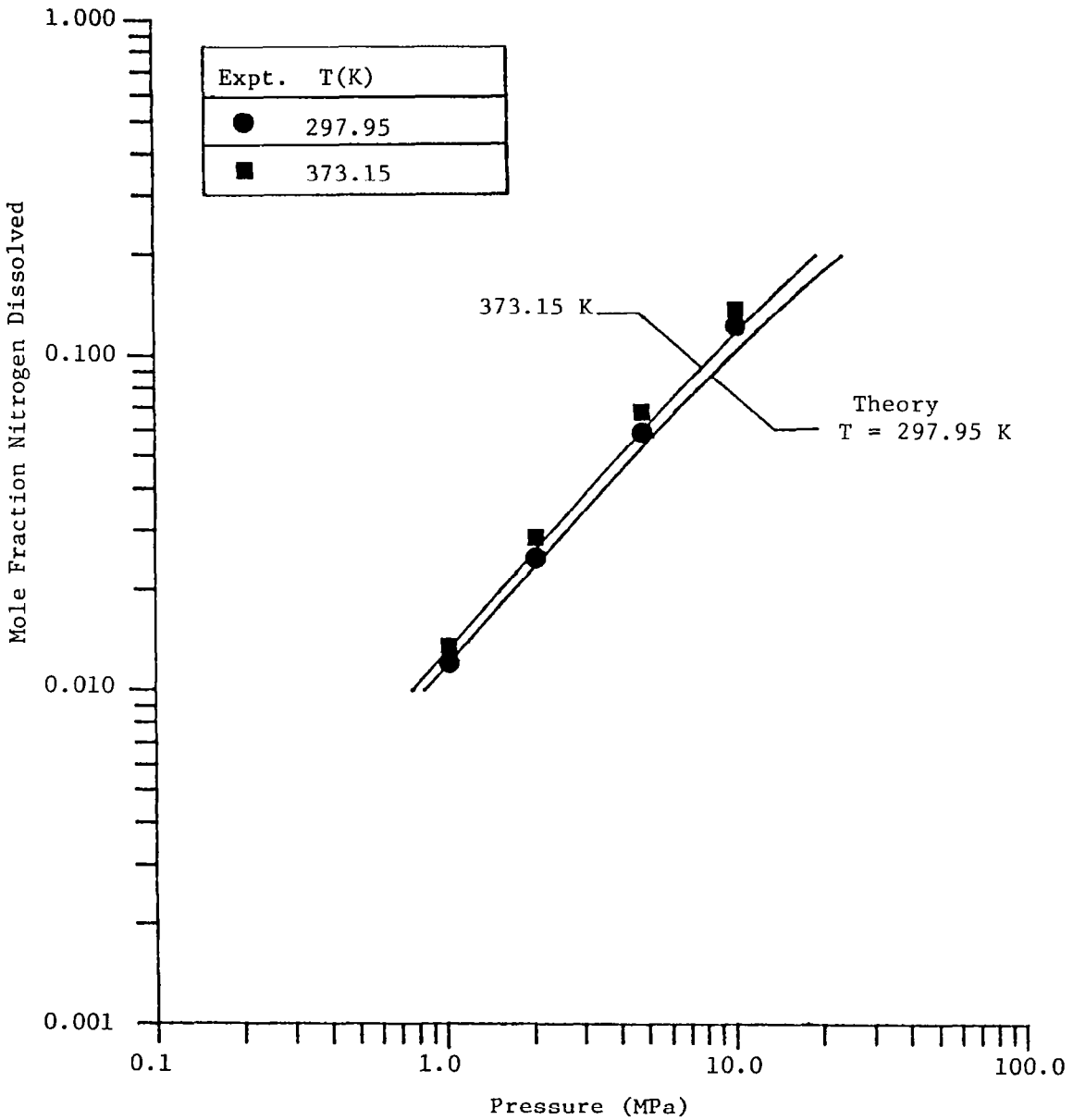

Figure 8. Solubility characteristics of Jet A (80) - nitrogen system.

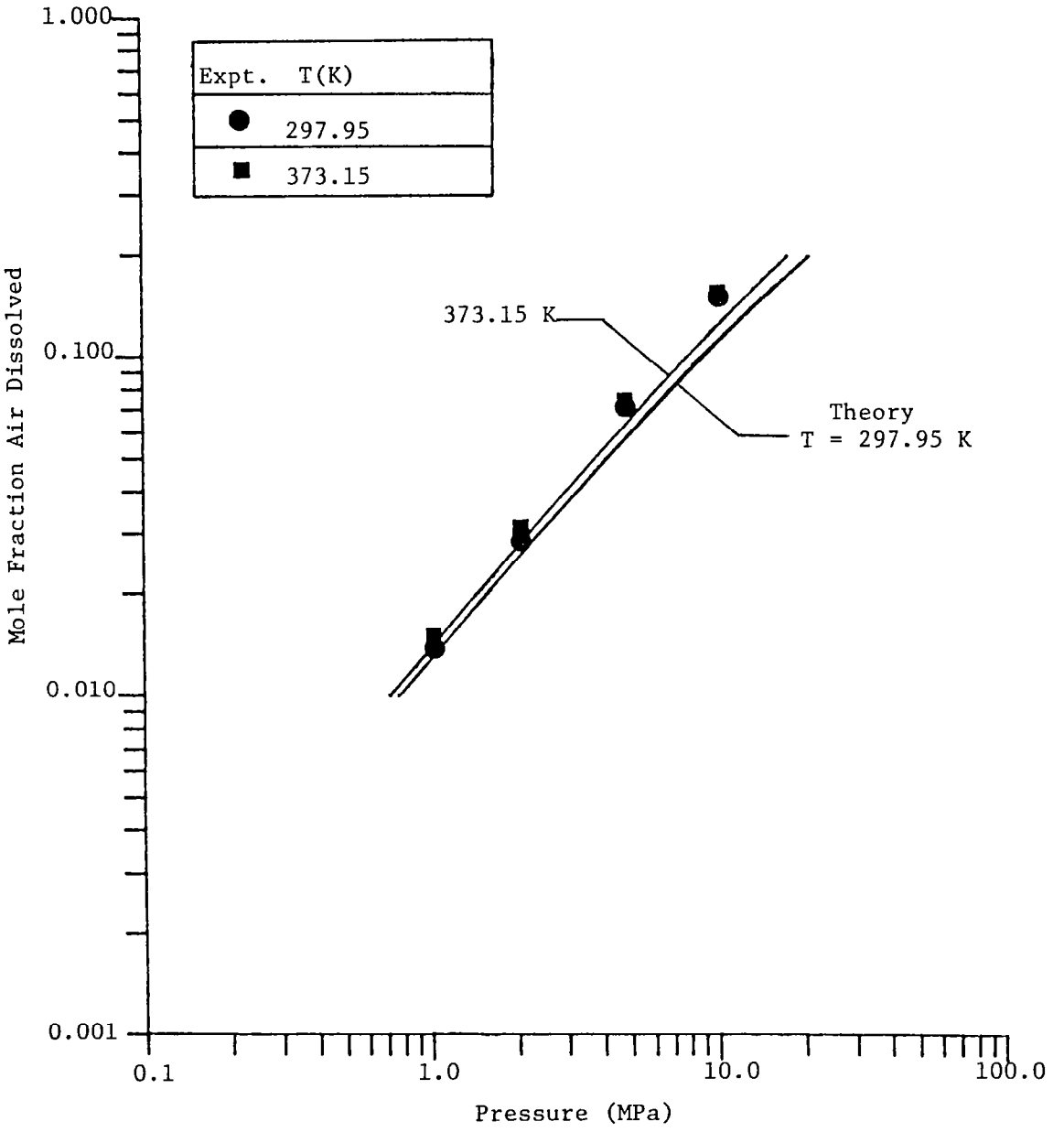

Figure 9. Solubility characteristics of Jet A (80) - air system.

4.2 Near-Critical Point Results

In addition to comparing the predictions of the Soave equation of state with the present measurements, earlier results discussed by Lazar [22] were also considered. This includes solubility measurements for the n-decane - nitrogen system [23], the n-hexane - nitrogen system [24], and the n-pentane - carbon dioxide system [25]. Solubility predictions for these cases are presented by Lazar [22], using the Redlich-Kwong equation of state.

Figure 10 is an illustration of the results for the n-decane - nitrogen system. This is a plot of equilibrium gas and liquid phase composition as a function of pressure, for a constant temperature. Liquid conditions are given by the curves on the left hand side of the figure. In addition to the measurements, predictions are shown for both the Redlich-Kwong and Soave equations of state. The comparison between both predictions and the measurements is seen to be excellent.

Figures 11 and 12 are illustrations of similar results for the n-hexane - nitrogen system at two different temperatures. As before, the liquid phase properties are represented by the curves at the left hand sides of the figures. In these cases, the liquid and gas phase carves are joined at high pressures. The point where they meet is the thermodynamic critical point for the system, at the given temperature. The Redlich-Kwong equation of state is in reasonably good agreement with the measurements over the complete range of the data. The Soave equation gives more accurate results than the Redlich-Kwong equation for conditions not too near the thermodynamic critical point. However, the Soave equation of state is not very satisfactory near the thermodynamic critical point.

A similar trend was noted for the n-pentane - carbon dioxide system. These results are illustrated in Figures 13 and 14. From these findings we conclude that the Soave equation can best be applied at moderate pressures, not too near the critical point of the mixture. The Redlich-Kwong equation of state provides a reasonable prediction over the entire test range, and is clearly superior for predictions of critical conditions, and properties near the critical point.

4.3 Predicted Results

Desirable levels of dissolved gas concentrations for the supercritical injection concept are not known at this time. Since present test conditions did not result in large quantities of dissolved gas, additional solubility computations were completed in order to investigate required injector inlet conditions for various dissolved gas levels. These computations employed the Soave equation of state and either nitrogen or the simplified air composition.

Figure 15 is an illustration of the predicted solubility properties of the Jet A (79) - nitrogen system. The concentrations of the gas (right hand curve) and liquid (left hand curve) phases are plotted as

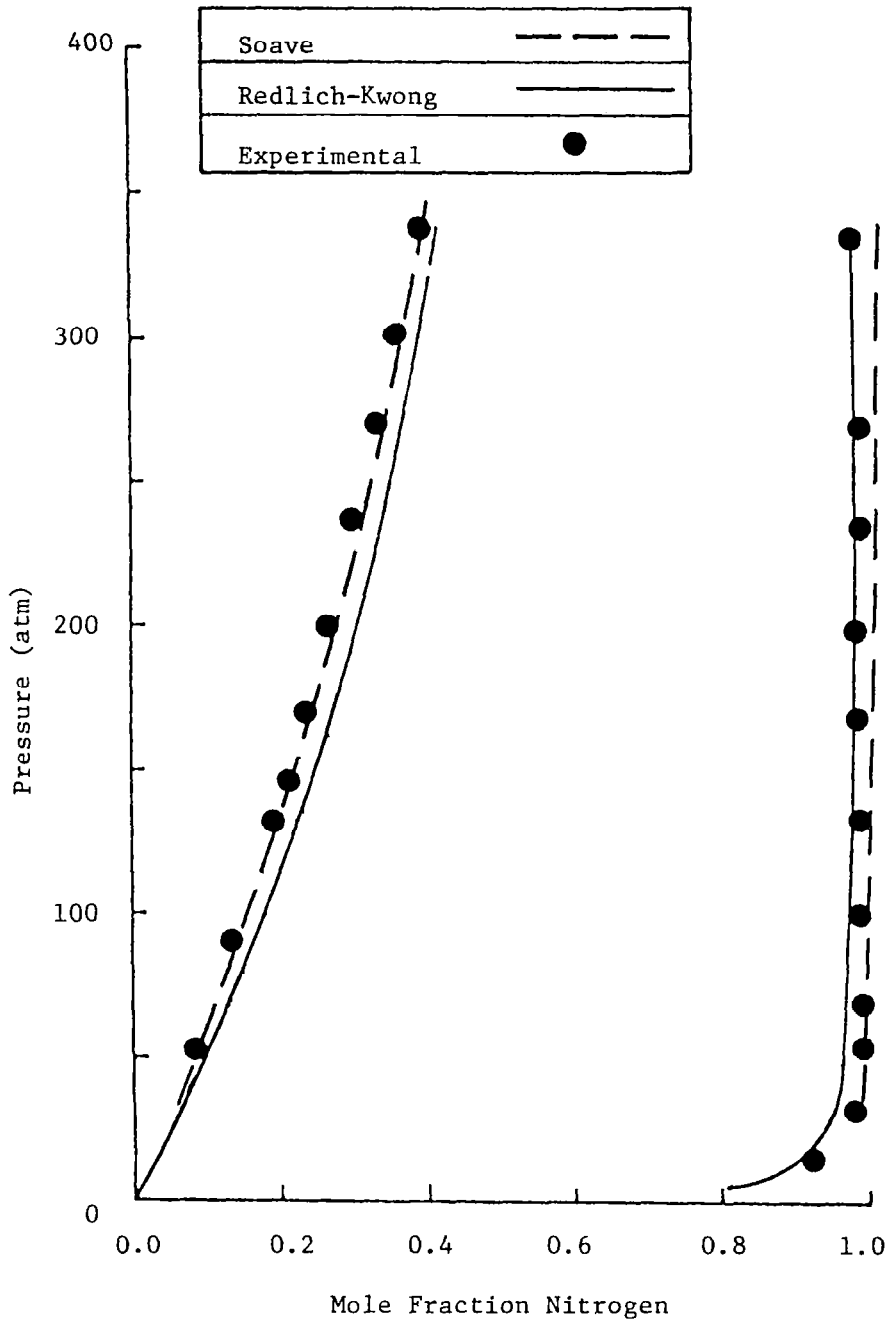

Figure 10. Phase equilibrium for the n-decane - nitrogen system at 411.1K; data from Ref. 23.

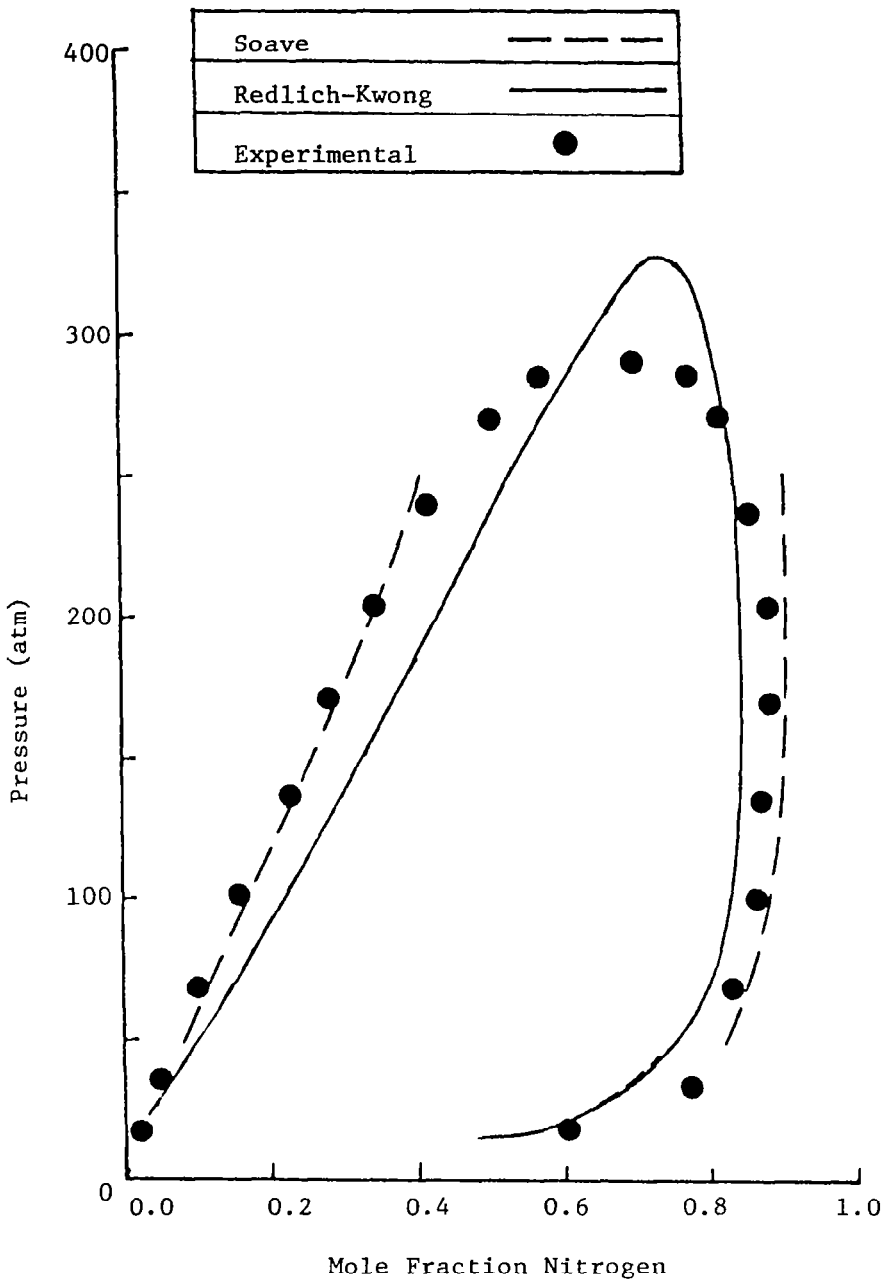

Figure 11. Phase equilibrium for the n-hexane - nitrogen system at 410.8 K; data from Ref. 24.

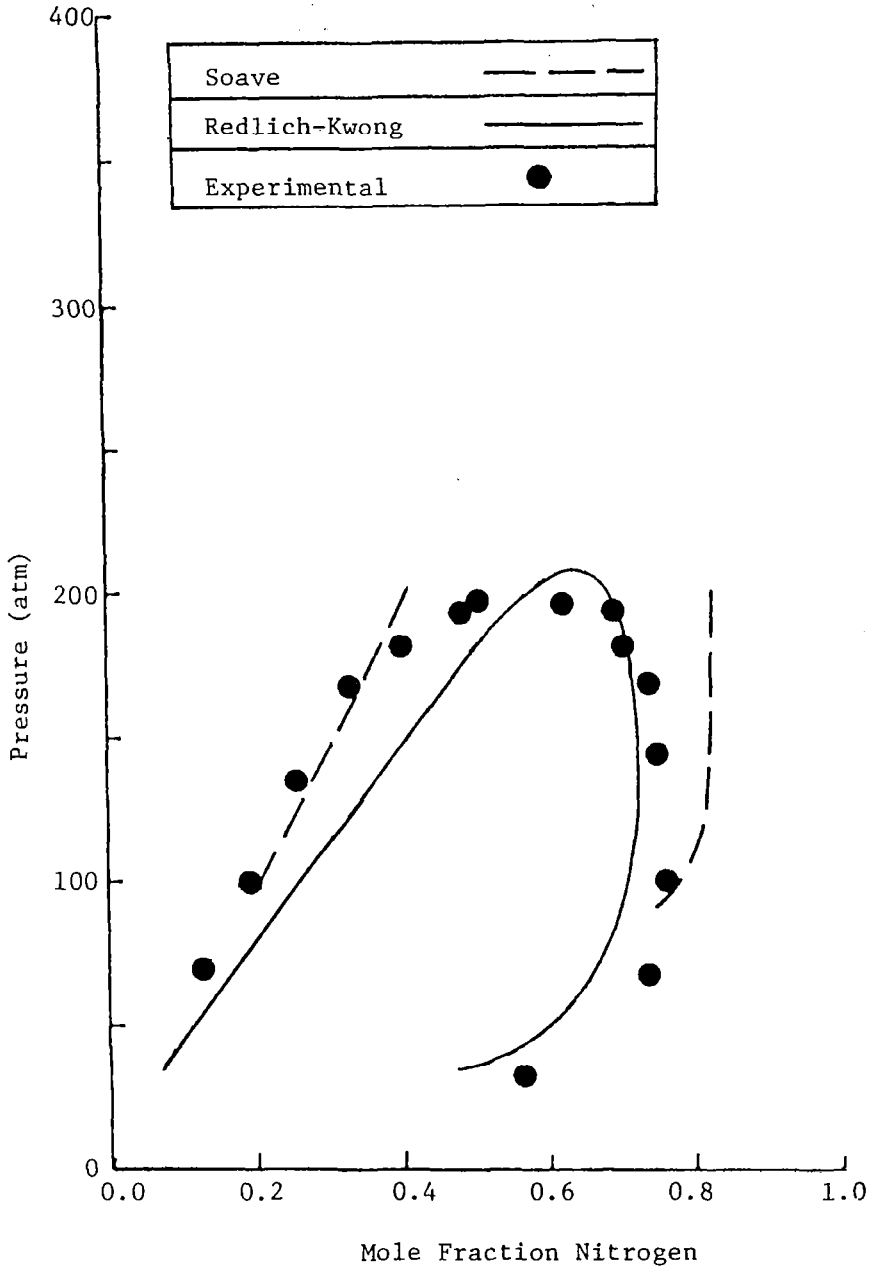

Figure 12. Phase equilibrium for the n-hexane - nitrogen system at 444.1K; data from Ref. 24.

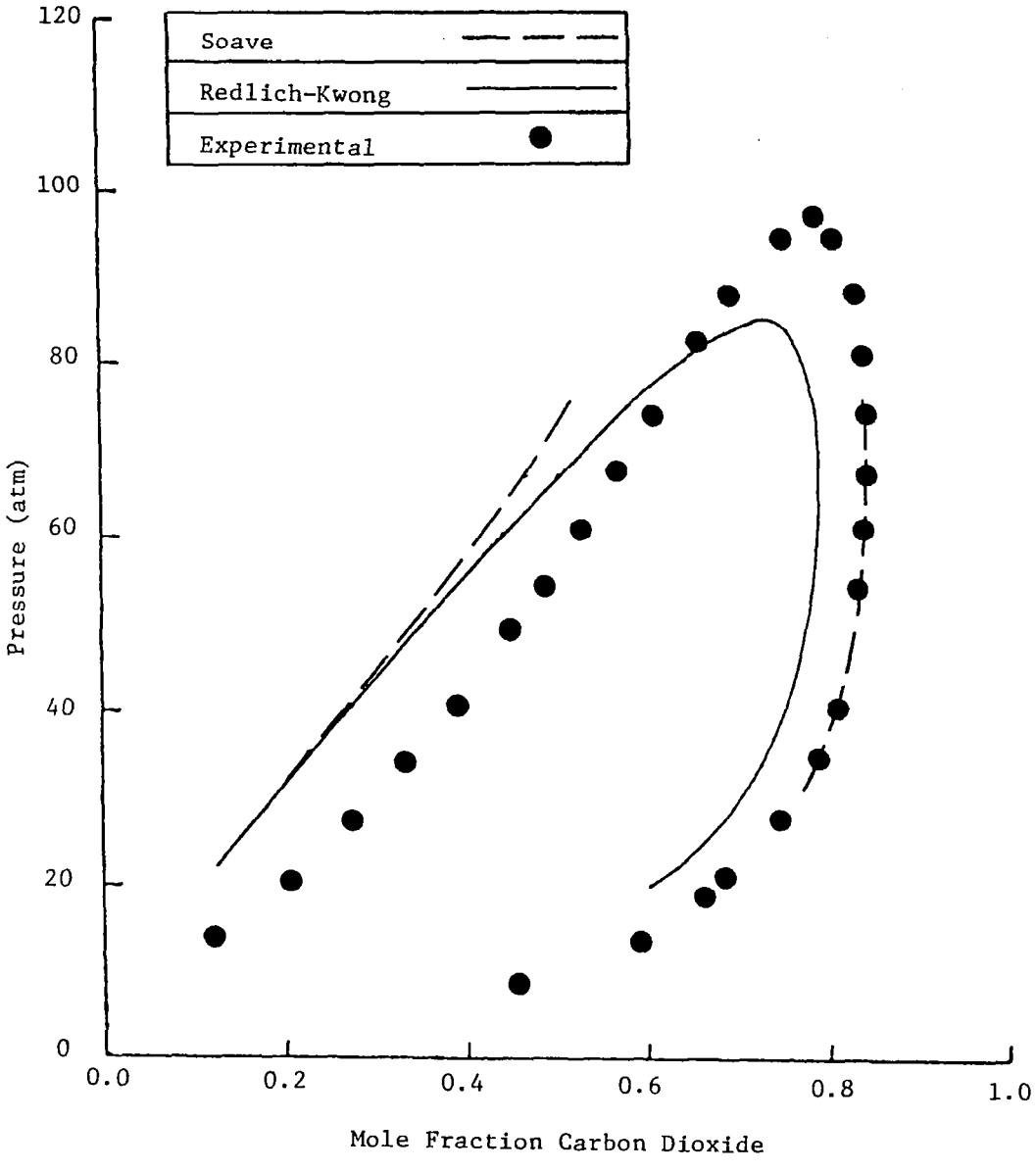

Figure 13. Phase equilibrium for the n-pentane - carbon dioxide system at 366.7 K; data from Ref. 25.

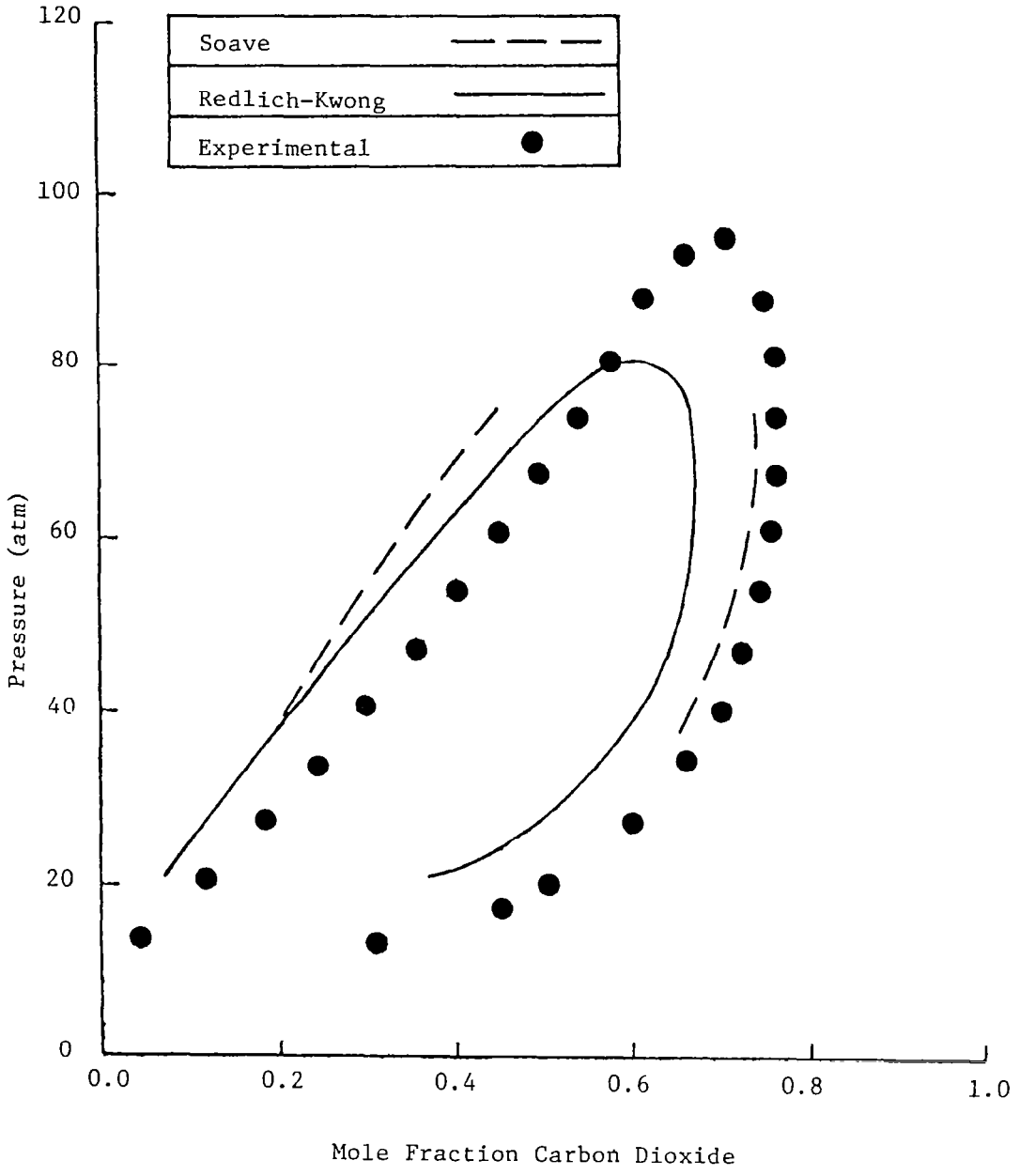

Figure 14. Phase equilibrium for the n-pentane - carbon dioxide system at 394.4K; data from Ref. 25.

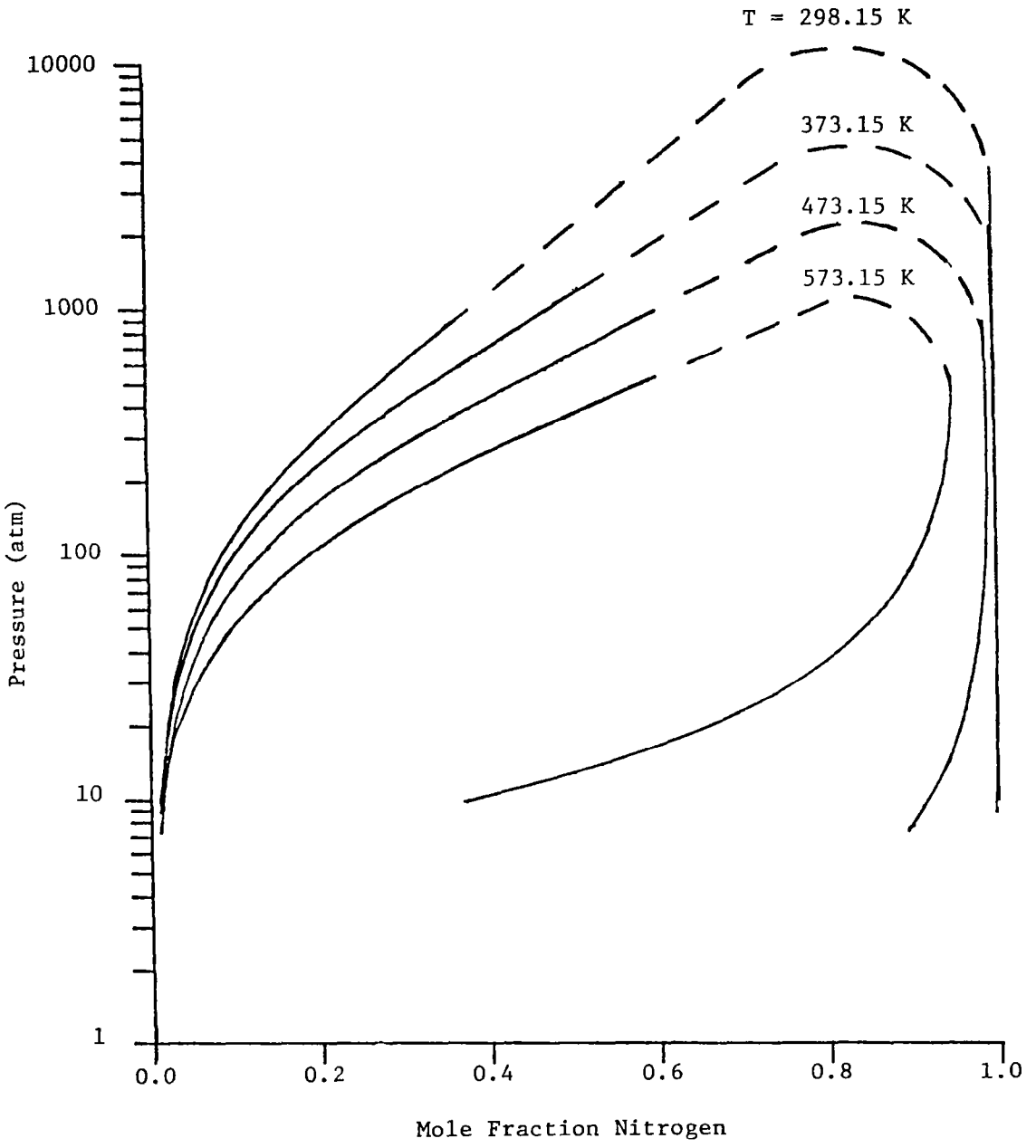

Figure 15. Predicted phase equilibrium for the Jet A (79) - nitrogen system.

a function of pressure, with temperature as a parameter. As before, both curves meet at the thermodynamic critical point where the temperature, pressure and concentrations of both phases are the same. The Soave equation of state is not very accurate near the critical point, as noted earlier, and the computational algorithm was not very stable in this region. Therefore, near-critical conditions were estimated, and are indicated by a dashed line.

The results illustrated in Figure 15 indicate that dissolved gas concentrations in the liquid phase increase as both the temperature and pressure of the system are increased. Maximum dissolved gas levels approach a mole fraction of 0.8 (estimated) at the critical point; however, such conditions require very high pressures. For pressures on the order of 100 atm, relatively high dissolved gas levels can still be achieved (mole fractions of 0.2-0.6) if temperatures on the order of 300°C can be employed.

Figure 16 is an illustration of similar results for the Jet A (79) - air system. These computations employed the simplified air composition; however, results for dry air were similar. Air solubilities in Jet A (79) are only slightly higher than nitrogen solubilities. This trend generally agrees with the present experimental results, described earlier.

5. Apparatus for Density Measurements

5.1 Available Test Methods

There are a variety of techniques available for measuring fluid densities. The most straight forward technique is the pycrometric method, which involves a direct weighing of the fluid sample in a vessel of known mass and volume. Another widely used technique is the hygrometric method, which involves determining the specific gravity of the fluid by employing a precalibrated float. The specific gravity of the fluid is directly proportional to the volume of fluid displaced by the precalibrated float. Both of these methods are only practical when dealing with fluids existing at atmospheric conditions. Jet A fuel-dissolved gas systems, however, require that density measurements be made in a high pressure environment. Therefore, these two methods were not convenient for this investigation.

The expansion technique is another common method for measuring fluid densities. This involves expanding a small known volume of fluid into a large precalibrated volume which is held at a known temperature. Measuring the pressure of the expanded fluid and employing an equation of state allows for the determination of the fluid density. Two aspects of this technique make it impractical for use in this investigation. First, a well proven equation of state must be employed. One of the objectives of this segment of the investigation is to gain further confidence in the Soave equation of state. Second, upon expansion, a portion of the saturated liquid jet fuel-dissolved gas system would flash

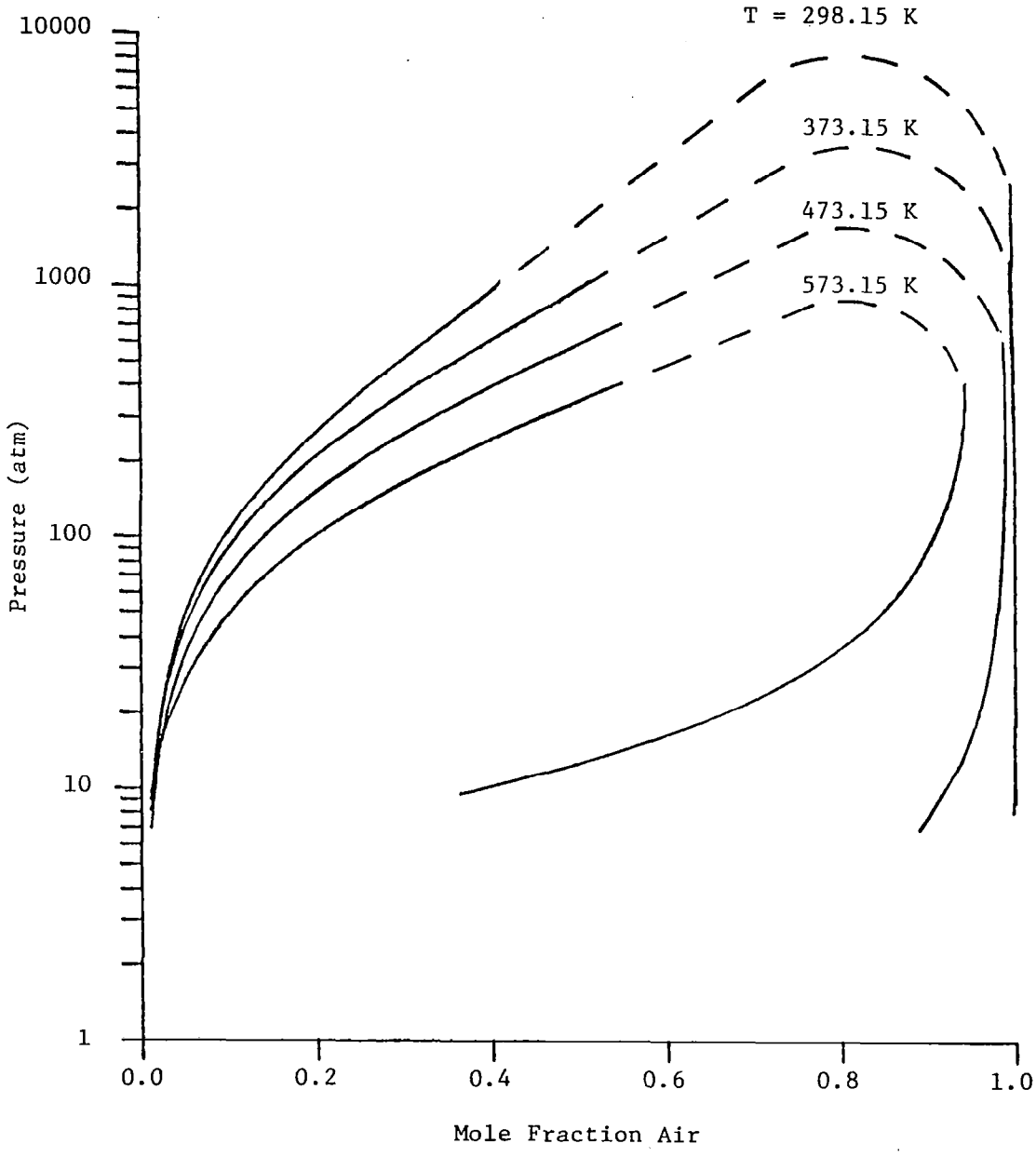

Figure 16. Predicted phase equilibrium for the Jet A (79) - air system.

to a vapor. The expansion chamber would then contain a two-phase system as opposed to the desired single-phase saturated liquid.

A fourth approach employs the principle of buoyancy. This method measures the density of the fluid by completely immersing a float of known mass and volume into the fluid, and subsequently measuring its apparent weight. Electromagnetic and magnetic balancing of a ferromagnetic float have been used for the measurement of the apparent weight. Both of these methods require the use of a transparent pressure vessel, a sight glass, or an auxiliary device for determining the position of the float or balance beam. As a result of the high pressure environment associated with the saturated liquid jet fuel-dissolved gas systems, the transparent pressure vessels and sight glass techniques become inconvenient.

Another technique based on the principle of buoyancy is that developed by Keramati, et al. [26]. This method allows for the direct measurement of fluid density by measuring the relative angular position of a completely immersed vertical disc containing two floats having different densities. This technique was specifically designed for density measurements of fluids at high pressures. In addition, this device was well tested and was immediately available for use in this laboratory. As a result, Keramati's high pressure density measuring device and technique was adopted during the present investigation for determination of the liquid densities of saturated Jet A fuel-dissolved gas systems.

5.2 Test Apparatus

A detailed description of Keramati's density measuring apparatus may be found in Reference [26]. This section contains only a brief review of that detailed description. Quotations are taken directly from Reference [26].

5.2.1 Theory of Apparatus

The float assembly, upon which the apparatus is based, is shown schematically in Figure 17. The assembly

> "consists of a disk C on the periphery of which two cylindrical floats A and B are permanently attached with a separation angle of ϕ. The two cylinders have the same nominal volume ($V_A = V_B$), but different densities denoted by ρ_A and ρ_B with $\rho_A < \rho_B$. A pivot is also permanently mounted through the center of the disk at point O. The two ends of the pivot which protrude out of the plane of the disk are supported by ring jewel bearings with spring-loaded end-stones. In normal operation the pivot is horizontal.
>
> "When the entire assembly, i.e., the disk, pivot, bearings, and the cylinders, is submerged in a fluid of unknown density ρ, the buoyant forces acting on the two cylinders will be different in

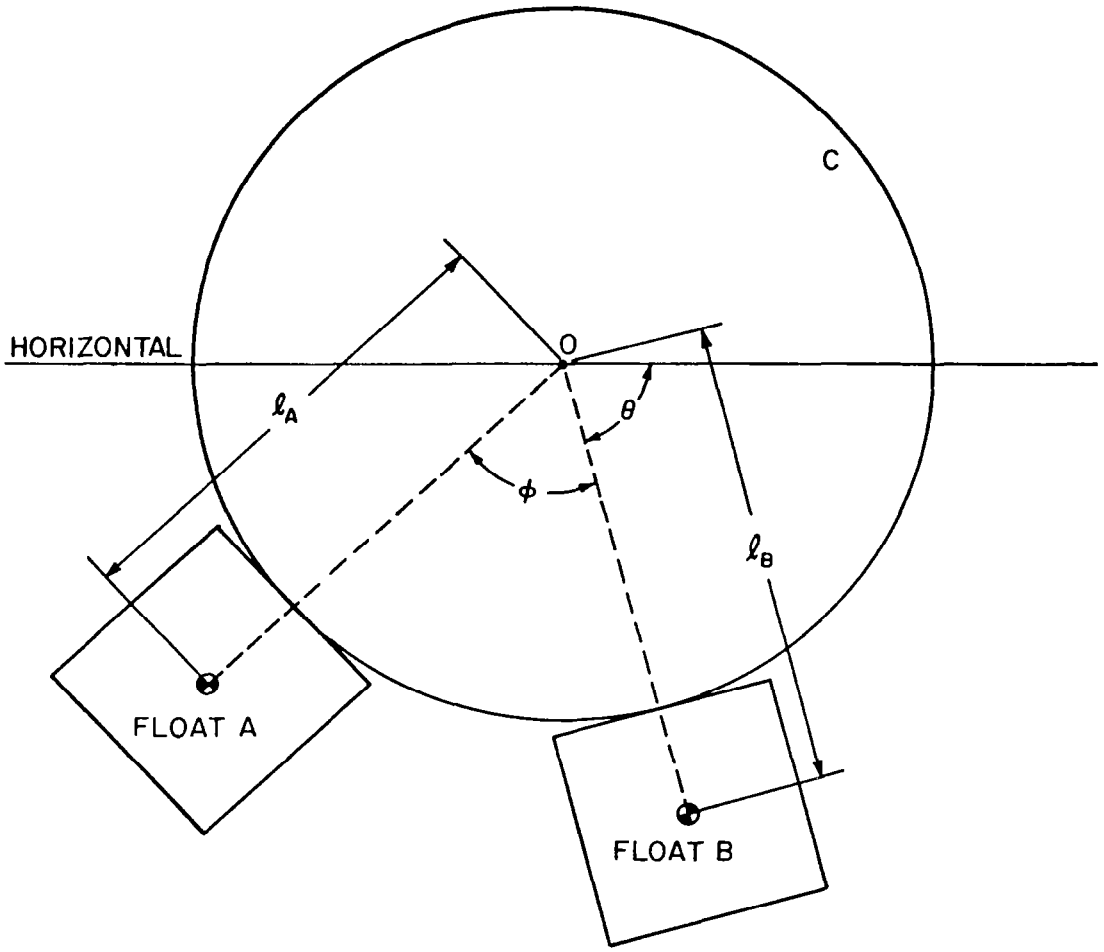

Figure 17. Sketch of the float assembly.

magnitude due to the difference in the densities ρ_A and ρ_B. This system of forces causes a net moment around the point 0. Thus, the assembly will be oriented angularly into a position that makes the net moment equal to zero. This angular position is measured by θ with respect to a fixed horizontal line as shown in Figure 17.

"A simple analysis reveals that when equilibrium is established

$$\rho = \frac{\rho_A V_A \ell_A \cos(\theta + \phi) + \rho_B V_B \ell_B \cos\theta}{V_A \ell_A \cos(\theta + \phi) + V_B \ell_B \cos\theta} \qquad (37)$$

with ℓ_A and ℓ_B defined in Figure 17. Thus, the problem of measuring density just involves measuring the angle θ."

The geometric details of the float assembly employed in this investigation are summarized in Table 5. For this specific case Eq. (37) was employed to compute the density as a function of θ. The results are illustrated in Figure 18. This particular float arrangement was chosen because of its enhanced sensitivity in the 800 to 900 kg/m^3 range. Preliminary theoretical density predictions indicated that this was the probable range of saturated liquid densities for Jet A fuel-dissolved gas systems.

5.2.2 Description of the Apparatus

The system used to measure the orientation cycle, θ, is shown in Figure 19. The arrangement consists of a simple direct current circuit. A high resistance ribbon made by Evanohm was mounted on the periphery of the disk over an arc of 180°, diametrically opposite the cylindrical floats. The high resistance ribbon is held in place by two brass screws which were tapped into the plexiglass disk. Two small insulated copper wires were welded onto each brass screw. These wires were light enough so that they did not significantly interfere with the rotation of the float assembly.

Connected in series with the high resistance ribbon is a 0-200 kΩ decade box. Completing the circuit is a constant two volt power supply. The two remaining small insulated copper wires attached to the brass screws are connected to a digital integrating microvoltmeter ($\pm$ 0.005 mV).

In addition, a contact switch was permanently positioned with respect to ground. The contact switch was designed to only make contact with the high resistance ribbon when the relay switch was connected. Otherwise, there is no contact or interference with the plexiglass disk or high resistance ribbon. A three volt power supply was required to activate the contact switch. A small insulated wire was connected to the contact

Table 5

GEOMETRY AND MATERIALS OF THE FLOAT ASSEMBLY

Disk:	
Material	Plexiglass
Diameter	116.84 mm
Thickness	12.70 mm
Cylinder A:	
Material	Epoxy
Volume	75077 mm^3
Density	662.3 kg/m^3
ℓ_A	79.86 mm
Cylinder B:	
Material	Magnesium
Volume	74955 mm^3
Density	1043.5 kg/m^3
ℓ_B	79.86 mm
Cylinder Separation Angle	45^o

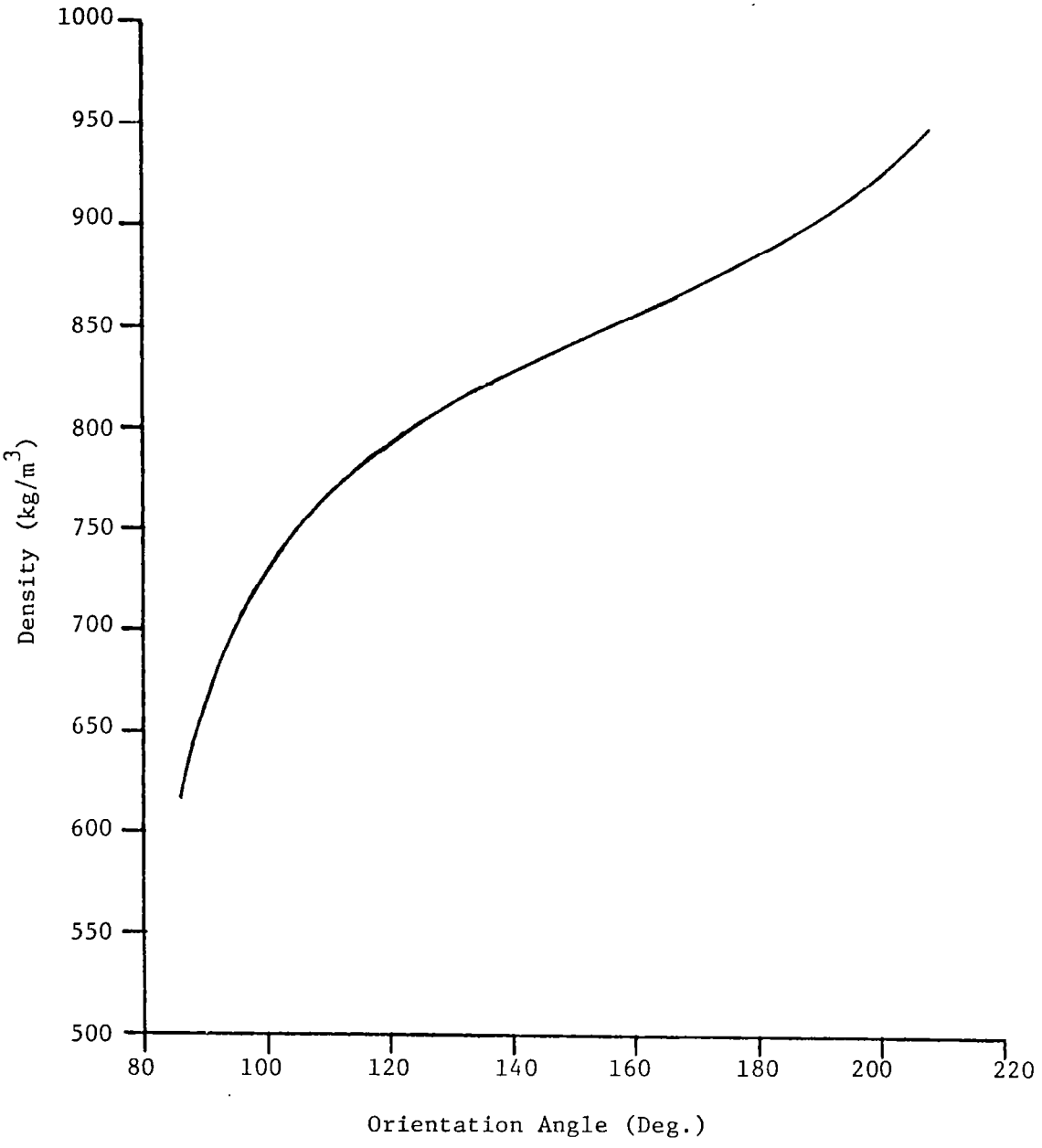

Figure 18. Sensitivity of the float assembly.

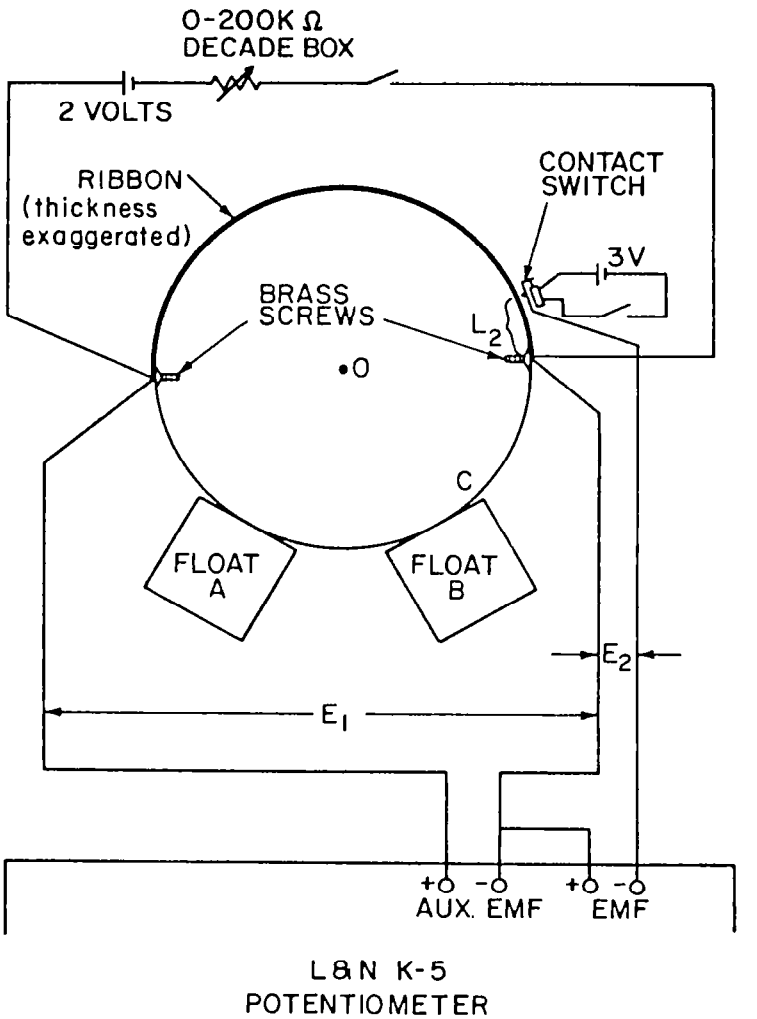

Figure 19. Sketch of the arrangements used for the measurements of the orientation angle.

switch from the digital integrating microvoltmeter. A toggle switch was employed at the digital integrating microvoltmeter to determine which voltage drop, E_1 or E_2 was to be measured. This entire assembly was installed in the pressure vessel.

The density measuring system as a whole is illustrated schematically in Figure 20. The system consists of the high pressure density measurement chamber, a 3000 ml high pressure sample preparation chamber, and a high pressure fluid sight chamber. The sample preparation chamber is connected in parallel to the density chamber by two flexible high pressure hoses. The flexible high pressure hoses allow the sample preparation chamber to be raised above or lowered below the density chamber for purposes of filling or draining the density chamber, respectively.

Connected to the top of the density chamber is a high pressure fluid sight chamber. This high pressure chamber contains a plexiglass high pressure viewing window used to determine when the density chamber was completely filled with fluid. The sight chamber also served as the junction by which the system is pressurized. The system may be pressurized with air or nitrogen. The system pressure level was determined with Heisse absolute pressure gauges (0.1 percent accuracy, 0-2.1 MPa and 0-10.3 MPa ranges, using two gauges). There were no provisions made during this investigation to regulate the temperature of the chamber.

5.3 Operation of the Apparatus

The operation of the apparatus proceeded as follows:

1) The sample preparation chamber was lowered below the density measurement chamber and filled with approximately two liters of fuel. The system was then pressurized with the desired gas.

2) Keeping the sample preparation chamber below the density measurement chamber, the sample was agitated for a period of 250-300 seconds to achieve equilibration.

3) Upon equilibration, the sample preparation chamber was raised above the density measurement chamber, allowing the sample fluid to drain into the density measurement chamber. To assure that the density measurement chamber was completely filled, the fluid sight chamber was checked for the presence of fluid. The sample preparation chamber was then secured at a position above the density measurement chamber.

4) A stable direct current of above 1 mA was then passed through the high resistance ribbon. This current was varied by adjusting the resistance of the decade box shown in Figure 19.

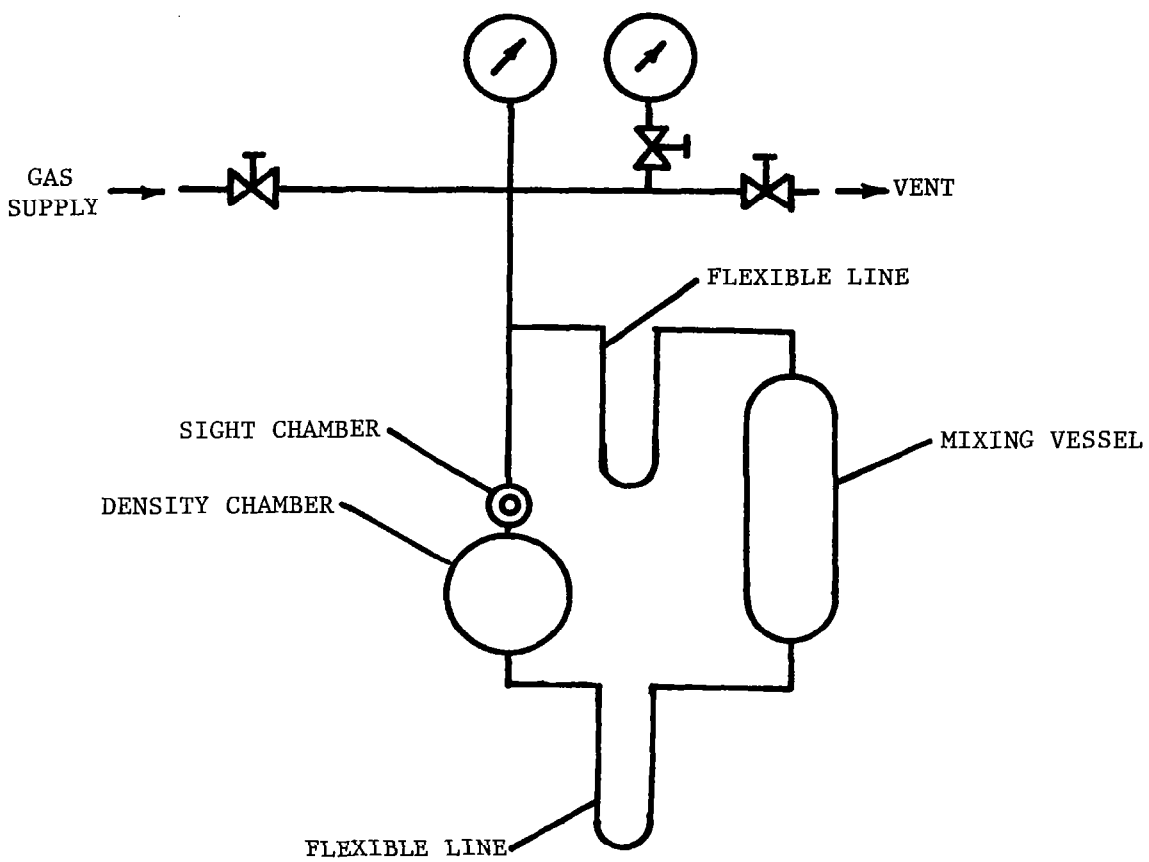

Figure 20. Schematic of density measuring system.

5) The voltage across the entire ribbon, E_1, was then measured using the digital integrating microvoltmeter.

6) The contact switch was then activated in order to make contact with the high resistance ribbon. Using the digital integrating microvoltmeter, the voltage E_2 was measured.

7) As a result of the linearity of the high resistance ribbon

$$\frac{L_1}{L_2} = \frac{E_1}{E_2} \tag{38}$$

where L_1 is the length of the entire ribbon and L_2 is the length of ribbon shown in Figure 19.

8) From the information in (7) above, the knowledge of the relative angular position of the contact switch with respect to the disk, and the separation angle ϕ, θ can be readily calculated. The density of the sample is then computed from Eq. (37).

6. Density Results and Discussion

Density measurements were completed for Jet A (79) - nitrogen and air, and Jet A (80) - air systems. The pressure range was 1.034-10.342 MPa, at an average sample temperature of 296.15K. The measurements were compared with the predictions of the Soave equation of state, employing the simplified air composition. The data is tabulated in Appendix C.

The comparison between predictions and measurements for the three systems considered is illustrated in Figures 21-23. The density of saturated mixtures of fuel and dissolved gas is plotted in these figures as a function of pressure. The agreement between predictions and measurements is readonably good, with discrepancies on the order of 2-3 percent. The region tested is not near the thermodynamic critical point, so that the Soave equation of state might be expected to yield good agreement, based on the solubility results discussed earlier.

Recalling that increased pressures yield increased gas solubilities in the liquid phase, the results illustrated in Figures 21-23 indicate that dissolved gas levels have a relatively small influence on liquid density over the range tested. This behavior is due to the fact that while increased pressures increase dissolved gas concentrations, tending to reduce the density, the density of both the gas and the liquid is increased as the pressure is increased. Therefore, these two compensating effects reduce the density variation. Comparing Figures 21 and 22

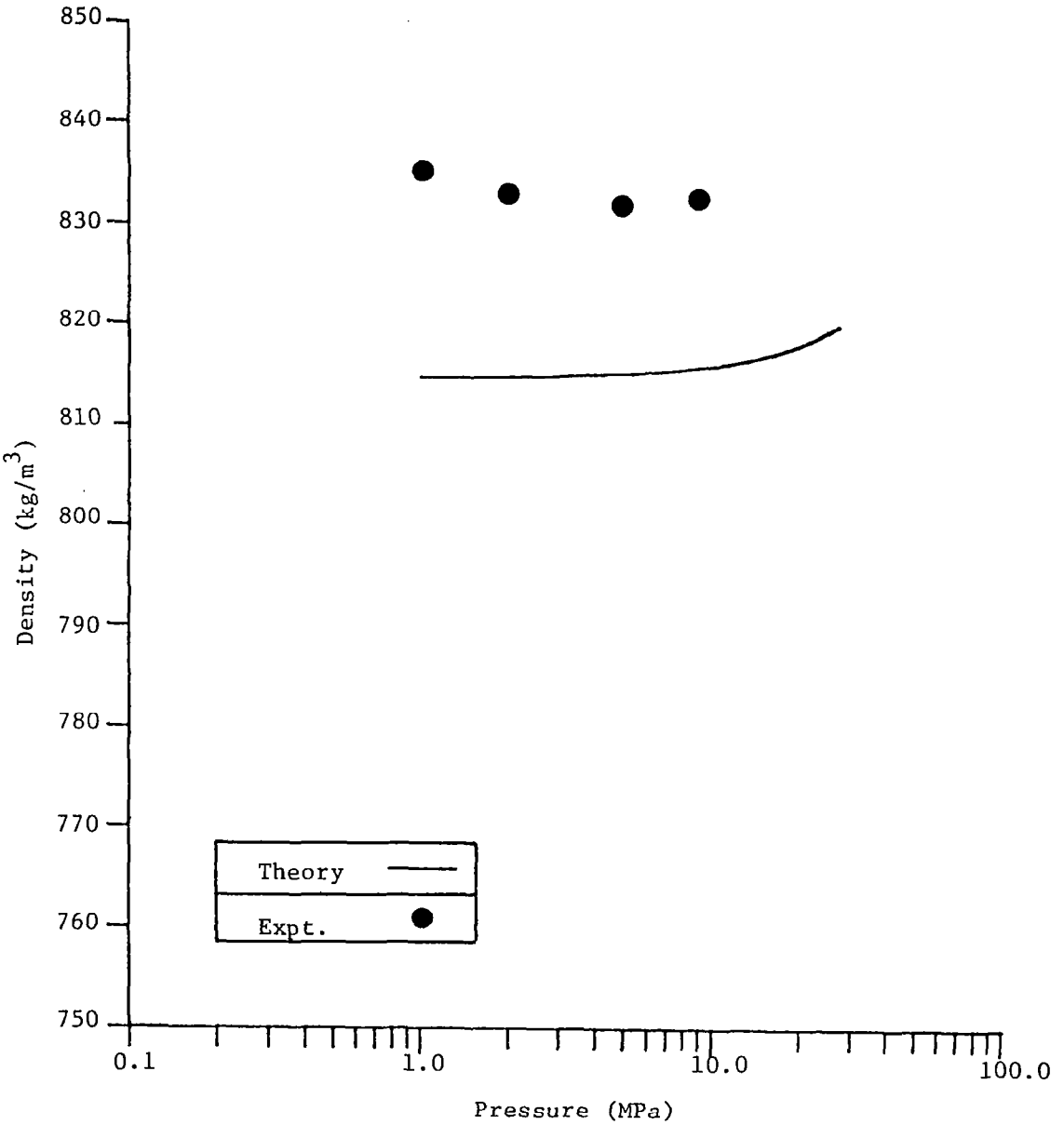

Figure 21. Density characteristics of Jet A (79) - nitrogen system, T = 296.15K.

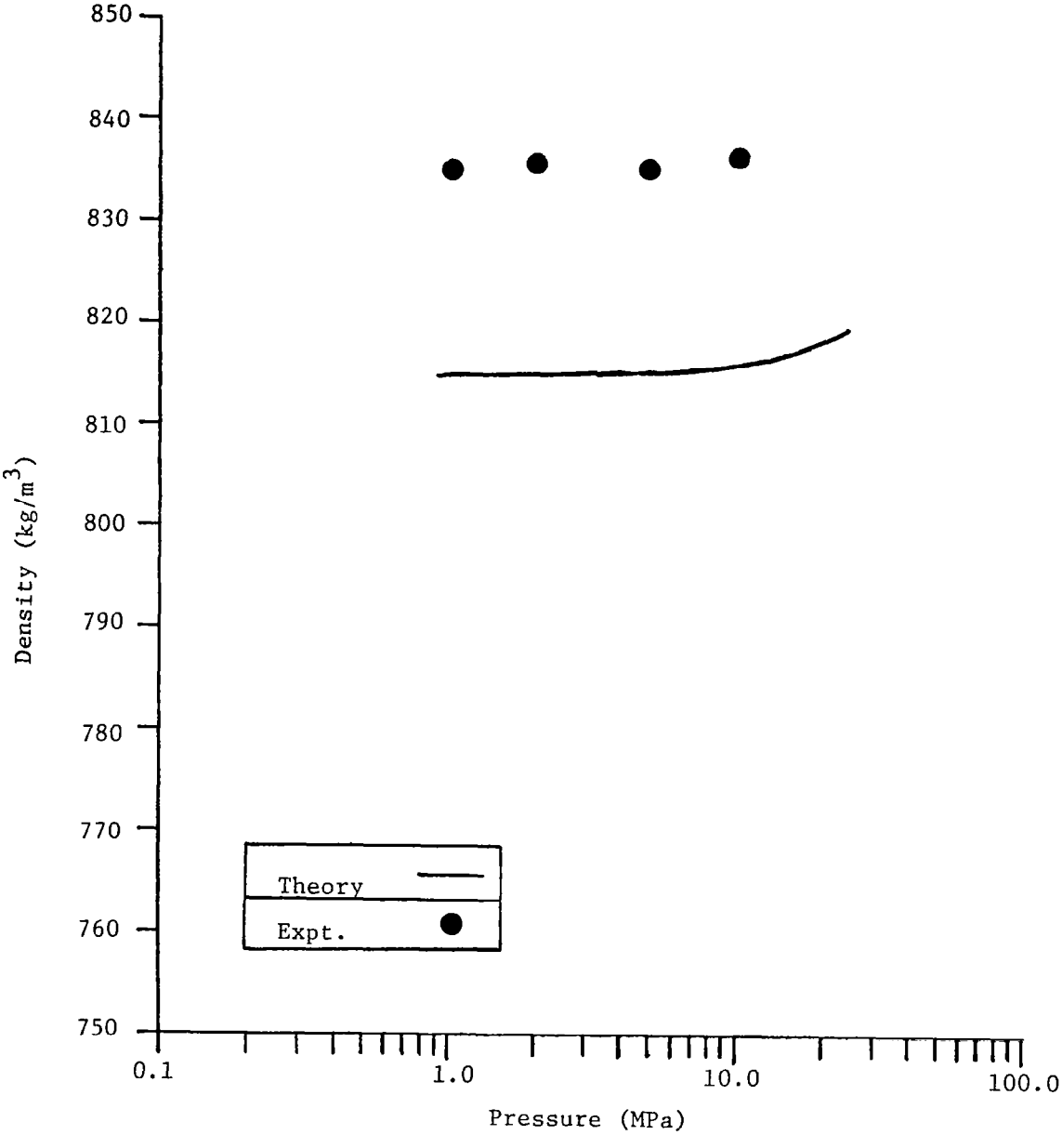

Figure 22. Density characteristics of Jet A (79) - air system, T = 296.15 K.

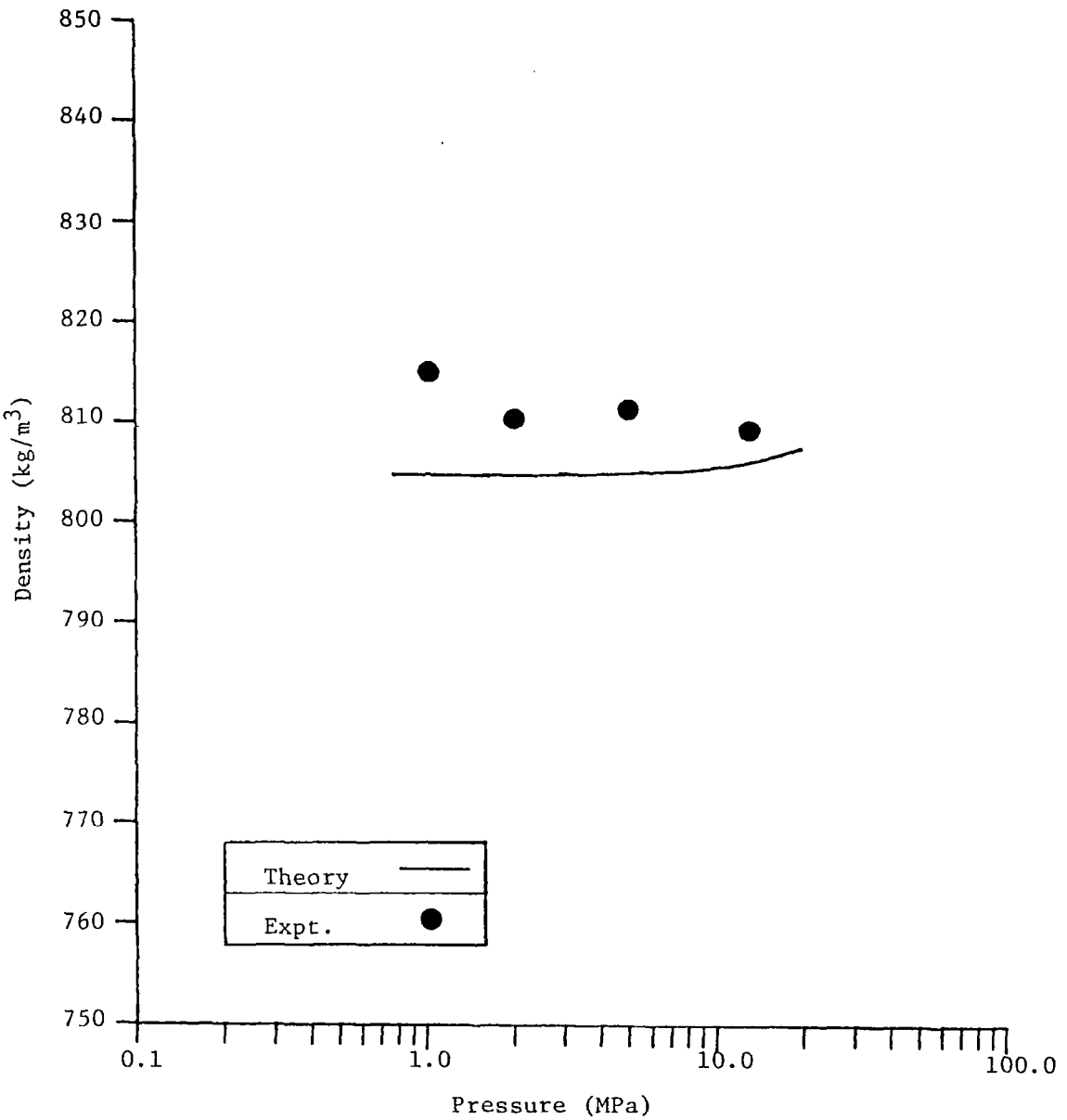

Figure 23. Density characteristics of Jet A (80) - air system, T = 296.15 K.

also shows that the density is relatively unchanged when air is substituted for nitrogen as the dissolved gas.

The effect of temperature on the density of saturated Jet A (79) - air mixtures was examined theoretically. The results are illustrated in Figure 24. In this figure, density is plotted as a function of pressure with temperature as a parameter. Predictions are provided for temperatures in the range 296.15-373.15K. Increasing the temperature tends to reduce the density, which is typical of most materials. For the range considered, temperature variations have a greater effect on mixture density than dissolved gas levels.

7. Isentropic Expansion

7.1 Computations

The effect of dissolved gases on atomization properties is influenced by the variation in the equilibrium state of the mixture as it passes through the injector [2-4]. The equilibrium states reached during expansion are influenced by frictional effects. Realistic limits on state conditions are an isentropic process (no friction or heat transfer) and a constant enthalpy process (strong frictional effects resulting in a negligible increase in kinetic energy during expansion, no heat transfer). Since frictional effects are generally moderate during liquid injection processes, the isentropic process was examined during this investigation, as the most realistic model for practical injectors.

Conditions upstream of the injector were assumed to be a saturated mixture of liquid and dissolved gas, at a given temperature and pressure. Conditions downstream of the injector are prescribed by the pressure and the fact that the injection process is assumed to be isentropic. For these conditions, once the expansion begins, the system enters the two-phase region, with saturated vapor and liquid phases present (at sufficiently low pressures, all the material would be a vapor; however, such conditions were not encountered during the present computations). Given the initial condition and the current pressure and entropy; the temperature, the composition of each phase, and the relative proportions of the phases (vapor fraction), must be determined.

The method used to solve for properties during an isentropic expansion follows the procedure outlined by Starling [15]. A flow diagram for the computation is illustrated in Figure 25. This computation was programmed as an option in the basic phase equilibrium routine. The program appears in Appendix A. The parameters used during these computations were the same as those employed for the solubility and density calculations. The quantity F appearing in Figure 25 is

$$F = \sum_i Z_i(1-K_i)/(K_iV+1-V) \qquad (39)$$

while

$$F' = \frac{\partial F}{\partial V} \qquad (40)$$

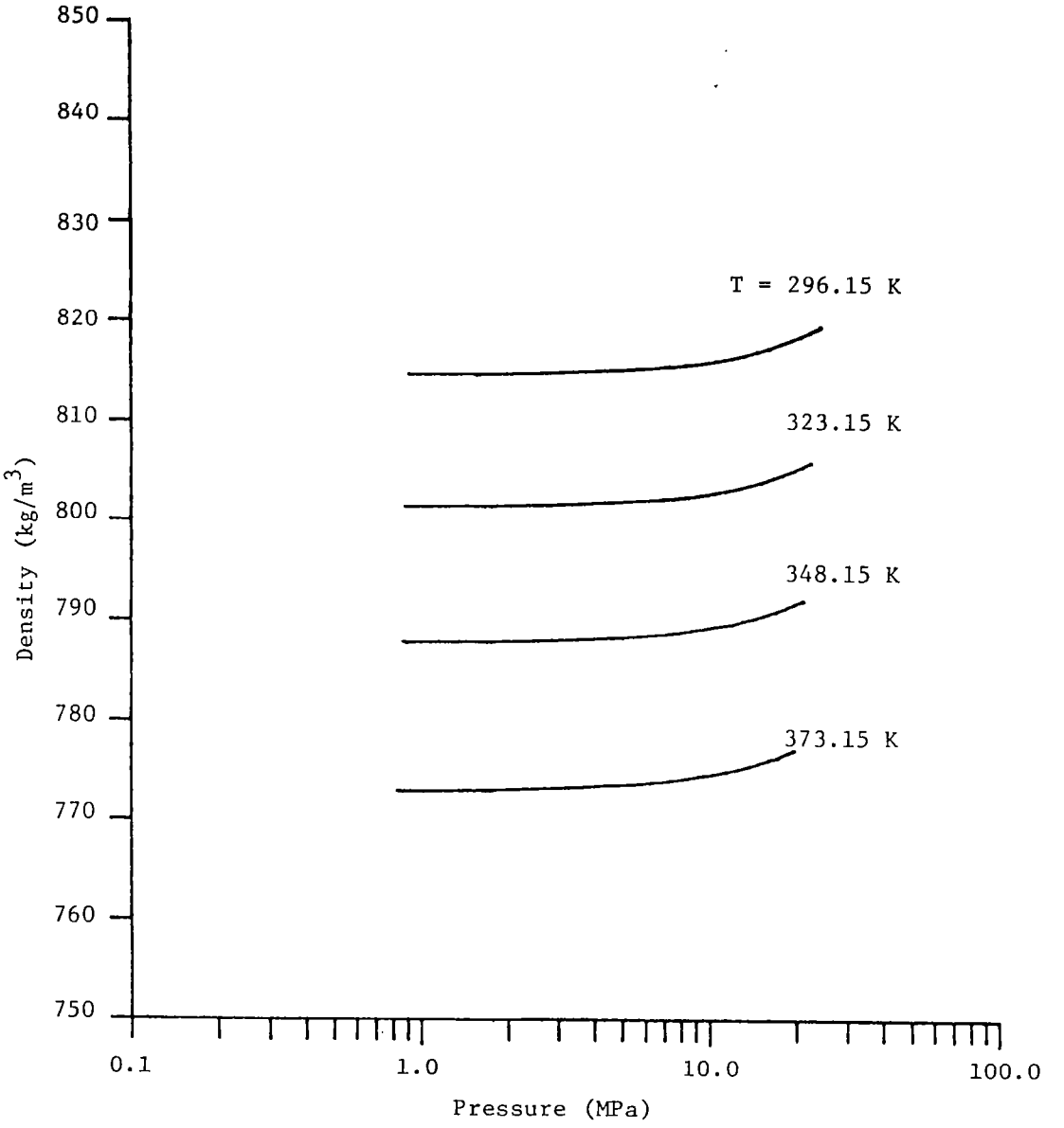

Figure 24. Density characteristics of Jet A (79) - air for various temperatures.

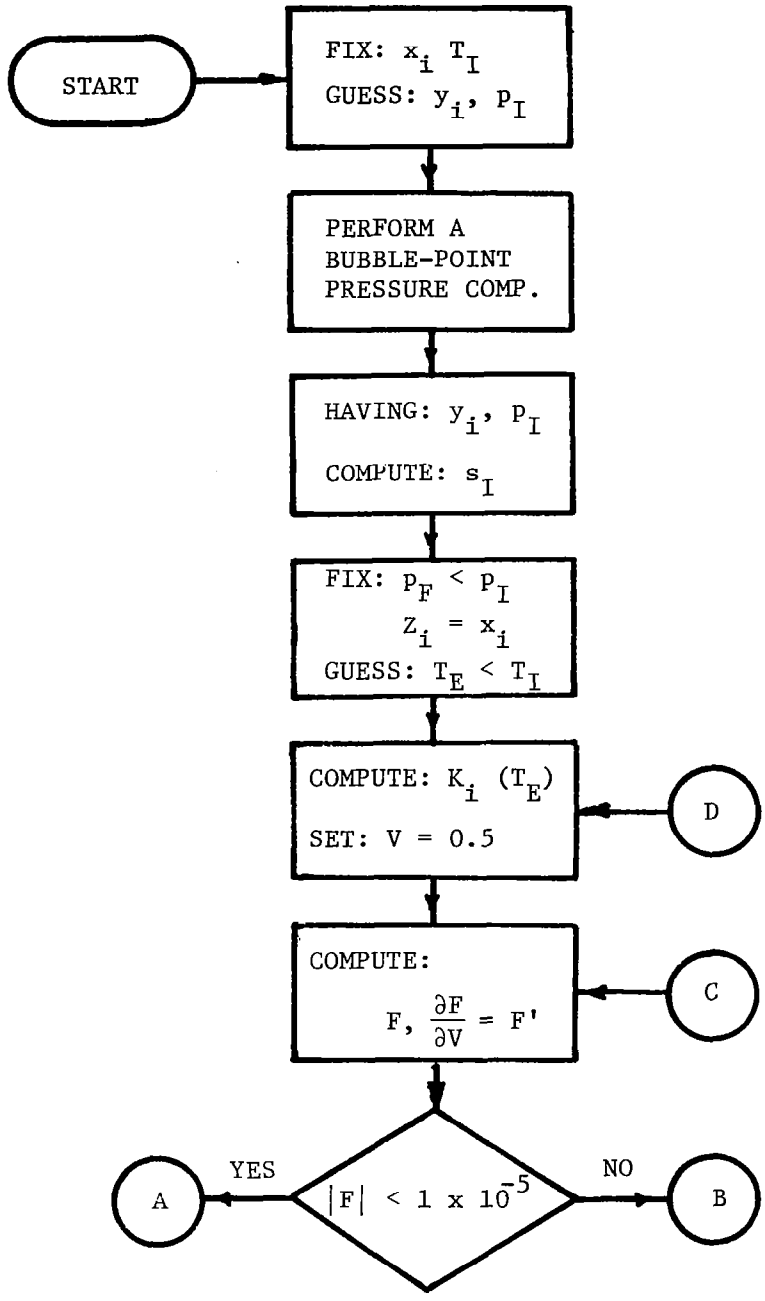

Figure 25. Schematic of isentropic expansion calculation.

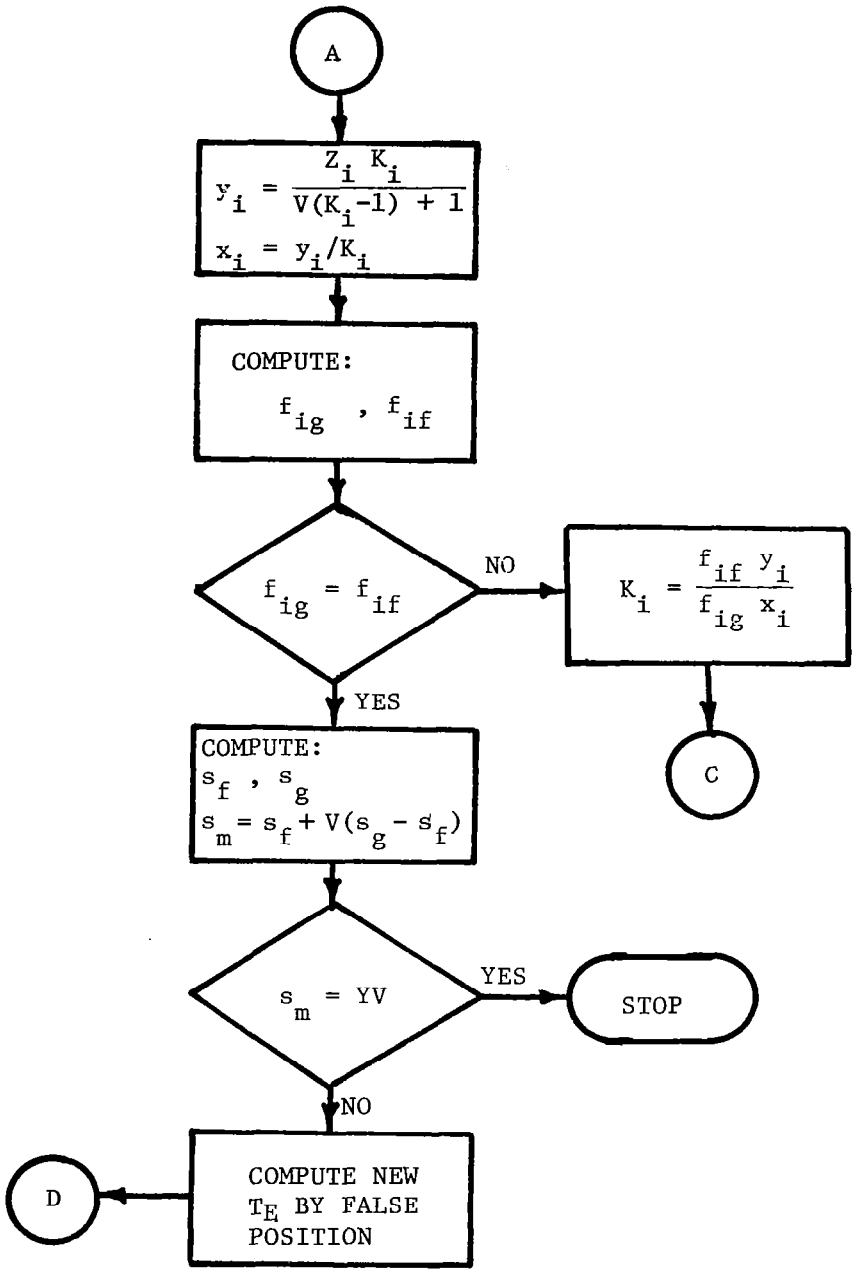

Figure 25. Schematic of isentropic expansion calculation (continued).

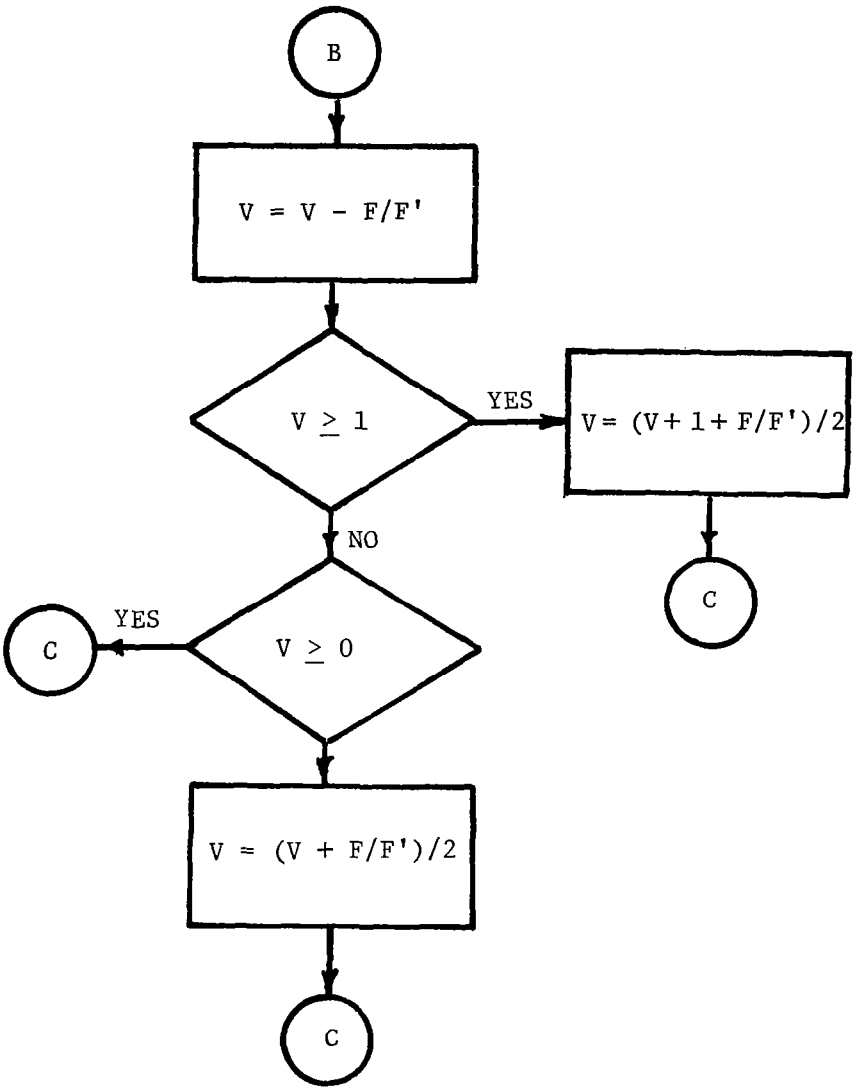

Figure 25. Schematic of isentropic expansion calculation (continued).

7.2 Results and Discussion

Figure 26 is an illustration of the variation of the mass fraction of vapor as initially saturated mixtures of Jet A (79) and air (simplified air) are expanded. These results are for an initial temperature of 298.15K, with initial dissolved air concentrations of 1 and 10 percent on a molal basis. The computations extend from the initial saturated pressure to 0.1 MPa. For this relatively low initial temperature, the vapor pressure of the fuel is quite low. Therefore, the vapor phase largely consists of air gases. The maximum vapor fraction for such conditions is limited by the initial mole fraction of dissolved gas.

Figures 27 and 28 are illustrations of similar results at higher initial temperatures. In this case, the higher vapor pressure of the fuel at higher temperatures causes an inflection in the vapor mass fraction plot as the pressure is reduced. This is due to flashing of the fuel vapor. Similar results would eventually be observed for the conditions of Figure 26, if lower back pressures were considered.

Figure 29 is an illustration of the mixture temperature as a function of back pressure during an isentropic expansion, for various saturated initial states. For the conditions shown, the expansion is nearly isothermal, similar to isentropic expansion processes for liquids.

Volumetric expansion ratios are plotted as a function of back pressure in Figures 30 and 31, for initial dissolved gas concentrations of 1 and 10 percent, respectively. The presence of dissolved gas yields expansion ratios significantly greater than unity, particularly for low back pressures. High initial temperatures result in larger expansion ratio values, as well, due to the effect of flashing. Since density ratio has a significant effect on the atomization of dissolved gas mixtures [2-4], we can expect that the greatest improvement of injection quality for the supercritical injection will be observed for high initial tempratures and pressures (yielding large initial concentrations of dissolved gas) and low back pressures.

The results of the isentropic expansion computations are summarized more completely in Table 6 for Jet A - simple air mixtures. The table provides the composition of both phases, the vapor fractions, temperature, mixture enthalpy, mixture entropy, mixture specific volume and volumetric expansion ratio, as a function of back pressure. Results are presented for initial dissolved air concentrations of 1 and 10 percent (molal), at initial temperatures of 298.15, 373.15 and 473.15K.

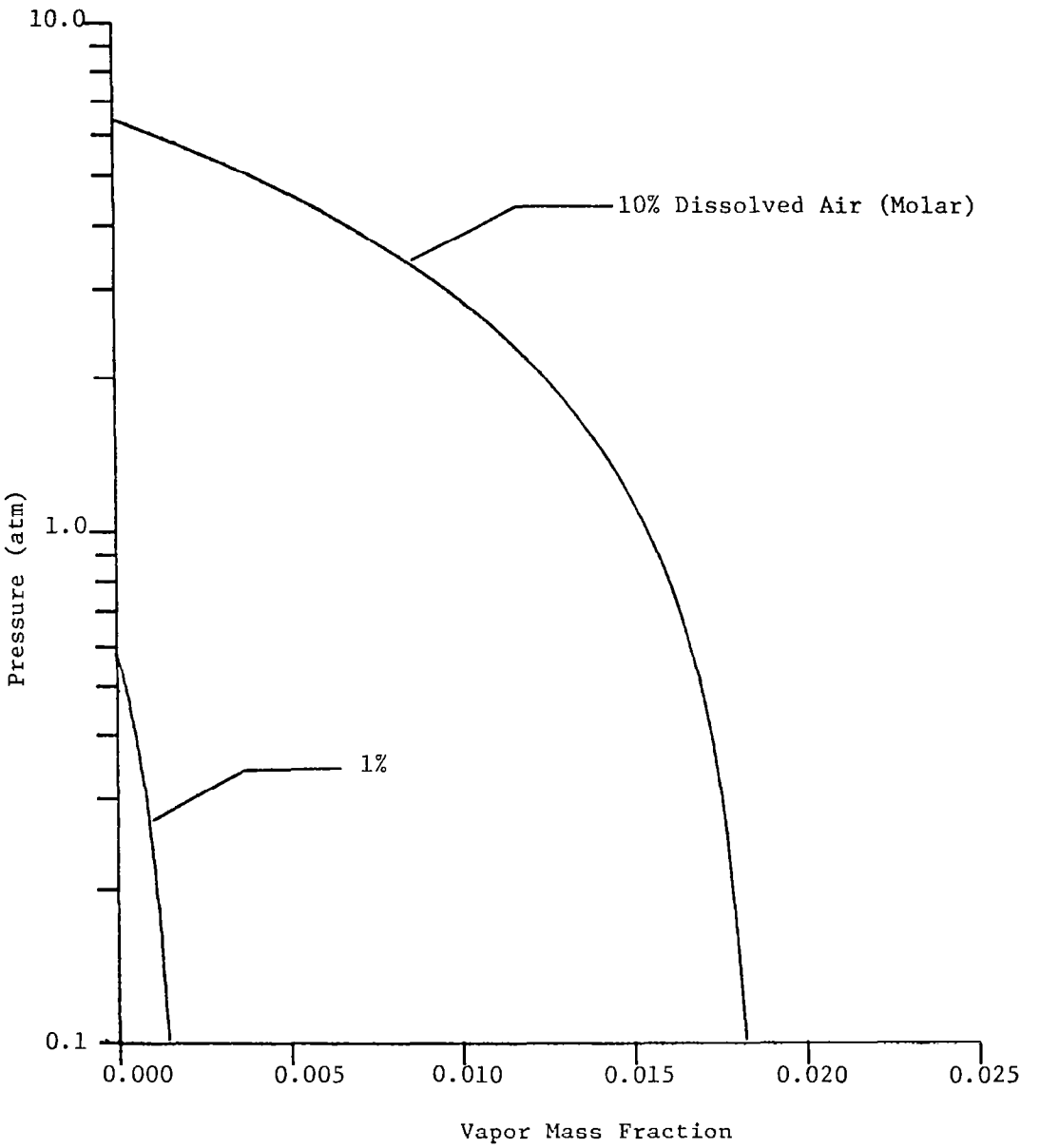

Figure 26. Vapor mole fraction during an isentropic expansion of initially saturated Jet A (79) - air mixtures at 298.15K.

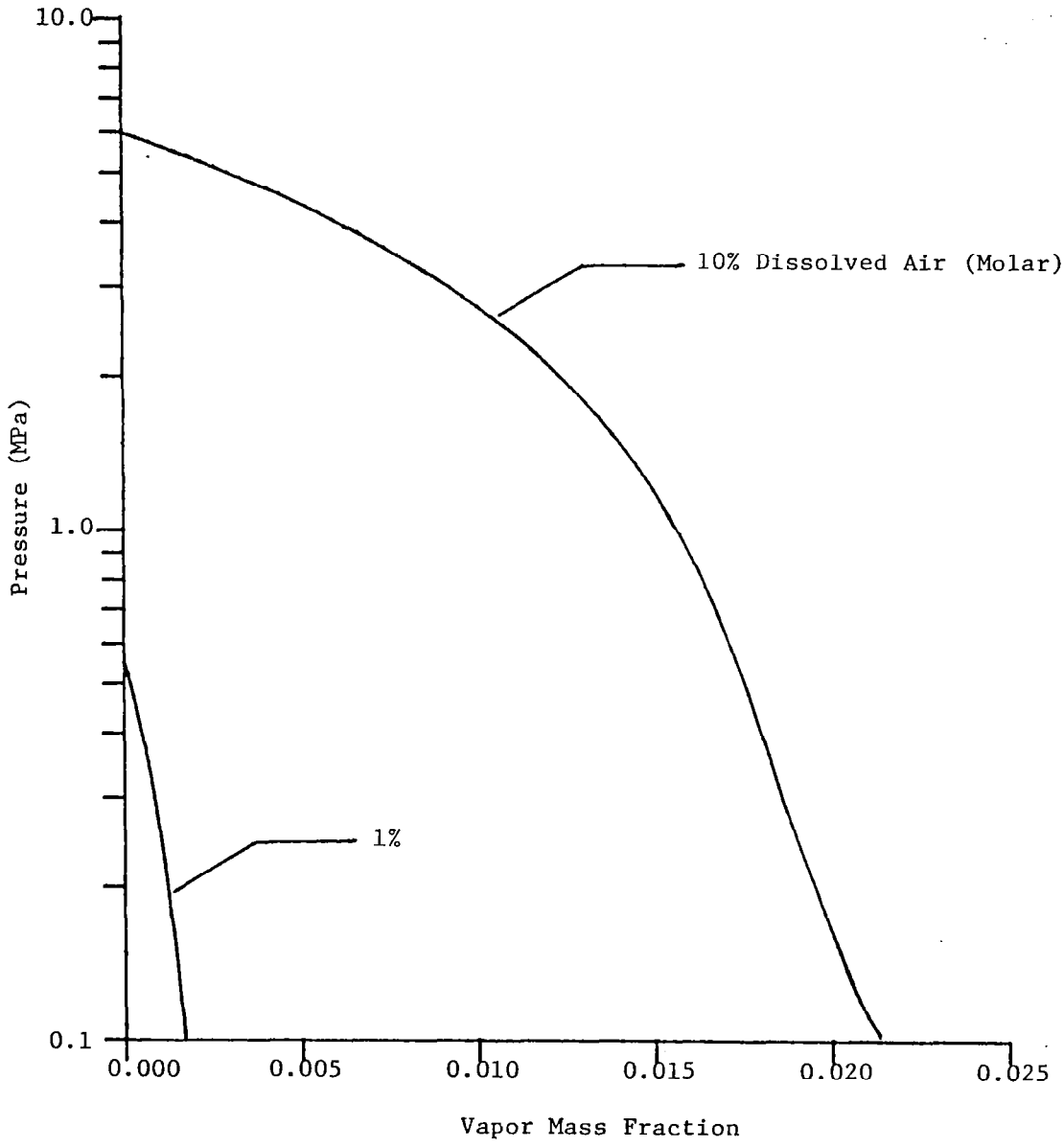

Figure 27. Vapor mole fraction during isentropic expansion of initially saturated Jet A (79) - air mixtures at 373.15 K.

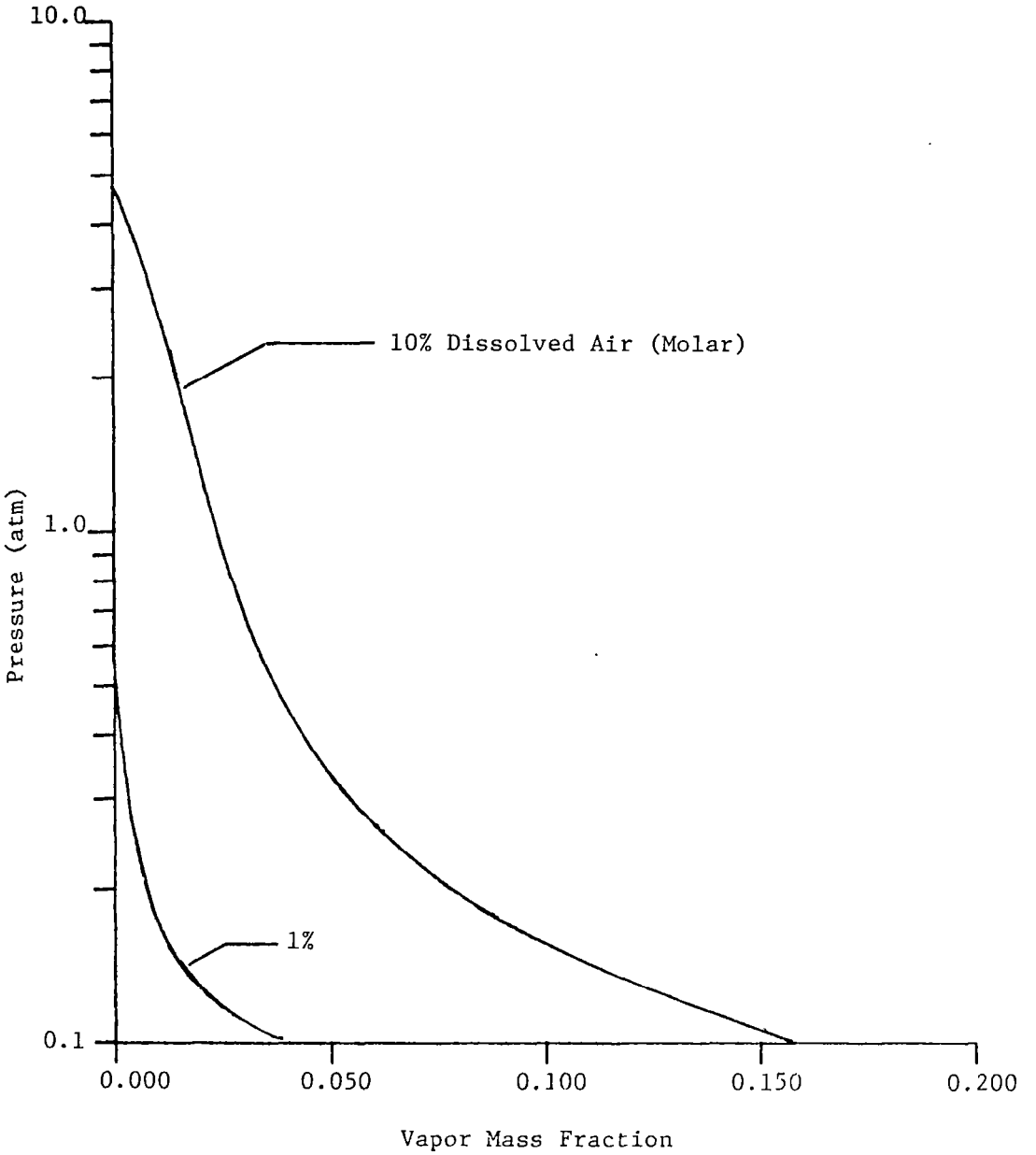

Figure 28. Vapor mole fraction during an isentropic expansion of initially saturated Jet A (79) - air mixtures at 473.15K.

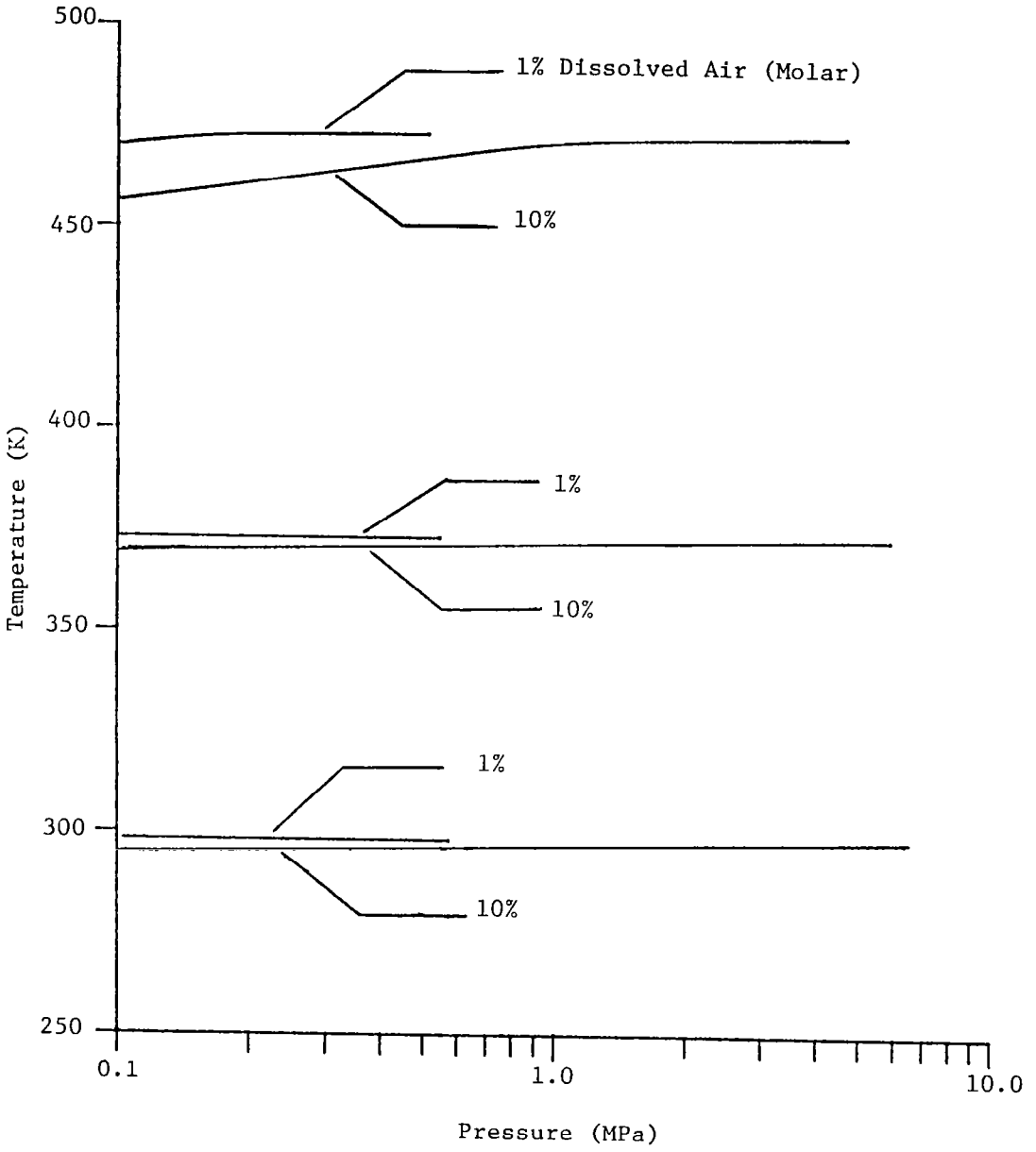

Figure 29. Mixture temperature during isentropic expansion of initially saturated mixtures of Jet A (79) and air.

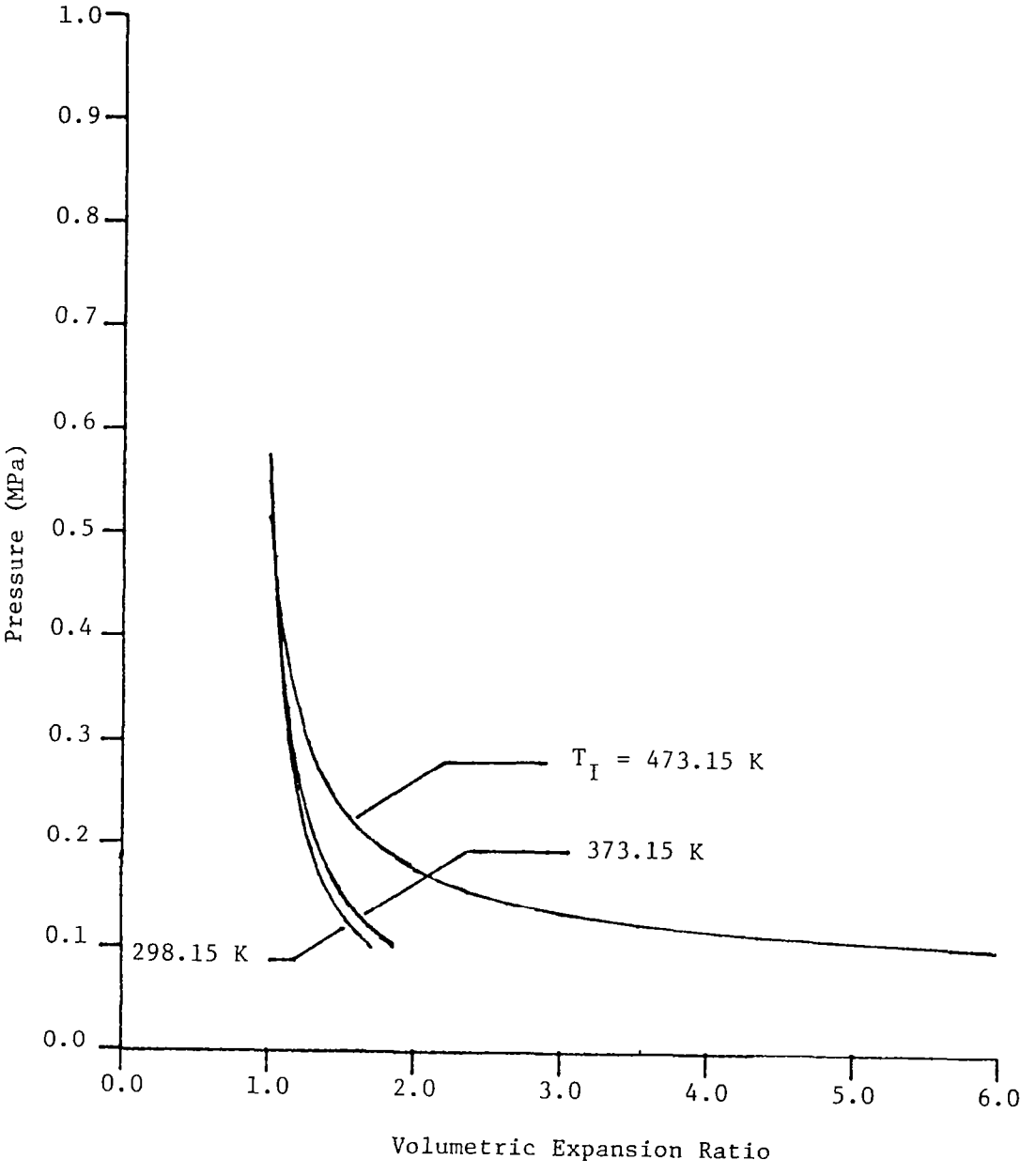

Figure 30. Volumetric expansion ratios during isentropic expansion of initially saturated mixtures of Jet A (79) and air, having an initial dissolved air concentration of 1% (molar).

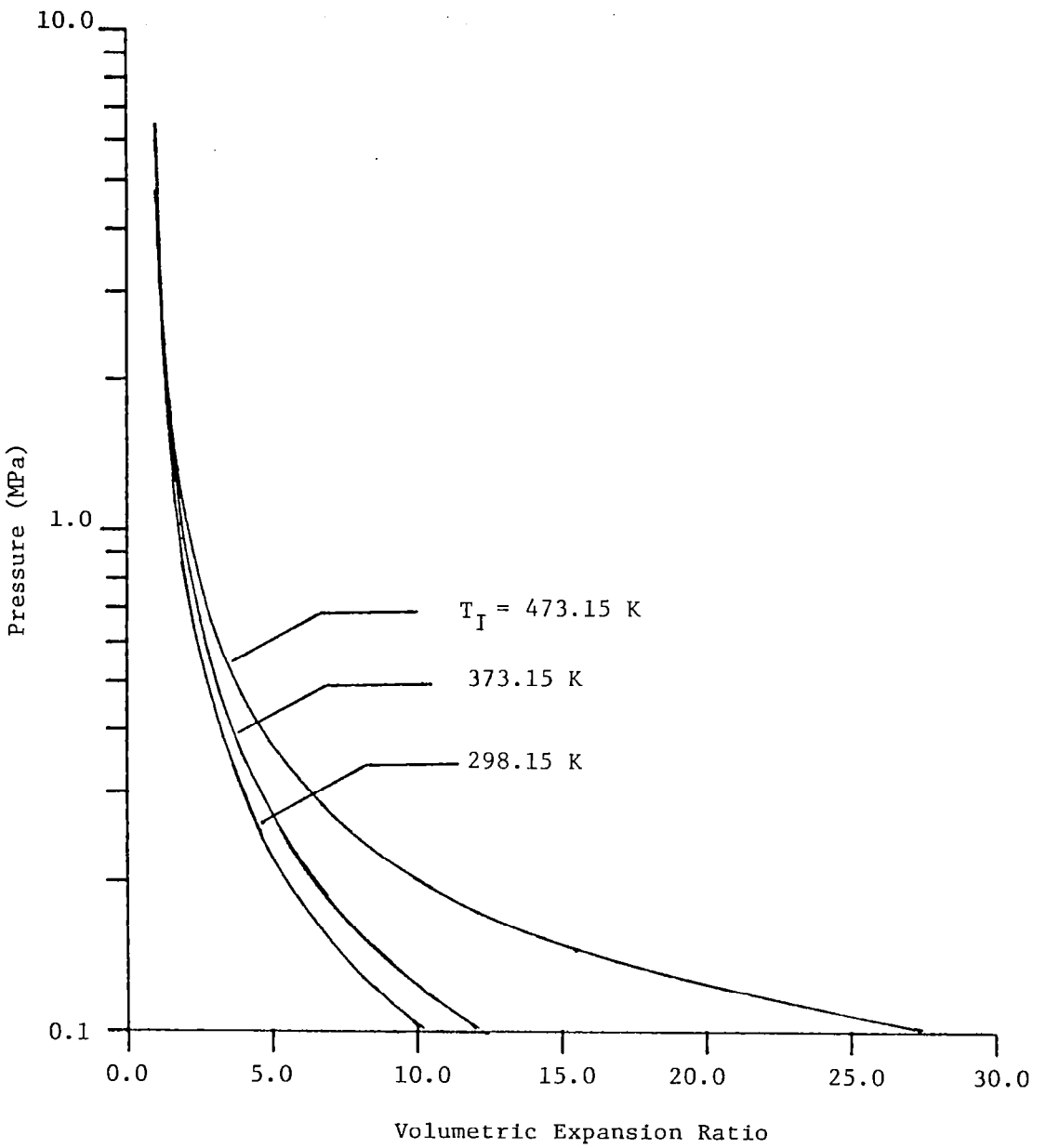

Figure 31. Volumetric expansion ratios during isentropic expansion of initially saturated mixtures of Jet A (79) and air, having an initial dissolved air concentration of 10% (molar).

Table 6A

SOLUBILITY PROPERTIES OF AN ISENTROPICALLY EXPANDED
JET A - SIMPLE AIR SATURATED LIQUID SYSTEM

Pressure (MPa)	Temperature (K)	x	Component	x_i	y_i
Inlet Condition:					
0.575089	298.15	0.00	Jet A	0.990000	0.000094
			N_2	0.007900	0.856035
			O_2	0.002100	0.143872
Outlet Conditions:					
0.460071	298.13	0.00033	Jet A	0.991939	0.000114
			N_2	0.006259	0.845923
			O_2	0.001803	0.153963
0.345053	298.10	0.00067	Jet A	0.993903	0.000147
			N_2	0.004640	0.834467
			O_2	0.001456	0.165386
0.230035	298.07	0.00101	Jet A	0.995899	0.000214
			N_2	0.003052	0.821432
			O_2	0.001050	0.178354
0.115018	298.02	0.00136	Jet A	0.997930	0.000414
			N_2	0.001501	0.806487
			O_2	0.000569	0.193099
0.101325	298.02	0.00140	Jet A	0.998175	0.000468
			N_2	0.001318	0.804548
			O_2	0.000506	0.194984

Table 6A (Continued)

THERMODYNAMIC MIXTURE PROPERTIES OF AN ISENTROPICALLY EXPANDED
JET A - SIMPLE AIR SATURATED LIQUID SYSTEM

Pressure (MPa)	Temperature (K)	x	h_m (kJ/kg)	s_m (kJ/kg-K)	$v_m \times 10^3$ (m^3/kg)	VR
Inlet Condition:						
0.575089	298.15	0.00	43.8128	0.6337	1.6904	1.0
Outlet Conditions:						
0.460071	298.13	0.00033	43.6151	0.6337	1.7463	1.0366
0.345053	298.10	0.00067	43.4081	0.6337	1.8570	1.0983
0.230035	298.07	0.00101	43.1841	0.6337	2.0671	1.2229
0.115018	298.02	0.00136	42.9181	0.6337	2.7037	1.5993
0.101325	298.02	0.00140	42.8800	0.6337	2.8741	1.7013

Table 6A (Continued)

THERMODYNAMIC PHASE PROPERTIES OF AN ISENTROPICALLY EXPANDED
JET A - SIMPLE AIR SATURATED LIQUID SYSTEM

Pressure (MPa)	Temperature (K)	x	h_f (kJ/kg)	h_g (kJ/kg)	s_f (kJ/kg-K)	s_g (kJ/kg-K)	$v_f \times 10^3$ (m^3/kg)	v_g (m^3/kg)
Inlet Condition:								
0.575078	298.15	0.00	43.8128	302.0635	0.6337	6.3785	1.6904	0.15060
Outlet Conditions:								
0.460071	298.13	0.00033	43.5293	301.8761	0.6318	6.4444	1.6904	1.18796
0.345053	298.10	0.00067	43.2355	301.6352	0.6298	6.5282	1.6905	0.25018
0.230035	298.07	0.00101	42.9231	301.3363	0.6276	6.6445	1.6906	0.37448
0.115018	298.02	0.00136	42.5668	301.0024	0.6253	6.8380	1.6906	0.74666
0.101325	298.02	0.00140	42.5177	300.9699	0.6249	6.8736	1.6905	0.84710

Table 6B

SOLUBILITY PROPERTIES OF AN ISENTROPICALLY EXPANDED
JET A - SIMPLE AIR SATURATED LIQUID SYSTEM

Pressure (MPa)	Temperature (K)	x	Component	x_i	y_i
Inlet Condition:					
6.404040	298.15	0.0	Jet A	0.900000	0.000032
			N_2	0.079000	0.853225
			O_2	0.021000	0.146743
Outlet Conditions:					
5.123232	297.94	0.00355	Jet A	0.917724	0.000030
			N_2	0.063932	0.844112
			O_2	0.018344	0.155857
3.842424	297.67	0.00716	Jet A	0.936455	0.000030
			N_2	0.048435	0.833563
			O_2	0.015110	0.166407
2.561616	297.31	0.01085	Jet A	0.956311	0.000032
			N_2	0.032556	0.821278
			O_2	0.011133	0.178689
1.280809	296.71	0.01463	Jet A	0.977434	0.000045
			N_2	0.016311	0.806894
			O_2	0.006195	0.193061
0.640404	296.15	0.01655	Jet A	0.988521	0.000074
			N_2	0.008200	0.798766
			O_2	0.003279	0.201160
0.101325	294.73	0.01823	Jet A	0.998157	0.000365
			N_2	0.001297	0.791164
			O_2	0.000545	0.208471

Table 6B (Continued)

THERMODYNAMIC MIXTURE PROPERTIES OF AN ISENTROPICALLY EXPANDED
JET A - SIMPLE AIR SATURATED LIQUID SYSTEM

Pressure (MPa)	Temperature (K)	x	h_m (kJ/kg)	s_m (kJ/kg-K)	$v_m \times 10^3$ (m^3/kg)	VR
Inlet Condition:						
6.404040	298.15	0.0	55.8162	0.7157	1.6840	1
Outlet Conditions:						
5.123232	297.94	0.00355	53.6269	0.7157	1.7391	1.0327
3.842424	297.67	0.00716	51.3444	0.7157	1.8348	1.0895
2.561616	297.31	0.01085	48.8853	0.7157	2.0326	1.2070
1.280808	296.71	0.01463	45.9823	0.7157	2.6404	1.5680
0.640404	296.15	0.01655	43.9886	0.7157	3.8652	2.2955
0.101325	294.73	0.01823	40.3308	0.7157	16.9077	10.0392

Table 6B (Continued)

THERMODYNAMIC PHASE PROPERTIES OF AN ISENTROPICALLY EXPANDED
JET A - SIMPLE AIR SATURATED LIQUID SYSTEM

Pressure (MPa)	Temperature (K)	x	h_f (kJ/kg)	h_g (kJ/kg)	s_f (kJ/kg-K)	s_g (kJ/kg-K)	$v_f \times 10^3$ (m^3/kg)	v_g (m^3/kg)
Inlet Condition:								
6.404040	298.15	0.0	55.8162	290.0026	0.7157	5.6406	1.6840	0.01356
Outlet Conditions:								
5.123232	297.94	0.00355	52.7792	291.7802	0.6979	5.7145	1.6852	0.01688
3.842424	297.67	0.00716	49.5976	293.5703	0.6789	5.8070	1.6863	0.02242
2.561616	297.31	0.01085	46.1825	295.3205	0.6584	5.9332	1.6873	0.03352
1.280808	296.71	0.01463	42.2581	296.8896	0.6351	6.1411	1.6880	0.06679
0.640404	296.15	0.01655	39.7226	297.4274	0.6209	6.3431	1.6886	0.13323
0.101325	294.73	0.01823	35.5647	297.0321	0.6015	6.8644	1.6870	0.83661

Table 6C

SOLUBILITY PROPERTIES OF AN ISENTROPICALLY EXPANDED
JET A - SIMPLE AIR SATURATED LIQUID SYSTEM

Pressure (MPa)	Temperature (K)	x	Component	x_i	y_i
Inlet Condition:					
0.550051	373.15	0.00	Jet A	0.990000	0.006575
			N_2	0.007900	0.834859
			O_2	0.002100	0.158566
Outlet Conditions:					
0.440041	373.13	0.00035	Jet A	0.991973	0.008096
			N_2	0.006258	0.825241
			O_2	0.001769	0.166663
0.330031	373.10	0.00072	Jet A	0.993963	0.010632
			N_2	0.004638	0.814034
			O_2	0.001399	0.175334
0.220020	373.06	0.00112	Jet A	0.995975	0.015698
			N_2	0.003043	0.799953
			O_2	0.000982	0.184349
0.110010	373.00	0.00163	Jet A	0.998009	0.030868
			N_2	0.001479	0.776931
			O_2	0.000513	0.192201
0.101325	372.99	0.00168	Jet A	0.998170	0.033464
			N_2	0.001357	0.773966
			O_2	0.000473	0.192569

Table 6C (Continued)

THERMODYNAMIC MIXTURE PROPERTIES OF AN ISENTROPICALLY EXPANDED
JET A - SIMPLE AIR SATURATED LIQUID SYSTEM

Pressure (MPa)	Temperature (K)	x	h_m (kJ/kg)	s_m (kJ/kg-K)	$v_m \times 10^3$ (m^3/kg)	VR
Inlet Condition:						
0.550051	373.15	0.00	214.6126	1.1435	1.7881	1.0
Outlet Conditions:						
0.440041	373.13	0.00035	214.4116	1.1435	1.8704	1.0466
0.330031	373.10	0.00072	214.1988	1.1435	2.0110	1.1250
0.220020	373.06	0.00112	213.9640	1.1435	2.2961	1.2839
0.110010	373.00	0.00163	213.6746	1.1435	3.1704	1.7722
0.101325	372.99	0.00168	213.6464	1.1435	1.3178	1.8575

Table 6C (Continued)

THERMODYNAMIC PHASE PROPERTIES OF AN ISENTROPICALLY EXPANDED
JET A - SIMPLE AIR SATURATED LIQUID SYSTEM

Pressure (MPa)	Temperature (K)	x	h_f (kJ/kg)	h_g (kJ/kg)	s_f (kJ/kg-K)	s_g (kJ/kg-K)	$v_f \times 10^3$ (m^3/kg)	v_g (m^3/kg)
Inlet Condition:								
0.550051	373.15	0.00	214.6126	383.2103	1.1435	6.4496	1.7881	0.19091
Outlet Conditions:								
0.440041	373.13	0.00035	214.3515	383.9725	1.1416	6.4730	1.7882	0.23655
0.330031	373.10	0.00072	214.0750	385.3838	1.1396	6.4871	1.7883	0.31115
0.220020	373.06	0.00112	213.7685	388.4043	1.1375	6.4676	1.7883	0.45515
0.110010	373.00	0.00163	213.3750	297.3406	1.1351	6.2805	1.7880	0.84983
0.101325	372.99	0.00168	213.3341	398.7897	1.1349	6.2417	1.7880	0.91241

Table 6D

SOLUBILITY PROPERTIES OF AN ISENTROPICALLY EXPANDED
JET A - SIMPLE AIR SATURATED LIQUID SYSTEM

Pressure (MPa)	Temperature (K)	x	Component	x_i	y_i
Inlet Condition:					
5.960325	373.15	0.0	Jet A	0.900000	0.001160
			N_2	0.079000	0.837533
			O_2	0.021000	0.161307
Outlet Conditions:					
4.768260	372.93	0.00369	Jet A	0.918305	0.001256
			N_2	0.063712	0.829635
			O_2	0.017983	0.169109
3.576195	372.66	0.00741	Jet A	0.937397	0.001441
			N_2	0.048125	0.820841
			O_2	0.014478	0.177718
2.384130	372.28	0.01117	Jet A	0.957346	0.001842
			N_2	0.032267	0.810943
			O_2	0.010387	0.187215
1.192065	371.65	0.01504	Jet A	0.978214	0.003090
			N_2	0.016185	0.799325
			O_2	0.005601	0.197586
0.596033	371.02	0.01719	Jet A	0.989013	0.005569
			N_2	0.008086	0.791614
			O_2	0.002906	0.202817
0.101325	369.22	0.02132	Jet A	0.998163	0.028356
			N_2	0.001339	0.768597
			O_2	0.000498	0.203047

Table 6D (Continued)

THERMODYNAMIC MIXTURE PROPERTIES OF AN ISENTROPICALLY EXPANDED
JET A - SIMPLE AIR SATURATED LIQUID SYSTEM

Pressure (MPa)	Temperature (K)	x	h_m (kJ/kg)	s_m (kJ/kg-K)	$v_m \times 10^3$ (m^3/kg)	VR
Inlet Condition:						
0.960325	373.15	0.0	224.6962	1.2219	1.7815	1.0
Outlet Conditions:						
4.768260	372.93	0.00369	222.5290	1.2219	1.8605	1.0444
3.576195	372.66	0.00741	220.2388	1.2219	1.9949	1.1198
2.384130	372.28	0.01117	217.7204	1.2219	2.2677	1.2729
1.192065	371.65	0.01504	214.6368	1.2219	3.0953	1.7374
0.596033	371.02	0.01719	212.4087	1.2219	4.7619	2.6727
0.101325	369.22	0.02132	208.1594	1.2219	21.4029	12.0146

Table 6D (Continued)

THERMODYNAMIC PHASE PROPERTIES OF AN ISENTROPICALLY EXPANDED
JET A - SIMPLE AIR SATURATED LIQUID SYSTEM

Pressure (MPa)	Temperature (K)	x	h_f (kJ/kg)	h_g (kJ/kg)	s_f (kJ/kg-K)	s_g (kJ/kg-K)	$v_f \times 10^3$ (m^3/kg)	v_g (m^3/kg)
Inlet Condition:								
5.960325	373.15	0.0	224.6962	373.4083	1.2219	5.8870	1.7815	0.01842
Outlet Conditions:								
4.768260	372.93	0.00369	221.9673	373.9807	1.2044	5.9536	1.7827	0.02287
3.576195	372.66	0.00741	219.0863	374.5902	1.1860	6.0363	1.7837	0.03027
2.384130	372.28	0.01117	215.9407	375.2832	1.1663	6.1467	1.7846	0.04503
1.192065	371.65	0.01504	212.1673	376.3685	1.1441	6.3160	1.7850	0.08891
0.596033	371.02	0.01719	209.5140	377.9361	1.1305	6.4479	1.7847	0.17498
0.101325	369.22	0.02132	204.1761	390.9883	1.1102	6.3480	1.7821	0.92208

Table 6E

SOLUBILITY PROPERTIES OF AN ISENTROPICALLY EXPANDED
JET A - SIMPLE AIR SATURATED LIQUID SYSTEM

Pressure (MPa)	Temperature (K)	x	Component	x_i	y_i
Inlet Condition:					
0.515210	473.15	0.0	Jet A	0.990000	0.179898
			N_2	0.007900	0.676503
Outlet Conditions:			O_2	0.002100	0.143599
Outlet Conditions:					
0.412168	473.07	0.00110	Jet A	0.992373	0.222450
			N_2	0.005959	0.222450
			O_2	0.001668	0.141976
0.309126	472.92	0.00282	Jet A	0.994760	0.292563
			N_2	0.004046	0.572588
			O_2	0.001194	0.134849
0.206084	472.57	0.00668	Jet A	0.997154	0.429191
			N_2	0.002169	0.457118
			$)_2$	0.000676	0.113692
0.101325	469.68	0.03824	Jet A	0.999486	0.792473
			N_2	0.000336	0.164356
			O_2	0.000128	0.043171

Table 6E (Continued)

THERMODYNAMIC MIXTURE PROPERTIES OF AN ISENTROPICALLY EXPANDED
JET A - SIMPLE AIR SATURATED LIQUID SYSTEM

Pressure (MPa)	Temperature (K)	x	h_m (kJ/kg)	s_m (kJ/kg-K)	$v_m \times 10^3$ (m^3/kg)	VR
Inlet Condition:						
0.515210	473.15	0.0	479.0957	1.7696	2.0089	1.0
Outlet Conditions:						
0.412168	473.07	0.00110	478.8808	1.7696	2.1793	1.0848
0.309126	472.92	0.00282	478.6415	1.7696	2.5073	1.2479
0.206084	472.57	0.00668	478.3469	1.7696	3.3880	1.6865
0.101325	469.63	0.03824	477.7625	1.7696	11.9976	5.9728

Table 6E (Continued)

THERMODYNAMIC PHASE PROPERTIES OF AN ISENTROPICALLY EXPANDED
JET A - SIMPLE AIR SATURATED LIQUID SYSTEM

Pressure (MPa)	Temperature (K)	x	h_f (kJ/kg)	h_g (kJ/kg)	s_f (kJ/kg-K)	s_g (kJ/kg-K)	$v_f \times 10^3$ (m^3/kg)	v_g (m^3/kg)
Inlet Condition:								
0.515210	473.15	0.0	479.0957	619.8631	1.7696	4.3113	2.0089	0.1400
Outlet Conditions:								
0.412168	473.07	0.00110	478.7084	635.3923	1.7671	4.0449	2.0088	0.1570
0.309126	472.92	0.00282	478.1426	655.1951	1.7642	3.6929	2.0084	0.1789
0.206084	472.57	0.00668	476.9844	680.9649	1.7600	3.2088	2.0074	0.2087
0.101325	469.68	0.03824	468.5428	709.6162	1.7402	2.5097	1.9984	0.0758

Table 6F

SOLUBILITY PROPERTIES OF AN ISENTROPICALLY EXPANDED
JET A - SIMPLE AIR SATURATED LIQUID SYSTEM

Pressure (MPa)	Temperature (K)	x	Component	x_i	y_i
Inlet Condition:					
4.716380	473.15	0.0	Jet A	0.900000	0.025596
			N_2	0.079000	0.802737
			O_2	0.021000	0.171667
Outlet Conditions:					
3.773104	472.88	0.00451	Jet A	0.918958	0.030061
			N_2	0.063436	0.793179
			O_2	0.017606	0.176760
2.829820	472.52	0.00936	Jet A	0.938609	0.037521
			N_2	0.047581	0.780861
			O_2	0.013810	0.181618
1.886552	471.96	0.01510	Jet A	0.958482	0.052342
			N_2	0.031454	0.762311
			O_2	0.009564	0.185347
0.943216	470.78	0.02457	Jet A	0.980085	0.095589
			N_2	0.015096	0.720888
			O_2	0.004820	0.183522
0.471638	468.98	0.03848	Jet A	0.990867	0.176596
			N_2	0.006879	0.653167
			O_2	0.002259	0.170237
0.101325	455.93	0.15708	Jet A	0.998979	0.561830
			N_2	0.000763	0.346303
			O_2	0.000258	0.091867

Table 6F (Continued)

THERMODYNAMIC MIXTURE PROPERTIES OF AN ISENTROPICALLY EXPANDED
JET A - SIMPLE AIR SATURATED LIQUID SYSTEM

Pressure (MPa)	Temperature (K)	x	h_m (kJ/kg)	s_m (kJ/kg-K)	$v_m \times 10^3$ (m^3/kg)	VR
Inlet Condition:						
4.716380	473.15	0.0	485.0349	1.8436	2.0022	1.0
Outlet Conditions:						
3.773104	472.88	0.00451	483.0870	1.8436	2.1385	1.0681
2.829828	472.52	0.00936	480.5181	1.8436	2.3700	1.2172
1.886552	471.96	0.01510	478.5431	1.8436	2.8455	1.4211
0.943276	470.78	0.002457	475.3175	1.8436	4.3584	2.1770
0.471638	468.98	0.03848	472.6569	1.8436	7.7954	3.8937
0.101325	455.93	0.15708	466.2086	1.8436	54.8576	27.4000

Table 6F (Continued)

THERMODYNAMIC PHASE PROPERTIES OF AN ISENTROPICALLY EXPANDED
JET A - SIMPLE AIR SATURATED LIQUID SYSTEM

Pressure (MPa)	Temperature (K)	x	h_f (kJ/kg)	h_g (kJ/kg)	s_f (kJ/kg-K)	s_g (kJ/kg-K)	$v_f \times 10^3$ (m^3/kg)	v_g (m^3/kg)
Inlet Condition:								
4.716380	473.15	0.0	485.0349	511.0828	1.8436	5.7093	2.0022	0.02632
Outlet Conditions:								
3.773104	472.88	0.00451	482.9387	515.8124	1.8262	5.6858	2.0029	0.03207
2.829828	472.52	0.00936	480.5704	523.4156	1.8079	5.6261	2.0034	0.04118
1.886552	471.96	0.01510	477.6422	537.3149	1.7880	5.4767	2.0032	0.05779
0.943276	470.78	0.02457	472.9334	569.9545	1.7636	5.0209	2.0011	0.9795
0.471638	468.98	0.03848	467.1582	610.0452	1.7438	4.3394	1.9964	0.15270
0.101325	455.91	0.15708	429.8282	661.4287	1.6571	2.8448	1.9594	0.33872

8. Summary and Conclusions

The overall objective of the present investigation was to determine the thermodynamic properties of Jet A fuel saturated with dissolved air at high pressures. This information is needed for subsequent development of the supercritical injector concept, proposed by Marek [1].

Supercritical injection involves dissolving air into a fuel prior to injection. When the saturated mixture passes through the injector, the reduction of pressure causes the air to come out of solution, similar to the flashing of a superheated liquid. Flashing is known to enhance atomization and the presence of air in the primary zone of a spray flame is known to reduce pollutant emissions; therefore, supercritical injection has the potential to improve the performance of spray burners.

The specific objectives of the present investigation were: (1) to measure the solubility and density characteristics of fuel-gas mixtures, (2) to correlate these results using basic thermodynamic theory, and (3) to theoretically examine the isentropic expansion characteristics of such mixtures. The practical fuel system, Jet A - air, was of primary concern; however, the systems Jet A - nitrogen, n-dodecane - nitrogen and n-dodecane - air were also considered, in order to help establish theoretical methods.

Specific test arrangements were developed for the solubility and density measurements. The range of the experiments included pressures of 1.03-10.34 MPa and temperatures of 298-373 K, for the systems mentioned earlier. Experimental results were also obtained from earlier studies [19-22] for evaluation of theoretical methods.

The theory involved application of the multicomponent forms of both the Redlich-Kwong [9], and Soave [13] equations of state; however, the present data was largely correlated using the Soave approach. A computer program, based on the work of Starling [15], was developed to facilitate computations of solubility, density and isentropic expansion properties.

The major conclusions of the investigation can be summarized as follows:

1. The present solubility and density measurements could be correlated by selecting reasonable values for the binary interaction parameters in the Soave equation of state. This was accomplished by treating Jet A as a pseudo-compound.

2. For the present test range, the solubility of air in Jet A was roughly proportional to pressure. The solubility also increased with temperature, but the temperature dependence was relatively weak. Maximum observed solubilities were at 373 K and 10.34 MPa, where the mass fraction of dissolved air in the liquid was 0.0227-0.0267, depending on the particular sample of Jet A tested.

3. The effect of dissolved air on liquid density was small. Temperature variations resulted in density variations typical of hydrocarbon blends.

4. Solubility predictions are reported over a wider range than the experiments. These results show that the mass fraction of dissolved air approaches a maximum of 0.6 near the thermodynamic critical point of the mixture.

5. Computations were completed for the isentropic expansion of initially saturated dissolved air - Jet A mixtures. The presence of dissolved air appreciably increases the volumetric expansion ratio of the flow, which should result in improved atomization, particularly at low back pressures.

6. The Soave equation of state provided the best correlation of data for conditions not too near the thermodynamic critical point. In contrast, the Redlich-Kwong equation of state provided a fair correlation over the entire range of the data, and was clearly superior in the near-critical region.

With thermodynamic properties and solubility levels established, current efforts are considering the supercritical injection concept. This involves evaluation of both injector atomization properties and combustion performance.

REFERENCES

1. Marek, J., Personal Communication, 1979.

2. Sher, E. and C. Elata, "Spray Formation from Pressure Cans by Flashing," Ind. Eng. Chem. Process Des. Dev., Vol. 16, pp. 237-242, 1977.

3. Brown, R. and J. L. York, "Sprays Formed by Flashing Liquid Jets," AIChE J., Vol. 8, pp. 149-153, 1962.

4. Suzuki, M., Yamamoto, T., Fatagami, N. and S. Maeda, "Atomization of a Superheated Liquid Jet," Proceedings of First International Conference on Liquid Atomization and Spray Systems, Tokyo, August 1978.

5. Faeth, G. M., Dominicis, D. P., Tulpinski, J. F. and D. R. Olson, "Supercritical Bipropellant Droplet Combustion," Twelfth Symposium (International) on Combustion, The Combustion Institute, Pittsburgh, pp. 9-18, 1969.

6. Lazar, R. S. and G. M. Faeth, "Bipropellant Droplet Combustion in the Vicinity of the Critical Point," Thirteenth Symposium (International) on Combustion, The Combustion Institute, Pittsburgh, pp. 801-811, 1970.

7. Canada, G. S. and G. M. Faeth, "Full Droplet Burning Rates at High Pressures," The Combustion Institute, Pittsburgh, pp. 1345-1354, 1972.

8. Canada, G. S. and G. M. Faeth, "Combustion of Liquid Fuels in a Flowing Combustion Gas Environment at High Pressures," The Combustion Institute, Pittsburgh, pp. 419-423, 1974.

9. Prausnitz, J. M. and P. L. Chueh, Computer Calculations for High Pressure Vapor-Liquid Equilibrium, Prentice-Hall, New York, 1968.

10. Graboski, M. S. and T. E. Daubert, "A Modified Soave Equation of State for Phase Equilibrium Calculations," Ind. Engr. Chem. Process Des. Dev., Vol. 17, pp. 443-448, 1978.

11. Graboski, M. S. and T. E. Daubert, "A Modified Soave Equation of State for Phase Equilibrium Calculations, 2. Systems Containing CO_2, H_2S, N_2 and CO," Ind. Engr. Chem. Process Des. Dev., Vol. 17, pp. 448-459, 1978.

12. Graboski, M. S. and T. E. Daubert, "A Modified Soave Equation of State for Phase Equilibrium Calculations, 3. Systems Containing Hydrogen," Ind. Engr. Chem. Process Des. Dev., Vol. 18, pp. 300-305, 1979.

13. Soave, G., "Equilibrium Constants from a Modified Redlich-Kwong Equation of State," Chem. Engr. Sci., Vol. 27, pp. 1197-1203, 1972.

14. Technical Data Book - Petroleum Refining, 3rd Edition, American Petroleum Institute, Washington, DC, 1976.

15. Starling, K. E., Fluid Thermodynamic Properties for Light Petroleum Systems, Gulf Publishing Company, Houston, 1973.

16. Reid, R. C. and T. W. Leland, Jr., "Pseudocritical Constants," AIChE J., Vol. 11, pp. 228-237, 1965.

17. Chueh, P. L. and J. M. Prausnitz, "Vapor-Liquid Equilibrium at High Vapor Pressures. Vapor Phase Fugacity Coefficients in Nonpolar and Quantum Gas Mixtures," Ind. Engr. Chem. Fundam., Vol. 6, pp. 492-504, 1967.

18. Faith, L. E., Ackerman, G. H. and H. T. Henderson, "Heat Sink Capability of Jet A Fuel: Heat Transfer and Coking Studies," NASA CR-72951.S-14115, 1971.

19. Harris, H. G. and J. M. Prausnitz, "Thermodynamic Properties of Binary Mixtures of I-Hexyne and Polar Organic Solvents, AIChE J., Vol. 14, pp. 737-740, 1968.

20. Muirbrook, N. K. and J. M. Prausnitz, "Multicomponent Vapor-Liquid Equilibria at High Pressures: Part I. Experimental Study of Nitrogen-Oxygen-Carbon Dioxide System at 0°C," AIChE J., Vol. 11, pp. 1092-1096, 1965.

21. Zennes, G. H. and L. I. Dana, "Liquid-Vapor Equilibrium Compositions of Carbon Dioxide-Oxygen-Nitrogen Mixtures," Chem. Engr. Prog. Symp. Series, Vol. 59, No. 44, pp. 36-41, 1963.

22. Lazar, R. S., "Bipropellant Droplet Combustion in the Vicinity of the Critical Point," Ph.D. Thesis, The Pennsylvania State University, University Park, Pennsylvania, 1970.

23. Azarnoosh, A. and S. S. McKetta, "Nitrogen-n-Decane System in the Two Phase Region," J. Chem. Engr. Data, Vol. 8, pp. 494-496, 1963.

24. Poston, R. S. and S. S. McKetta, "Vapor-Liquid Equilibrium in the n-Hexane-Nitrogen System," J. Chem. Engr. Data, Vol. 11, pp. 364-365, 1966.

25. Poettmann, F. H. and D. L. Katz, "Phase Behavior of Binary Carbon Dioxide-Paraffin Systems," Ind. Engr. Chem., Vol. 37, pp. 847-853, 1945.

26. Keramati, B. and C. H. Wolgemuth, "Device for the Direct Measurement of Fluid Densities," Rev. Sci. Instr., Vol. 46, pp. 1513-1577, 1975.

APPENDIX A

COMPUTER PROGRAM

```
C  MAIN PROGRAM
      IMPLICIT REAL*8 (A-H,O-Z)
      COMMON/VLE01/NC,NTYPE,MOD,MODF,NOUT
      COMMON/VLE04/DELP,PF,TF,PI,TI,P,T
      COMMON/VLE05/XK(10),X(10),Y(10),Z(10)
      COMMON/VLE07/FS
      COMMON/VLE10/V,FL,XX,VR
      COMMON/VLE11/VLM,VVM,DENL,DENV,RMWL,RMWV,RMWF
      COMMON/VLE14/HL,HV,SL,SV,HM,SM
      CALL INPUT
      CALL INDEP
      MOD=0
      XV=DLOG(PI)
      FS=0.0D0
      CALL SERCH(XV)
      PI=DEXP(XV)
      SUMY=0.0D0
      DO 10 I=1,NC
   10 SUMY=SUMY+Y(I)
      DO 20 I=1,NC
      Z(I)=X(I)
   20 Y(I)=Y(I)/SUMY
      T=TI
      P=PI
      V=0.0D0
      CALL DENSIT
      CALL DEPART
      CALL IDEAL
      CALL ABSOL
      XX=0.0D0
      VL=1.0D0/DENL
      VM=VL
      VMS=VM
      HM=HL
      VR=1.0D0
      SM=SL
      CALL OUTPUT
      IF(NTYPE.EQ.0) GO TO 999
      PF=PI*DELP
      NA=0
      IF((TF-TI).LE.0.0D0) GO TO 30
      WRITE(6,100)
      GO TO 999
   30 FS=SM
      P=PF
      XV=T
      MOD=1
      CALL SERCH(XV)
      T=XV
      VL=1.0D0/DENL
      VV=1.0D0/DENV
      VM=XX*VV+(1.0D0-XX)*VL
      VR=VM/VMS
      CALL OUTPUT
      IF(NA.EQ.1)GO TO 999
      DELP=DELP-0.20
      PF=PI*DELP
      IF(PF.GT.14.696D0) GO TO 40
      READ(5,*)DELP
```

```
      NA=1
      PF=PI*DELP
   40 GO TO 30
  999 STOP
  100 FORMAT('0','TF>TI CALCULATION ABORTED')
      END
      SUBROUTINE INPUT
      IMPLICIT REAL*8 (A-H,O-Z)
      COMMON/VLE01/NC,NTYPE,MOD,MODF,NOUT
      COMMON/VLE02/AK(10,10),RMW(10),PC(10),TC(10),W(10),ID(10),NAME(10)
      COMMON/VLE03/A(10),B(10),C(10),D(10),E(10),F(10),G(10)
      COMMON/VLE04/DELP,PF,TF,PI,TI,P,T
      COMMON/VLE05/XK(10),X(10),Y(10),Z(10)
      COMMON/VLE15/ZC(10)
      CHARACTER * 15 NAME
      READ(5,100)NC,NTYPE
      DO 10 I=1,NC
   10 READ(5,200)ID(I),NAME(I),RMW(I),TC(I),PC(I),ZC(I),W(I)
      DO 20 I=1,NC
      READ(5,*) A(I),B(I),C(I),D(I)
   20 READ(5,*)E(I),F(I),G(I)
      NC1=NC-1
      DO 40 I=1,NC
   40 AK(I,I)=0.0D0
      DO 50 I=1,NC1
      I1=I+1
      DO 50 J=I1,NC
      READ(5,*)AK(I,J)
   50 AK(J,I)=AK(I,J)
C  ECHOE PROPERTY DATA
      WRITE(6,300)
      DO 60 I=1,NC
   60 WRITE(6,400)I,NAME(I),ID(I),RMW(I),TC(I),PC(I),ZC(I),W(I)
      WRITE(6,500)
      DO 70 I=1,NC
   70 WRITE(6,600)NAME(I),A(I),B(I),C(I),D(I),E(I),F(I),G(I)
      WRITE(6,700)
      DO 80 I=1,NC1
      I1=I+1
      DO 80 J=I1,NC
   80 WRITE(6,800)I,J,AK(I,J)
      READ(5,*)TI,PI
      DO 90 I=1,NC
   90 READ(5,*)X(I),Y(I)
      WRITE(6,900)PI
      DO 110 I=1,NC
  110 WRITE(6,1000)I,Y(I)
      IF(NTYPE.EQ.0) GO TO 120
      READ(5,*)TF,DELP
      WRITE(6,1100)
      GO TO 130
  120 WRITE(6,1200)
  130 RETURN
  100 FORMAT(2I2)
  200 FORMAT(I3,T5,A15,5F10.4)
  300 FORMAT('1',29('*'),'CRITICAL PROPERTY DATA',29('*'),
     1       //' ',T38,'IDNO.',T48,'MW',T58,'TC',T68,'PC',T78,'ZC',T88,'W
     2')
```

```
 400 FORMAT(' ','COMPONENT  ',I2,':  ',A15,T39,I2,T45,F8.3,T55,F8.3,T65
    1,F8.3,T76,F6.4,T85,F7.4)
 500 FORMAT('0',19('*'),'IDEAL GAS ISOBARIC HEAT CAPACITY CONSTANTS',
    119('*'),//' ',T25,'A',T40,'B',T55,'C',T70,'D',T85,'E',T100,'F',
    2T115,'G')
 600 FORMAT(' ',A15,T18,1P1D12.5,T33,1P1D12.5,
    1T48,1P1D12.5,T63,1P1D12.5,T78,1P1D12.5,T93,1P1D12.5,T108,1P1D12.5)
 700 FORMAT('0','SOAVE BINARY INTERACTION COEFFICIENTS :')
 800 FORMAT(' ',T16,'K(',I2,',',I2,')=',F6.4)
 900 FORMAT('0','BUBBLE PT. INITIAL GUESSES :',
    1      /' ',T16,'PI=',F10.3,'PSIA')
1000 FORMAT(' ',T16,'Y(',I1,')=',F8.6)
1100 FORMAT('0',26('*'),'ISENTROPIC EXPANSION PROCESS',26('*'),
    1      /' ',80('*'),
    2      //' ',10('*-'),'INLET VLE BUBBLE PT PRESSURE CALCULATION',
    310('*-'),/)
1200 FORMAT('0',20('*-'),'VLE BUBBLE PT. PRESSURE CALCULATION',
    120('*-'))
     END
     SUBROUTINE INDEP
     IMPLICIT REAL*8 (A-H,O-Z)
     COMMON/VLE01/NC,NTYPE,MOD,MODF,NOUT
     COMMON/VLE02/AK(10,10),RMW(10),PC(10),TC(10),W(10),ID(10),NAME(10)
     COMMON/VLE06/ALPHA(10),SA(10),SB(10),S(10)
     CHARACTER * 15 NAME
     R=10.731
     DO 10 I=1,NC
     TCR=TC(I)+459.67D0
     SA(I)=(0.42747D0*(R*TCR)**2)/PC(I)
     SB(I)=0.08664D0*R*TCR/PC(I)
  10 S(I)=0.48508D0+1.55171D0*W(I)-0.151613D0*W(I)**2
     RETURN
     END
     SUBROUTINE SERCH(XV)
     IMPLICIT REAL*8 (A-H,O-Z)
     COMMON/VLE01/NC,NTYPE,MOD,MODF,NOUT
     COMMON/VLE07/FS
     DIMENSION XN(60),FN(60)
     IT=1
     ITM=50
     IF(MOD)10,10,20
  10 CALL BUBBLE(XV,YV)
     GO TO 30
  20 CALL FLASH(XV,YV)
  30 XN(IT)=XV
     FN(IT)=YV
     IT=IT+1
     IF(IT-3)40,40,50
  40 XV=XV*1.01
     IF(MOD)10,10,20
  50 XINC=-(XN(IT-1)-XN(IT-2))/(FN(IT-1)-FN(IT-2))*(FN(IT-1)-FS)
  60 DXN=DABS(XINC)-0.5D0*DABS(XN(IT-1))
     IF(DXN)80,80,70
  70 XINC=0.5D0*XINC
     GO TO 60
  80 XN(IT)=XN(IT-1)+XINC
     DELTA=DABS(XN(IT)-XN(IT-1))
     IF(DELTA-1.0D-05)130,130,90
  90 IF(IT-ITM)110,110,120
```

```
  110 XV=XN(IT)
      IF(MOD)10,10,20
  120 WRITE(6,100)
  130 XV=XN(IT)
      RETURN
  100 FORMAT('SERCH ITERATION LIMIT EXCEEDED')
      END
      SUBROUTINE BUBBLE(XV,YV)
      IMPLICIT REAL*8 (A-H,O-Z)
      COMMON/VLE01/NC,NTYPE,MOD,MODF,NOUT
      COMMON/VLE04/DELP,PF,TF,PI,TI,P,T
      COMMON/VLE08/ZLS,ZVS,ZL,ZV
      COMMON/VLE09/PHIL(10),PHIV(10),FUL(10),FUV(10)
      COMMON/VLE05/XK(10),X(10),Y(10),Z(10)
      NOUT=0
      MODF=0
      T=TI
      P=DEXP(XV)
C CALL FUGAC TO CALCULATE LIQUID PHASE FUGACITY OF EACH COMPONENT
      CALL FUGAC
      ZLS=ZL
      IF(NOUT)10,10,999
   10 MODF=1
      ITN=1
      ITNM=30
C  BEGIN INNER VAPOR FUGACITY LOOP
C  CALL FUGAC TO CALCULATE VAPOR PHASE FUGACITY OF EACH COMPONENT
   20 CALL FUGAC
      ZVS=ZV
      IF(NOUT)30,30,999
   30 DO 40 I=1,NC
      XK(I)=(FUL(I)*Y(I))/(FUV(I)*X(I))
      IF(DABS(XK(I)).GE.1.0D-12) GO TO 40
      XK(I)=1.0D-12
   40 CONTINUE
C  CHECK IF THE INDIVIDUAL FUGACITIES OF THE LIQUID AND VAPOR PHASES
C  OF EACH COMPONENT ARE EQUAL.
      DO 50 I=1,NC
      DELFU=FUL(I)/FUV(I)-1.0D0
      IF(DABS(DELFU).GE.1.0D-04) GO TO 60
   50 CONTINUE
      GO TO 90
   60 ITN=ITN+1
      IF(ITN.GT.ITNM)GO TO 80
      DO 70 I=1,NC
   70 Y(I)=X(I)*XK(I)
      GO TO 20
   80 WRITE(6,100)
      GO TO 999
   90 SUM=0.0D0
      DO 110 I=1,NC
  110 SUM=SUM+X(I)*XK(I)
C  CALCULATE DEVIATIONOF SUM FROM ITS REQUIRED VALUE OF 1.0
      YV=SUM-1.0D0
  999 RETURN
  100 FORMAT('0','FUGACITIES FAILED TO CONVERGE IN ITNM ITERATIONS')
      END
      SUBROUTINE FLASH(XV,YV)
```

```
      IMPLICIT REAL*8 (A-H,O-Z)
      COMMON/VLE01/NC,NTYPE,MOD,MODF,NOUT
      COMMON/VLE04/DELP,PF,TF,PI,TI,P,T
      COMMON/VLE05/XK(10),X(10),Y(10),Z(10)
      COMMON/VLE08/ZLS,ZVS,ZL,ZV
      COMMON/VLE09/PHIL(10),PHIV(10),FUL(10),FUV(10)
      COMMON/VLE10/V,FL,XX,VR
      COMMON/VLE11/VLM,VVM,DENL,DENV,RMWL,RMWV,RMWF
      COMMON/VLE14/HL,HV,SL,SV,HM,SM
      T=XV
      ITN=1
      ITNM=20
      CALL KI
    1 FL=0.5D0
        ITMAX=50
C*************************************************************
      TESTV=0.0D0
      TESTL=0.0D0
      DO 5 I=1,NC
      TESTL=TESTL+XK(I)*Z(I)
    5 TESTV=TESTV+Z(I)/XK(I)
      IF(TESTL-1.0D0)7,160,7
    7 IF(TESTV-1.0D0)8,210,8
C*************************************************************
    8 IT=0
      V=1.0D0-FL
   10 FVA=0.0D0
      FVAD=0.0D0
      DO 20 I=1,NC
      FVA=FVA+(Z(I)*(XK(I)-1.0D0))/(V*(XK(I)-1.0D0)+1.0D0)
      WW=(XK(I)-1.0D0)/(V*(XK(I)-1.0D0)+1.0D0)
   20 FVAD=FVAD+Z(I)*WW**2
      IF(DABS(FVA)-1.0D-05)80,30,30
   30 CONTINUE
      V=V+FVA/FVAD
      IF(IT-ITMAX)40,70,70
   40 CONTINUE
      IT=IT+1
      IF(V-1.0D0)50,50,240
   50 IF(V)250,60,60
   60 CONTINUE
      GO TO 10
   70 WRITE(6,100)V,IT
      GO TO 120
   80 FL=1.0D0-V
      SUMX=0.0D0
      SUMY=0.0D0
      DO 90 I=1,NC
       Y(I)=(Z(I)*XK(I))/(V*(XK(I)-1.0D0)+1.0D0)
      X(I)=Y(I)/XK(I)
      SUMX=SUMX+X(I)
      SUMY=SUMY+Y(I)
   90 CONTINUE
      DO 110 I=1,NC
      X(I)=X(I)/SUMX
      Y(I)=Y(I)/SUMY
  110 CONTINUE
      GO TO 260
```

```
  120 IF(V)160,160,130
  130 IF(V-1.0D0)140,210,210
  140 ITMAX=100
      IF(IT-ITMAX)10,10,150
  150 WRITE(6,200)V,IT
      GO TO 80
C*****************************************************************
  160 WRITE(6,300)
      V=0.0D0
      DO 170 I=1,NC
      X(I)=Z(I)
  170 Y(I)=Z(I)*XK(I)
      SUMY=0.0D0
      DO 180 I=1,NC
  180 SUMY=SUMY+Y(I)
      DO 190 I=1,NC
      Y(I)=Y(I)/SUMY
  190 XK(I)=Y(I)/X(I)
      RETURN
C*****************************************************************
C*****************************************************************
  210 WRITE(6,400)
      V=1.0D0
      DO 220 I=1,NC
      X(I)=Z(I)/XK(I)
  220 Y(I)=Z(I)
      SUMX=0.0D0
      DO 230 I=1,NC
  230 SUMX=SUMX+X(I)
      DO 235 I=1,NC
      X(I)=X(I)/SUMX
  235 XK(I)=Y(I)/X(I)
      RETURN
C*****************************************************************
  240 V=V-FVA/FVAD
      V=V+(1.0D0-V)/2.0D0
      GO TO 10
  250 V=V-FVA/FVAD
      V=V*0.5D0
      GO TO 10
  260 MODF=0
      CALL FUGAC
      ZLS=ZL
      IF(NOUT)270,270,999
  270 MODF=1
      CALL FUGAC
      ZVS=ZV
      IF(NOUT)280,280,999
  280 DO 290 I=1,NC
      XK(I)=(FUL(I)*Y(I))/(FUV(I)*X(I))
      IF(DABS(XK(I)).GE.1.0D-12)GO TO 290
      XK(I)=1.0D-12
  290 CONTINUE
      DO 310 I=1,NC
      DELFU=FUL(I)/FUV(I)-1.0D0
      IF(DABS(DELFU).GE.1.0D-04) GO TO 320
  310 CONTINUE
      GO TO 340
  320 ITN=ITN+1
```

```
      IF(ITN.GT.ITNM)GO TO 330
      GO TO 1
  330 WRITE(6,500)
      GO TO 999
  340 CALL DENSIT
      CALL DEPART
      CALL IDEAL
      CALL ABSOL
C  CALCULATE MASS FRACTION
      XX=V*RMWV/RMWF
      HM=XX*HV+(1.0D0-XX)*HL
      SM=XX*SV+(1.0D0-XX)*SL
      YV=SM
  999 RETURN
  100 FORMAT('0','FLASH ITERATION LIMIT EXCEEDED V=',F6.2,'IT=',I3)
  200 FORMAT('0','SECOND FLASH ITERATION LIMIT EXCEEDED V=',F6.2,'IT=',
     1I3)
  300 FORMAT('0','FLASH GIVES V<0')
  400 FORMAT('0','FLASH GIVES V>0')
  500 FORMAT('0','FUGACITY ITERATION LIMIT EXCEEDED')
      END
      SUBROUTINE FUGAC
      IMPLICIT REAL*8 (A-H,O-Z)
      COMMON/VLE01/NC,NTYPE,MOD,MODF,NOUT
      COMMON/VLE02/AK(10,10),RMW(10),PC(10),TC(10),W(10),ID(10),NAME(10)
      COMMON/VLE04/DELP,PF,TF,PI,TI,P,T
      COMMON/VLE05/XK(10),X(10),Y(10),Z(10)
      COMMON/VLE06/ALPHA(10),SA(10),SB(10),S(10)
      COMMON/VLE08/ZLS,ZVS,ZL,ZV
      COMMON/VLE09/PHIL(10),PHIV(10),FUL(10),FUV(10)
      DIMENSION XY(10),ALPHAA(10,10)
      CHARACTER * 15 NAME
      IF(MODF.EQ.1)GO TO 20
      DO 10 I=1,NC
   10 XY(I)=X(I)
      GO TO 40
   20 DO 30 I=1,NC
   30 XY(I)=Y(I)
   40 TR=T+459.67D0
      XB=0.0D0
      XALPHA=0.0D0
      DO 50 I=1,NC
      TC1=TC(I)+459.67D0
      T1=TR/TC1
      ALPHA(I)=(1.0D0+S(I)*(1.0D0-DSQRT(T1)))**2
   50 XB=XB+XY(I)*SB(I)
      DO 55 I=1,NC
      DO 55 J=1,NC
      ALPHAA(I,J)=(1.0D0-AK(I,J))*DSQRT(ALPHA(I)*SA(I)*ALPHA(J)*SA(J))
   55 XALPHA=XALPHA+XY(I)*XY(J)*ALPHAA(I,J)
      R=10.7313D0
      TR=T+459.67D0
      A=XALPHA*P/(R*TR)**2
      B=XB*P/(R*TR)
      XP=-1.0D0
      Q=A-B-(B*B)
      R=-(A*B)
C CALL THE CUBIC SOLVER TO SOLVE THE SOAVE CUBIC COMPRESSIBILITY
```

```
C EQUATION. CUBIC RETURNS ONLY TWO OF THE THREE POSSIBLE ROOTS. THE
C SMALLEST ROOT MUST BE USED FOR THE LIQUID PHASE(ZL), AND THE
C GREATEST ROOT MUST BE USED FOR THE VAPOR PHASE(ZV).
      CALL CUBIC(XP,Q,R,ZV,ZL)
      IF(MODF.EQ.1) GO TO 60
      XZ=ZL
      GO TO 70
   60 XZ=ZV
   70 IF((XZ-B).LE.0.0D0.OR.(1.0D0+B/XZ).LE.0.0D0)NOUT=1
      IF(NOUT.NE.1) GO TO 80
      WRITE(6,100)
  100 FORMAT('0','COMPRESSIBILITY FACTORS SUPPLIED BY CUBIC WILL NOT
     1 YIELD A PHYSICALLY REALISTIC FUGACITY COEFFICIENT.')
      GO TO 999
   80 DO 120 I=1,NC
      SUM=0.0D0
      DO 90 J=1,NC
C CALCULATE THE FUGACITY COEFFICIENT PHI AND THE FUGACITY.
   90 SUM=SUM+XY(J)*ALPHAA(I,J)
      PHI1=(SB(I)/XB)*(XZ-1.0D0)
      PHI2=DLOG(XZ-B)
      PHI3=2.0D0*SUM/XALPHA-SB(I)/XB
      PHI4=DLOG(1.0D0+B/XZ)
      PHI=PHI1-PHI2-A/B*PHI3*PHI4
      IF(MODF.EQ.1) GO TO 110
      PHIL(I)=DEXP(PHI)
      FUL(I)=XY(I)*P*DEXP(PHI)
      GO TO 120
  110 PHIV(I)=DEXP(PHI)
      FUV(I)=XY(I)*P*DEXP(PHI)
  120 CONTINUE
  999 RETURN
      END
      SUBROUTINE CUBIC(XP,Q,R,ZH,ZL)
C THIS SUBROUTINE SOLVES FOR THE THREE ROOTS OF THE SOAVE CUBIC
C COMPRESSIBILITY EQUATION. IT RETURNS WITH ONLY THE HIGH AND LOW
C ROOTS, FOR THE VAPOR AND LIQUID PHASES RESPECTIVELY.
      IMPLICIT REAL*8 (A-H,O-Z)
      COMMON/VLE01/NC,NTYPE,MOD,MODF,NOUT
      DIMENSION RT(3),ANS(2)
      P=XP
      DO 50 I=1,3
50    RT(I)=0.0D0
      A=Q-(P*P/3.D0)
      B=2.0D0*P*P*P/27.D0-P*Q/3.D0+R
      NOUT=0
      IF(A.EQ.0.D0.OR.B.EQ.0.D0) GO TO 20
      ANS(1)=DLOG10(DABS(A))*3.D0
      ANS(2)=DLOG10(DABS(B))*2.D0
      DO 10 I=1,2
10    IF(ANS(I).LE.-78.268D0.OR.ANS(I).GE.75.859D0) NOUT=1
   20 IF(NOUT) 70,70,500
70    YY=B*B/4.D0+A*A*A/27.D0
      ZZ=-B/2.D0
      IF(YY) 100,101,102
100   PHI=DARCOS((-B/2.D0)/DSQRT(-A*A*A/27.D0))
      RT(1)=2.D0*DSQRT(-A/3.D0)*DCOS(PHI/3.D0)-P/3.D0
      RT(2)=2.D0*DSQRT(-A/3.D0)*DCOS(PHI/3.D0+2.0944D0)-P/3.D0
      RT(3)=2.D0*DSQRT(-A/3.D0)*DCOS(PHI/3.D0+4.1888D0)-P/3.D0
```

```
      GO TO 300
101   RT(1)=2.D0*ZZ**(1.D0/3.D0)-P/3.D0
      RT(2)=-ZZ**(1.D0/3.D0)-P/3.D0
      RT(3)=RT(2)
      GO TO 300
102   EXPON=1.D0/3.D0
      Y=DSQRT(YY)
      IF((ZZ+Y).LT.0.) GO TO 103
      AA=(ZZ+Y)**EXPON
      GO TO 104
103   AA=-(DABS(ZZ+Y)**EXPON)
104   IF((ZZ-Y).LT.0.) GO TO 105
      BB=(ZZ-Y)**EXPON
      GO TO 106
105   BB=-(DABS(ZZ-Y)**EXPON)
106   DO 107 I=1,3
  107 RT(I)=AA+BB-P/3.D0
300   ZH=RT(1)
      ZL=RT(1)
      DO 400 I=2,3
      IF(RT(I).GT.ZH) ZH=RT(I)
400   IF(RT(I).LT.ZL) ZL=RT(I)
500   RETURN
      END
      SUBROUTINE KI
      IMPLICIT REAL*8 (A-H,O-Z)
      COMMON/VLE01/NC,NTYPE,MOD,MODF,NOUT
      COMMON/VLE02/AK(10,10),RMW(10),PC(10),TC(10),W(10),ID(10),NAME(10)
      COMMON/VLE04/DELP,PF,TF,PI,TI,P,T
      COMMON/VLE05/XK(10),X(10),Y(10),Z(10)
      COMMON/VLE15/ZC(10)
      CHARACTER * 15 NAME
      DO 40 I=1,NC
      TCR=TC(I)
      TR1=T
      TR=TR1/TCR
      IF(TR1-TCR)10,10,20
   10 ALPR=(4.92D0*W(I)+5.81D0)*DLOG(TR)-8.38D-02*(4.92D0*W(I)+2.06D0)*
     1(36.0D0/TR-35.0D0-TR**6+42.0D0*DLOG(TR))
      GO TO 30
   20 ALPR=-(16.26D0-73.85D0*ZC(I)+90.0D0*ZC(I)**2)*(1.0D0-TR)/TR-
     110.0D0**(-8.68D0*(TR-1.8D0+6.2D0*ZC(I))**2)
   30 XK(I)=PC(I)/P*DEXP(ALPR)
      IF(DABS(XK(I)).GT.1.0D-12) GO TO 40
      XK(I)=1.0D-12
   40 CONTINUE
      RETURN
      END
      SUBROUTINE DENSIT
      IMPLICIT REAL*8 (A-H,O-Z)
      COMMON/VLE01/NC,NTYPE,MOD,MODF,NOUT
      COMMON/VLE04/DELP,PF,TF,PI,TI,P,T
      COMMON/VLE05/XK(10),X(10),Y(10),Z(10)
      COMMON/VLE08/ZLS,ZVS,ZL,ZV
      COMMON/VLE11/VLM,VVM,DENL,DENV,RMWL,RMWV,RMWF
      COMMON/VLE02/AK(10,10),RMW(10),PC(10),TC(10),W(10),ID(10),NAME(10)
      CHARACTER * 15 NAME
      R=10.731D0
      TR=T+459.67D0
```

```
C   CALCULATE THE LIQUID AND VAPOR MOLAR DENSITIES
      DENLM=P/(ZLS*R*TR)
      DENVM=P/(ZVS*R*TR)
C   CALCULATE MOLAR SPECIFIC VOLUME
      VLM=1.0D0/DENLM
      VVM=1.0D0/DENVM
      RMWL=0.0D0
      RMWV=0.0D0
      RMWF=0.0D0
C   CALCULATE THE AVERAGE MOLECULAR WEIGHT OF THE LIQUID AND
C   VAPOR PHASES.
      DO 10 I=1,NC
      RMWF=RMWF+Z(I)*RMW(I)
      RMWL=RMWL+X(I)*RMW(I)
   10 RMWV=RMWV+Y(I)*RMW(I)
C   CALCULATE THE LIQUID AND VAPOR GRAVIMETRIC DENSITIES
      DENL=DENLM*RMWL
      DENV=DENVM*RMWV
      RETURN
      END
      SUBROUTINE DEPART
C   SUBROUTINE DEPART CALCULATES THE ENTHALPY AND ENTROPY (DEPART)URES
C   FROM THE IDEAL GAS STATE FOR BOTH THE LIQUID AND VAPOR PHASES. THIS
C   IS DONE USING EXPRESSIONS DERIVED FROM THE SOAVE EQUATION OF STATE.
      IMPLICIT REAL*8 (A-H,O-Z)
      COMMON/VLE01/NC,NTYPE,MOD,MODF,NOUT
      COMMON/VLE02/AK(10,10),RMW(10),PC(10),TC(10),W(10),ID(10),NAME(10
      COMMON/VLE04/DELP,PF,TF,PI,TI,P,T
      COMMON/VLE05/XK(10),X(10),Y(10),Z(10)
      COMMON/VLE06/ALPHA(10),SA(10),SB(10),S(10)
      COMMON/VLE08/ZLS,ZVS,ZL,ZV
      COMMON/VLE11/VLM,VVM,DENL,DENV,RMWL,RMWV,RMWF
      COMMON/VLE12/HDEPL,HDEPV,SDEPL,SDEPV
      CHARACTER * 15 NAME
      DIMENSION BETA(10,10),XY(10)
      MODD=0
   10 IF(MODD.NE.0) GO TO 30
      DO 20 I=1,NC
   20 XY(I)=X(I)
      XZ=ZLS
      V=VLM
      GO TO 50
   30 DO 40 I=1,NC
   40 XY(I)=Y(I)
      XZ=ZVS
      V=VVM
   50 XB=0.0D0
      XALPHA=0.0D0
      PALPHA=0.0D0
      R=10.731D0
      CONV=144.0D0/778.16D0
      TR=T+459.67
      DO 60 I=1,NC
      TCI=TC(I)+459.67
      XB=XB+XY(I)*SB(I)
      DO 60 J=1,NC
      TCJ=TC(J)+459.67
      BETA(I,J)=XY(I)*XY(J)*(1.0D0-AK(I,J))*DSQRT(SA(I)*SA(J))
```

```
      XALPHA=XALPHA+BETA(I,J)*DSQRT(ALPHA(I)*ALPHA(J))
      A1=S(J)*DSQRT(ALPHA(I)/(TR*TC(J)))
      A2=S(I)*DSQRT(ALPHA(J)/(TR*TC(I)))
   60 PALPHA=PALPHA+(BETA(I,J)/2.0D0)*(A1+A2)
      PALPHA=-PALPHA
      H1=(XALPHA-TR*PALPHA)/XB
      H2=DLOG(V/(V+XB))
      H3=R*TR*(XZ-1.0D0)
      HDEP=H1*H2+H3
      S1=-R*DLOG(V/(V-XB))
      S2=-(PALPHA/XB)*DLOG(V/(V+XB))
      PREF=14.696D0
      S3A=0.0D0
      DO 70 I=1,NC
   70 S3A=S3A+XY(I)*DLOG((V*PREF)/(XY(I)*R*TR))
      S3=R*S3A
      SDEP=S1+S2+S3
      IF(MODD.NE.0)GO TO 80
      MODD=1
C  CONVERSION FROM FT-LBF TO BTU ENERGY UNITS
      HDEPL=HDEP*CONV
      SDEPL=SDEP*CONV
      GO TO 10
   80 HDEPV=HDEP*CONV
      SDEPV=SDEP*CONV
      RETURN
      END
      SUBROUTINE IDEAL
C  SUBROUTINE IDEAL CALCULATES THE (IDEAL) GAS STATE ENTHALPY AND
C  ENTROPY FOR THE VAPOR LIQUID EQUILIBRIUM SYSTEM.
      IMPLICIT REAL*8 (A-H,O-Z)
      COMMON/VLE01/NC,NTYPE,MOD,MODF,NOUT
      COMMON/VLE02/AK(10,10),RMW(10),PC(10),TC(10),W(10),ID(10),NAME(10)
      COMMON/VLE03/A(10),B(10),C(10),D(10),E(10),F(10),G(10)
      COMMON/VLE04/DELP,PF,TF,PI,TI,P,T
      COMMON/VLE05/XK(10),X(10),Y(10),Z(10)
      COMMON/VLE13/HOL,HOV,SOL,SOV
      COMMON/VLE11/VLM,VVM,DENL,DENV,RMWL,RMWV,RMWF
      DIMENSION WL(10),WV(10),HO(10),SO(10)
      CHARACTER * 15 NAME
      HREF=500.0D0
      TR=T+459.67D0
      TREF=536.67D0
      T1=TR
      T2=TR**2
      T3=TR**3
      T4=TR**4
      T5=TR**5
C  CALCULATE INDIVIDUAL COMPONENT IDEAL GAS ENTHALPIES AND ENTROPIES
      DO 10 I=1,NC
      H1=A(I)
      H2=B(I)*T1
      H3=C(I)*T2
      H4=D(I)*T3
      H5=E(I)*T4
      H6=F(I)*T5
      HO(I)=H1+H2+H3+H4+H5+H6
      S1=B(I)*DLOG(T1)
      S2=2.0D0*C(I)*T1
```

```
      S3=1.5D0*D(I)*T2
      S4=(4.0D0/3.0D0)*E(I)*T3
      S5=(5.0D0/4.0D0)*F(I)*T4
      S6=G(I)
      SO(I)=S1+S2+S3+S4+S5+S6
   10 CONTINUE
C  CALCULATE WEIGHT FRACTIONS
      DO 20 I=1,NC
      WV(I)=Y(I)*RMW(I)/RMWV
   20 WL(I)=X(I)*RMW(I)/RMWL
C  CALCULATE THE MIXTURE IDEAL GAS ENTHALPY AND ENTROPY FOR BOTH
C  LIQUID AND VAPOR PHASES.
      HOL=0.0D0
      SOL=0.0D0
      HOV=0.0D0
      SOV=0.0D0
C  NOTE THAT UNLIKE ENTHALPY, THE IDEAL GAS ENTROPY OF THE MIXTURE
C  INCLUDES A CORRECTION FOR MIXING(FINAL LOGARITHMIC TERM)
      R1=1.986D0
      PREF=14.696D0
      DO 40 I=1,NC
      HOL=HOL+WL(I)*HO(I)
      HOV=HOV+WV(I)*HO(I)
      SOL=SOL+WL(I)*SO(I)
      SOV=SOV+WV(I)*SO(I)
   40 CONTINUE
      RETURN
      END
      SUBROUTINE ABSOL
C  SUBROUTINE ABSOL CALCULATES THE (ABSOL)UTE ENTHALPY AND ENTROPY OF
C  THE MIXTURE AT THE SYSTEM TEMPERATURE AND PRESSURE.
      IMPLICIT REAL*8 (A-H,O-Z)
      COMMON/VLE11/VLM,VVM,DENL,DENV,RMWL,RMWV,RMWF
      COMMON/VLE12/HDEPL,HDEPV,SDEPL,SDEPV
      COMMON/VLE13/HOL,HOV,SOL,SOV
      COMMON/VLE14/HL,HV,SL,SV,HM,SM
C  REDEFINE DEPARTURES TO GRAVIMETRIC BASIS
      HDEPL=HDEPL/RMWL
      HDEPV=HDEPV/RMWV
      SDEPL=SDEPL/RMWL
      SDEPV=SDEPV/RMWV
C  CALCULATE ABSOLUTE GRAVIMETRIC ENTHALPIES AND ENTROPIES
      HL=HOL+HDEPL
      HV=HOV+HDEPV
      SL=SOL+SDEPL
      SV=SOV+SDEPV
      RETURN
      END
      SUBROUTINE OUTPUT
      IMPLICIT REAL*8 (A-H,O-Z)
      COMMON/VLE01/NC,NTYPE,MOD,MODF,NOUT
      COMMON/VLE02/AK(10,10),RMW(10),PC(10),TC(10),W(10),ID(10),NAME(10)
      COMMON/VLE04/DELP,PF,TF,PI,TI,P,T
      COMMON/VLE05/XK(10),X(10),Y(10),Z(10)
      COMMON/VLE08/ZLS,ZVS,ZL,ZV
      COMMON/VLE10/V,FL,XX,VR
      COMMON/VLE11/VLM,VVM,DENL,DENV,RMWL,RMWV,RMWF
      COMMON/VLE14/HL,HV,SL,SV,HM,SM
      COMMON/VLE16/DENLK,DENVK,HMK,HLK,HVK,SMK,SVK,SLK,TK,PK
```

```
      CHARACTER * 15 NAME
      CALL CONVER
   30 IF(MOD)37,37,35
   35 WRITE(6,1200)
   37 WRITE(6,400)TK,PK
      WRITE(6,500)
      WRITE(6,600)
      DO 40 I=1,NC
   40 WRITE(6,700)NAME(I),Z(I),X(I),Y(I)
      WRITE(6,800)XX
      WRITE(6,900)RMWF,RMWV,RMWL
      WRITE(6,1000)DENVK,DENLK
      IF(MOD)60,60,50
   50 WRITE(6,1050)VR,DELP
   60 WRITE(6,1100)HMK,HVK,HLK,SMK,SVK,SLK
      WRITE(16,1300)PK,TK
      RETURN
  400 FORMAT(5X,' TEMPERATURE=',F8.2,' DEG.K',5X,' PRESSURE=',F9.6,' MPA
     1',//)
  500 FORMAT(31X,'MOLE FRACTION',/25X,26('-'))
  600 FORMAT(25X,' FEED',4X,'LIQUID',4X,'VAPOR',/)
  700 FORMAT(6X,A15,3(3X,F8.6))
  800 FORMAT(//,5X,' VAPOR MASS FRACTION=',F8.5,/)
  900 FORMAT(5X,' FEED MW=',F8.3,4X,' VAPOR MW=',F8.3,4X,' LIQUID MW=',F
     18.3,/)
 1000 FORMAT(5X,' VAPOR DENSITY=',F8.4,' KG PER CU-M',4X,'LIQ DENSITY=
     1',F8.4,' KG PER CU-M',/)
 1050 FORMAT(5X,' VOLUMETRIC EXPANSION RATIO=',F8.4,5X,'PRESSURE RATIO='
     1,F6.4,/)
 1100 FORMAT(5X,' MIXTURE ENTHALPY=',F10.4,' KJ/KG',
     1       /5X,' VAPOR   ENTHALPY=',F10.4,' KJ/KG',
     2       /5X,' LIQUID  ENTHALPY=',F10.4,' KJ/KG',
     3       /5X,' MIXTURE ENTROPY=',F10.4,' KJ/KG-K',
     4       /5X,' VAPOR   ENTROPY=',F10.4,' KJ/KG-K',
     5       /5X,' LIQUID  ENTROPY=',F10.4,' KJ/KG-K')
 1200 FORMAT(//' ',10('*-'),'OUTLET VLE FLASH CALCULATION',10('*-'),/)
 1300 FORMAT(1P2D20.6)
      END
      SUBROUTINE CONVER
      IMPLICIT REAL*8 (A-H,O-Z)
      COMMON/VLE04/DELP,PF,TF,PI,TI,P,T
      COMMON/VLE11/VLM,VVM,DENL,DENV,RMWL,RMWV,RMWF
      COMMON/VLE14/HL,HV,SL,SV,HM,SM
      COMMON/VLE16/DENLK,DENVK,HMK,HLK,HVK,SMK,SVK,SLK,TK,PK
      TK=(T-32.0D0)*(5.0D0/9.0D0)+273.15D0
      PK=P*0.0068947D0
      DENVK=DENV*16.018459D0
      DENLK=DENL*16.018459D0
      HMK=HM*2.32596D0
      HVK=HV*2.32596D0
      HLK=HL*2.32596D0
      SMK=SM*4.18673D0
      SVK=SV*4.18673D0
      SLK=SL*4.18673D0
      RETURN
      END
```

APPENDIX B

SUMMARY OF SOLUBILITY DATA

Table 7

SOLUBILITY PROPERTIES OF n-DODECANE-NITROGEN SYSTEM

Pressure (MPa)	Temperature (K)	Barometric[a] Pressure (mm Hg)	$(\frac{H_g}{H_f})_{avg.}$	x_g	Predicted Pressure[b] (MPa)
1.03	300.15	736.73	1.6350	0.0146	1.01
1.03	373.15	725.93	1.6250	0.0143	0.91
2.07	298.15	737.11	3.0050	0.0265	1.86
2.07	373.15	725.93	3.4250	0.0296	1.90
4.82	297.15	737.36	7.2550	0.0616	4.54
4.82	373.15	725.68	8.2650	0.0685	4.58
10.34	297.15	737.62	16.7950	0.1319	10.80
10.34	373.15	725.81	18.3400	0.1404	10.10

[a]Ambient temperature = 298.15K.

[b]Equilibrium pressure at test temperature and measured composition.

Table 8

SOLUBILITY PROPERTIES OF n-DODECANE-AIR SYSTEM

Pressure (MPa)	Temperature (K)	Barometric[a] Pressure (mm Hg)	$(\frac{H_g}{H_f})_{avg.}$	x_g	Predicted Pressure[b] (MPa)
1.03	248.82	738.29	1.5900	0.0142	0.90
1.03	373.15	731.52	1.8250	0.0161	0.96
2.07	297.40	738.00	3.5600	0.0312	2.02
2.07	373.15	727.33	3.8200	0.0330	1.99
4.82	297.65	737.62	9.6000	0.0722	4.93
4.82	373.15	727.46	9.3200	0.0768	4.84
10.34	297.15	737.87	19.3600	0.1491	11.37
10.34	373.15	727.20	21.0250	0.1579	10.85

[a]Ambient temperature = 298.15K.

[b]Equilibrium pressure at test temperature and measured composition.

Table 9

SOLUBILITY PROPERTIES OF JET A (79) - NITROGEN SYSTEM

Pressure (MPa)	Temperature (K)	Barometric[a] Pressure (mm Hg)	$(\frac{H_g}{H_f})_{avg.}$	x_g	Predicted Pressure (MPa)
1.03	298.15	724.15	1.0850	0.0094	0.95
1.03	373.15	727.46	1.3300	0.0116	1.09
2.07	298.65	730.50	2.2550	0.0196	2.01
2.07	373.65	727.96	2.7950	0.0240	2.19
4.82	298.40	737.24	5.3800	0.0458	4.92
4.82	373.15	727.84	6.7050	0.0558	5.29
10.34	296.65	722.12	12.8000	0.1006	15.02
10.34	373.15	727.96	15.2700	0.1186	12.22

[a]Ambient temperature = 298.15K.

Table 10

SOLUBILITY PROPERTIES OF JET A (79) - AIR SYSTEM

Pressure (MPa)	Temperature (K)	Barometric[a] Pressure (mm Hg)	$(\frac{H_g}{H_f})_{avg.}$	x_g	Predicted Pressure (MPa)
1.03	295.82	732.87	1.3467	0.0118	1.08
1.03	373.15	732.28	1.5100	0.0132	1.10
2.07	296.65	732.66	2.7600	0.0239	2.24
2.07	373.15	731.90	3.2250	0.0278	2.36
4.82	298.15	732.16	6.8300	0.0571	5.64
4.82	373.15	731.52	7.6600	0.0635	5.61
10.34	297.15	731.90	15.1600	0.1184	13.11
10.34	373.15	731.39	16.9600	0.1306	12.55

[a]Ambient temperature = 298.15K.

Table 11

SOLUBILITY PROPERTIES OF JET A (80) - NITROGEN SYSTEM

Pressure (MPa)	Temperature (K)	Barometric[a] Pressure (mm Hg)	$(\frac{H_g}{H_f})_{avg}$	x_g	Predicted Pressure (MPa)
1.03	299.15	727.96	1.2600	0.0121	1.03
1.03	373.15	731.77	1.4000	0.0135	1.04
2.07	298.65	728.09	2.6500	0.0251	2.17
2.07	373.15	729.23	3.0250	0.0286	2.24
4.82	298.65	728.47	6.5000	0.0594	5.43
4.82	373.15	729.23	7.5100	0.0680	5.57
10.34	299.15	727.20	14.6300	0.1242	12.70
10.34	373.15	727.46	16.5300	0.1381	12.34

[a]Ambient temperature = 298.15K.

Table 12

SOLUBILITY PROPERTIES OF JET A (80) - AIR SYSTEM

Pressure (MPa)	Temperature (K)	Barometric[a] Pressure (mm Hg)	$(\frac{H_g}{H_f})_{avg}$	x_g	Predicted Pressure (MPa)
1.03	297.65	725.17	1.4550	0.0139	1.08
1.03	373.15	732.41	1.5550	0.0150	1.08
2.07	298.15	725.42	3.0800	0.0289	2.29
2.07	373.15	732.28	3.3050	0.0312	2.28
4.82	297.15	725.81	7.8700	0.0707	5.97
4.82	373.15	732.03	8.1050	0.0733	5.60
10.34	297.40	726.19	18.4050	0.1512	14.61
10.34	373.15	731.77	18.6650	0.1540	12.95

[a]Ambient temperature = 298.15K.

Table 13

DENSITY CHARACTERISTICS OF JET A (79) - NITROGEN SYSTEM

Temperature (K)	Pressure (MPa)	Density (kg/m^3)	Predicted Density (kg/m^3)
296.15	1.03421	835.3	815.0
296.15	2.02705	833.0	815.1
296.65	5.03316	831.9	815.3
296.15	9.26652	832.5	815.4

Table 14

DENSITY CHARACTERISTICS OF JET A (79) - AIR SYSTEM

Temperature (K)	Pressure (MPa)	Density (kg/m^3)	Predicted Density (kg/m^3)
296.15	0.098595	835.9	----
296.15	1.03421	835.0	814.8
296.65	2.02705	835.7	814.9
296.15	5.03316	835.2	815.1
296.15	10.3421	836.4	815.4

APPENDIX C

SUMMARY OF DENSITY DATA

Table 15

DENSITY CHARACTERISTICS OF JET A (80) - AIR SYSTEM

Temperature (K)	Pressure (MPa)	Density (kg/m^3)	Predicted Density (kg/m^3)
296.15	0.098595	815.3	----
296.15	1.03421	815.1	804.8
295.15	2.02705	810.5	804.9
297.65	5.03316	811.4	805.0
297.65	10.3421	810.3	805.2